

INVESTIGATION OF GEOMETRIC PROPERTIES OF MEDIA PARTICLES FOR FLOATING MEDIA FILTER

by

Bashir Brika

Thesis submitted in partial fulfillment
of the requirements for the Degree

of

MASTER OF SCIENCE IN ENGINEERING
(CHEMICAL ENGINEERING)

in the Department of Process Engineering
at the University of Stellenbosch

Supervised by

Prof. S.M. Bradshaw
Prof. E.P. Jacobs

STELLENBOSCH

December 2010

Declaration

I, the undersigned, hereby declare that the work contained in this thesis is my own original work and that I have not previously in its entirety or in part submitted it at any university for a degree.

Signature

31st May 2010

Date

Copyright © 2010 Stellenbosch University

All rights reserved

Abstract

In a floating medium filter, polymeric beads with a density less than that of water form a floating bed which removes suspended material. Polyolefinic beads (polypropylene and polyethylene) are commonly used as filter media in this application. The geometric properties of the beads, and to a lesser extent the surface properties, strongly influence the performance of the filter. In the case of water treatment, the primary performance requirement is the production of a filtrate with turbidity ≤ 1.0 NTU. The influence of geometric properties on the performance of existing upflow filtration systems has not been extensively researched. The aim of this thesis was therefore to investigate the effects of floating medium granule size and shape on the performance of the floating medium filter (FMF). Towards this goal a pilot plant consisting of a dosing and flocculation unit and a clear PVC column with an inner diameter of 0.3 m and height of 2.8 m was designed and constructed, allowing the effect of media type, bed depth and filtration conditions to be investigated.

Artificial feed water for use during the experimental work was made up by dissolving 250 mg/L of bentonite in tap water (≈ 60 NTU). Four median grain sizes ($d_{50} = 2.28, 3.03, 3.30,$ and 4.07 mm) of polypropylene plastic granules were used. Two media shapes (cubic and disc) were evaluated. The effect of filtration rising velocity, medium depth, and coagulant chemical dosage were investigated using a complete 2^3 full factorial experimental design. Filter performance was evaluated in terms of filtrate turbidity and headloss development. The direction of filtration was upward in all the experiments.

It was found that optimal conditions for turbidity removal were low filtration rate ($36.8 \text{ L/m}^2 \cdot \text{min}$), longer media depth (0.6 m) and optimum coagulant dose (23 mg/L). At these conditions the best medium was the one with $d_{50} = 2.28$ mm, for which a minimum turbidity of 0.4 NTU was achieved, and which was able to provide 624 L of filtrate of < 1.0 NTU using a bed of 0.014 m^3 . For this medium headloss was 109 mm H_2O at breakthrough, while the other three media showed a headloss of 42 mm H_2O at breakthrough. Visual observation indicated that removal of solids took place primarily in the first 0.3 m of the floating bed in the case of the smallest medium, but that solids removal took place over the full depth of the bed for the

other three media. It was found that bed depth had the strongest influence on performance for a given medium type.

Experimental observation showed that coagulant dosage played an important role in floc size. A higher coagulant dosage (23 mg/L) resulted in a larger floc size which gave better performance. A lower velocity gradient was favourable for the formation of larger flocs. Some effect of media shape was noted, although it appeared that media size was dominant.

It is concluded that FMF show promise for application in the water treatment. FMF, however, can be applied successfully as pre-filtration unit for treatment of high turbid water. Proper medium selection in conjunction with operating conditions can enhance performance of the filter. Smaller medium would give better turbidity removal but high headloss development and more frequent backwashing becomes necessary than with larger medium.

Opsomming

In 'n dryfmediumfilter vorm polimeriese korrels met 'n laer digtheid as dié van water 'n dryfbedding wat swewende materiaal verwyder. Poli-olefiniese korrels (polipropileen en poliëtileen) word algemeen in hierdie toepassing as filtermedia aangewend. Die geometriese kenmerke, en in 'n mindere mate die oppervlakkenmerke, van die korrels het 'n groot invloed op die funksionering van die filter. In geval van waterbehandeling is die hoof funksioneringsvereiste die produksie van 'n filtraat met 'n troebelheid van ≤ 1.0 NTU ("nephelometric turbidity units"). Die invloed van die geometriese kenmerke van filtermedia op die funksionering van bestaande stroomop-filtreerstelsels is nog nie omvattend nagevors nie. Die doel van hierdie tesis is dus om ondersoek in te stel na die uitwerking van die korrelgrootte en -vorm van 'n dryfmedium op die funksionering van die dryfmediumfilter (DMF). Hiervoor is 'n proefaanleg met 'n doseer- en uitvlokkingsseenheid sowel as 'n deursigtige pilaar van polivinielchloried (PVC) met 'n binnedeursnee van 0.3 m en 'n hoogte van 2.8 m ontwerp en gebou, met behulp waarvan verskillende mediumtipes, beddingdieptes en filtreeromstandighede ondersoek kon word.

'n Kunsmatige watertoevoer vir die proefneming is vervaardig deur 250 mg/L bentoniet in kraanwater op te los (≈ 60 NTU). Polipropileenplastiekkorrels met vier verskillende deursnee ($d_{50} = 2.28; 3.03; 3.30$ en 4.07 mm) is gebruik, en twee mediumvorme (kubus- en skyfvormig) is beoordeel. Die uitwerking van filtrasiestygingsnelheid, mediumdiepte en die dosis koaguleermiddel is met behulp van 'n volledige 2^3 -faktoriaalontwerp ondersoek. Filterfunksionering is aan die hand van filtraattroebelheid en verlies aan drukhoogte beoordeel. Alle proefnemings is teen 'n opwaartse filtrasierigting uitgevoer.

Daar is bevind dat die beste omstandighede vir die verwydering van troebelheid 'n lae filtrasiemoed (36.8 L/m² per minuut), 'n groter mediumdiepte (0.6 m) en 'n optimale dosis koaguleermiddel (23 mg/L) is. In hierdie omstandighede was die beste medium die een met 'n d_{50} van 2.28 mm, waarvoor 'n minimum troebelheid van 0.4 NTU verkry is, en wat 624 L filtraat van 1.0 NTU met behulp van 'n bedding van 0.014 m³ kon lewer. By deurbraak het hierdie medium egter 'n drukhoogteverlies van 109 mm H₂O getoon, teenoor die ander drie

media se 42 mm H₂O op dieselfde punt. Visuele waarneming dui daarop dat, met die kleinste medium, vaste stowwe hoofsaaklik oor die eerste 0.3 m van die dryfbedding verwyder is, teenoor die volle diepte van die bedding vir die ander drie media. Beddingdiepte blyk dus die grootste invloed te hê op funksionering wat enige bepaalde mediumtipe betref.

Proefwaarneming toon dat die dosis koaguleermiddel 'n belangrike rol in vlokgrötte speel. 'n Hoër dosis koaguleermiddel (23 mg/L) het 'n groter vlokgrötte en dus beter funksionering tot gevolg. 'n Laer stygsnelheid blyk ook die beste te wees vir die vorming van groter vlokke. Hoewel mediumvorm oënskynlik 'n mate van 'n rol speel, is mediumgrötte eerder die dominante faktor.

Volgens die studie blyk DMF belowend vir aanwending in waterbehandeling te wees, veral as voorfiltreereenheid vir die behandeling van baie troebel water. Behoorlike mediumkeuse saam met die regte bedryfsomstandighede kan die funksionering van die filter verder verbeter. Kleiner media sal troebelheid beter verwyder, maar het 'n groot verlies aan drukhoogte tot gevolg, en sal dus meer gereelde terugspoeling as groter media verg.

Acknowledgements

In the name of Allah the most Gracious and the most Merciful

All praise and glory goes to Almighty Allah (the most Gracious and the most Merciful) who gave me the patience and courage to carry out this work.

I pay my sincere appreciation and gratitude to my thesis supervisors Prof. Steven Bradshaw and Prof EP Jacobs for their valuable guidance, constant endeavor and the numerous moments of attention they devoted throughout the course of this research.

My thanks extend to my coordinator Dr. Ian Goldie for his cooperation, motivation and encouragement.

Sincere thanks to Stephanus Victor and the people from Ikusasa Chemicals for the construction of the pilot plant.

Sincere thanks to Sarel Pieterse and Raymond Swarts from the City of Cape Town Metropolitan Scientific Services for the helpful discussions and for allowing me to conduct some of my experiments at their facility.

Special thanks to Eddy Bosman from the Department of Civil Engineering at Stellenbosch University for the very useful discussions that we had together. It has really helped me a lot.

Special thanks to my English assistant Dr. Margie Hurndall for her very careful editing of my thesis.

Profound thanks from the core of my heart to all my family members (my mother in particular) for their prayers, support, understanding, encouragement and never ending love.

Special thanks to my fiancée (my future wife) for her support and understanding the situation of being far away for a long time.

Last but not least, I would like to take this opportunity to thank the National Bureau for Research and Development in Tripoli-Libya for the financial support.

Table of contents

<i>Abstract</i>	<i>ii</i>
<i>Opsomming</i>	<i>iv</i>
<i>Acknowledgements</i>	<i>vi</i>
<i>Table of contents</i>	<i>viii</i>
<i>List of figures</i>	<i>xi</i>
<i>List of tables</i>	<i>xiii</i>
<i>List of abbreviations and symbols</i>	<i>xiv</i>
1 Introduction	1
1.1 Background	1
1.2 Floating media filter	2
1.3 Objectives of study	2
1.4 Methodology	3
1.5 Thesis structure	3
2 Literature review	5
2.1 Introduction	5
2.2 Theory of filtration	6
2.2.1 Coagulation and flocculation.....	6
2.2.2 Principal mechanisms of filtration.....	7
2.3 Conventional filters	10
2.3.1 Slow sand filter.....	11
2.3.2 Rapid sand filters.....	12
2.4 Filter modification	14
2.4.1 Direct filtration.....	14
2.4.2 Contact flocculation-filtration.....	15
2.4.3 Upflow filtration.....	17
2.4.4 Horizontal filter using floating media.....	20
2.5 Headloss development	21
2.5.1 Headloss development in direct filtration.....	22
2.5.2 Headloss development in contact flocculation-filtration.....	22
2.5.3 Headloss development in upflow filtration.....	23
2.5.4 Headloss development in a reverse-graded dual media filter.....	24
2.6 Filter backwashing	24
2.7 Effect of physical parameters on filtration performance	26
2.7.1 Filtration rate.....	26
2.7.2 Filter media.....	28
2.7.3 Chemical dosage.....	30
3 Development of a pilot floating media filter	31
3.1 Scope of this chapter	31

3.2	Background	31
3.3	Literature review of recent research on upflow filtration using floating media	32
3.4	Summary and discussion of pertinent aspects of the literature study.....	42
3.4.1	Backwashing system	42
3.4.2	Filter column	43
3.5	Design of the major components of the plant.....	43
3.6	Final design and installation	45
3.6.1	Process description.....	45
3.6.2	Construction materials.....	47
3.6.3	Ancillary equipment.....	47
3.6.4	Conclusion	50
4	<i>Experimental.....</i>	<i>51</i>
4.1	Introduction.....	51
4.2	Experimental setup	51
4.2.1	Raw water mixing and feeding system.....	51
4.2.2	Chemical dosing system.....	52
4.2.3	Filter unit.....	53
4.2.4	Backwashing system	53
4.3	Pilot plant preliminary experimental runs	54
4.4	Measurements	54
4.4.1	Turbidity.....	54
4.4.2	Headloss development.....	55
4.5	Filter media classification.....	55
4.5.1	Size analysis	55
4.5.2	Shape analysis	55
4.6	Filter media properties.....	58
4.6.1	Voidage in the FMF	58
4.6.2	Particle size	59
4.6.3	Reynolds Number.....	60
4.6.4	Flocculation in filter beds.....	60
5	<i>Design of experiments</i>	<i>62</i>
5.1	Introduction.....	62
5.2	Factorial experiments.....	62
5.2.1	Two-level full factorial design	62
5.2.2	Process of designing an experiment	65
6	<i>Results and discussion.....</i>	<i>68</i>
6.1	Introduction.....	68
6.2	Filter efficiency.....	68
6.3	Turbidity breakthrough.....	68
6.4	Results obtained from preliminary plant experiments.....	69
6.5	Results obtained from actual experimentation	70
6.6	Effects of physical parameters.....	72
6.6.1	Filtration rising velocity	72
6.6.2	Medium size	75
6.6.3	Medium shape	79
6.6.4	Medium depth	81

6.6.5	Coagulant dosage	83
6.7	Headloss development	87
6.8	Backwashing.....	89
6.8.1	Backwashing of plastic media	89
6.8.2	Backwashing of combined media and LLDPE powder.....	91
6.9	Experimental design	92
6.9.1	Statistical analysis	94
6.9.2	Discussion of the 2 ³ factorial design results for medium ii (3.30 mm, sharp-edged cubic medium) 94	
6.9.3	Discussion of the 2 ⁴ factorial design results.....	97
7	Conclusions.....	103
	Recommendations	106
	References.....	107
	Appendix A Pilot plant design drawings	114
	Appendix B Calculations.....	121
	Appendix C Dosing pump and Jar test.....	128
	Appendix D Turbidity and headloss profiles	135
	Appendix E Factorial design results.....	159
	Discussion of the 2 ³ factorial design results of medium i	160
	Discussion of the 2 ³ factorial design results of medium iii	162
	Appendix F Materials and equipment data sheet.....	166

List of figures

Figure 1.1: Flow diagram of the proposed study methodology.....	4
Figure 2.1: Schematic of a conventional slow sand filter [after Collins et al., 1991].....	11
Figure 2.2: Particle removal mechanisms that potentially could be involved in slow sand filters [after Weber-Shirk and Dick, 1999].....	12
Figure 2.3: Schematic of a conventional rapid sand filter.....	13
Figure 2.4: Direct filtration flow schemes [after Odira, 1985].....	15
Figure 2.5: Schematic representation of contact flocculation filtration.....	17
Figure 2.6: Upflow grid filter (after Hamann and McKinney, 1967).....	18
Figure 2.7: Schematic representation of the Haberer process [after Stukenburg and Hesby, 1991].....	20
Figure 2.8: Filter headloss versus filter run time [after Ødegaard and Helness, 1999].....	23
Figure 2.9: Headloss development rate versus sludge accumulation rate.....	24
Figure 2.10: Headloss vs. filtration time at different filtration velocities (polypropylene & polystyrene media, downflow filtration) [after Sundarakumar, 1996].....	27
Figure 2.11: Shapes of plastic media that have been used in floating media filter to date.....	29
Figure 3.1: Schematic diagram of an upflow system filtration system in which floating media are used [after You and Kim, 2001].....	33
Figure 3.2: Experimental setup of an upflow filter [after Visvanathan et al., 1996].....	35
Figure 3.3: Flow diagram of bench-scale and pilot-scale floating media filter.....	36
Figure 3.4: Experimental pilot plant [after Ødegaard and Helness, 1999].....	38
Figure 3.5: Schematic of a backwashing apparatus [after Fitzpatrick, 1998].....	39
Figure 3.6: Schematic diagram of floating media filter [after Verster, 2005].....	40
Figure 3.7: Schematic diagram of the upflow filtration unit [after Zouboulis et al. 2002].....	41
Figure 3.8: Simplified flow diagram for water treatment in this study using floating media with flocculation....	46
Figure 3.9: The floating medium filtration pilot plant.....	48
Figure 3.10: Piezometer panel.....	49
Figure 3.11: Feed water tank and platform ladder.....	49
Figure 4.1: Schematic diagram of the upflow floating media filtration unit designed for use in this study.....	52
Figure 4.2: Particles classification chart [adapted from Lees, 1964; Janoo, 1998].....	56
Figure 4.3: Different sizes and shapes of plastic media that were tested in this study. From left to right: smooth cubic (medium i), large cubic (medium ii), disc (medium iii), and small lace-cut cubic (medium iv).....	57
Figure 5.1: Geometric representation of the 2 ³ design.....	64
Figure 6.1: Effect of filtration rising velocity on filtrate turbidity for all media.....	72
Figure 6.2: Effect of filtration rate on initial filter headloss.....	74
Figure 6.3: Effect of medium size on filtrate turbidity. Filtration velocity: (a) 2 m/h,.....	75
Figure 6.4: Filter headloss as a function of filtration time. Filtration velocity: (a) 2 m/h, (b) 4 m/h; media depth 600 mm; chemical dose 23 mg/L.....	76
Figure 6.5: Effect of medium size on filtrate turbidity. Filtration velocity: 2 m/h; media depth: 600 mm; coagulant dose: 23 mg/L.....	78
Figure 6.6: Effect of medium shape on filtrate turbidity. Filtration rate: (a) 36.8 L/m ² ·min, (b) 73.6 L/m ² ·min; media depth: (a) 200 mm, (b) 600 mm; coagulant dose: 23 mg/L.....	79
Figure 6.7: SEM images showing the surface morphologies of (a) a cubic-shaped medium; and (b) a disc-shaped medium.....	80
Figure 6.8: Effect of media depth on filtrate turbidity. Filtration velocity: 2m/h; chemical dose: 23 mg/L; medium: (a) i, (b) iii.....	81
Figure 6.9: Effect of media depth on filtrate turbidity. Filtration velocity: 2m/h; chemical dose: 23 mg/L; medium: medium iv.....	82

<i>Figure 6.10: Headloss development as a function of filtration time. Filtration velocity: 2 m/h; chemical dose: 23 mg/L; medium: medium i.</i>	83
<i>Figure 6.11: Effect of coagulant dose on filtrate turbidity. Filtration velocity: 2m/h; media depth: 200 mm; medium: (a) i, (b) ii.</i>	84
<i>Figure 6.12: Headloss development as a function of filtration time. Filtration velocity:</i>	85
<i>Figure 6.14: Headloss variation along filter bed at given time. Filtration velocity: 2 m/h, media depth: 600 mm, chemical dose: 23 mg/L, medium: iv.</i>	88
<i>Figure 6.15: Time vs. backwash water turbidity for media iii. Backwash method: (a) air + water, (b) water only.</i>	91
<i>Figure 6.17: Factorial experimental trials conducted with medium ii.</i>	93
<i>Figure 6.18: Factorial experimental trials conducted with medium iii.</i>	93
<i>Figure 6.19: Pareto chart.</i>	94
<i>Figure 6.20: 3D response surface graph for turbidity removal vs. filtration rising velocity and chemical dose.</i>	96
<i>Figure 6.21: 3D response surface graph for turbidity removal vs. media depth and</i>	97
<i>Figure 6.22: Effect of medium shape on Turbidity (a).</i>	98
<i>Figure 6.23: Effect of the medium shape on Turbidity (b).</i>	98
<i>Figure 6.24: Effect of interaction CD.</i>	99
<i>Figure 6.25: Pareto chart of main effects in the factorial 2⁴ design.</i>	100
<i>Figure 6.26: Effect of the medium shape on Turbidity at optimal chemical dose.</i>	101
<i>Figure 6.27: Effect of the medium shape on Turbidity at low level of chemical dose.</i>	101
<i>Figure 6.28: Effect of interaction CD.</i>	102

List of tables

<i>Table 4.1: Summary of filter media particle analysis</i>	<i>57</i>
<i>Table 4.2: Floating media particle characteristics.....</i>	<i>60</i>
<i>Table 5.1: The 2³ design: (a) the design matrix, and (b) the algebraic signs for calculating effects.....</i>	<i>63</i>
<i>Table 5.2: Factors and details of the levels for the treatment combinations in the 2³ design.....</i>	<i>66</i>
<i>Table 5.3: Experiments generated from DOE.....</i>	<i>67</i>
<i>Table 6.1: Operating conditions of the preliminary experiments</i>	<i>69</i>
<i>Table 6.2: Summary of preliminary experiments</i>	<i>70</i>
<i>Table 6.3: Summary of results</i>	<i>71</i>
<i>Table 6.4: Summary of calculated parameters at bed depth of 200 mm.....</i>	<i>86</i>

List of abbreviations and symbols

mL	milliliter
L	liter
g	gram
kg	Kilogram
H	hour
pH	Hydrogen ion exponent
COD	Chemical oxygen demand
BOD ₅	Biological Oxygen Demand
CBOD ₅	Carbonaceous Biological Oxygen Demand
FMF	Floating Media Filter
F ⁺³	Ferric ion
Al ₂ (SO ₄) ₃ .H ₂ O	Alum
PVC	Polyvinyl chloride
PLC	Programmable Logic Control
μm	micrometer
p	flatness ratio
q	elongation ratio
F	Shape factor
ψ	Sphericity
C°	degrees Celsius
NTU	Nephelometric Turbidity Unit
LLDPE	Linear Low Density Polyethylene

ϕ_{FMF}	Bed voidage
M	mass of floating media in FMF
A	Cross-sectional area of FMF column
V_p	Volume of 1 gram of floating media particles
w	mass of particles
ρ_s	solid density of floating media particles
ρ_b	bulk density of floating media particles
V_{sphere}	Volume of sphere
d_e	equivalent diameter
d_{50}	median grain size
Re	Reynolds number
D_p	equivalent spherical diameter
μ	dynamic viscosity of the fluid
ν	kinematic viscosity
V_s	Superficial velocity
ε	Void fraction of the bed (porosity)
g	the gravitational acceleration
G	Velocity gradient
Δh	headloss across the filter bed
t	detention time in the filter bed
f	porosity of the filter medium

1 Introduction

1.1 Background

Two thirds of the earth's surface is covered by water and the human body consists of 75% water. It is therefore very clear that water is one of the most essential requirements for life on earth. Water is involved in all bodily functions: digestion, assimilation, elimination, respiration, maintaining temperature (homeostasis), and integrity and the strength of all bodily structures.

Our water today is unfortunately no longer pure: it contains hundreds of deadly commercial chemicals, in addition to bacteria, viruses, and inorganic minerals. Particulate matter, both man-made or natural is commonly present in water, and requires removal. These particulates can either be in solid or dissolved state. All these harmful constituents in water cause it to be often unsuitable for human consumption. Over the past few decades a major concern has been how to produce water that is pure enough for its intended use, most commonly human consumption.

Filtration is the most well-known method for removing clay and suspended solids from surface water. Slow sand filters and rapid sand filters are widely used for the removal of suspended solids present in water, but sand filters have a number of limitations and drawbacks such as high energy requirements for backwashing. One of the most serious problems involves maintaining bed homogeneity during operation. Inhomogeneities in the bed lead to formation of channels in the bed, poor distribution of the liquid flow through the bed, and thus very low particulate removal. Such inhomogeneities may also allow air to be trapped in the bed, also leading to the formation of channels and poor distribution of the liquid [Ngo and Vigneswaran, 1995, Schwartzkopf, 2006]. Over the past decade, many modifications have been made in efforts to minimize the shortcomings of conventional sand filters.

1.2 Floating media filter

A floating media filter (FMF) can be defined as a filter that is designed to use a floating medium such as expanded polystyrene or polypropylene or polyethylene in granulated or granular form that has a lower specific gravity than that of the water to be filtered. In such filters the floating medium resides in the upper compartment of the filter. Water flows vertically upward through the bed [Akitoshi, 1980].

Floating media filters differ from the conventional sand filters in many ways: the density of media particles is less than that of the water to be filtered; and a retaining grating is placed at the top of the filter in order to maintain the media inside the filter under submerged conditions [El Etriby and Menlibia 1997].

Floating media filters have the following advantages over conventional sand filters. They do not require as much energy and water for backwashing as required by sand filters. Floating media filters do not require large land area and large quantity of filter media as required by sand filters [Ngo and Vigneswaran, 1995].

1.3 Objectives of study

The main objective of this study was to investigate the effect of the geometric properties (size and shape) of the medium used in FMF on the performance of the filter. In order to achieve this objective the following aims were set:

- select design parameters for an upflow floating media filter;
- locate suitable media and chemicals required to remove turbidity from raw water;
- characterise the media in terms of size and shape;
- determine the optimum coagulant dosage that needs to be added to the liquid flow for the purpose of forming flocs;
- determine the variables required to achieve efficient removal of turbidity from raw water;

- try to obtain an understanding of the mechanisms involved in the floating media filtration process;
- determine the filter performance under various operating conditions, e.g. filtration rates, media bed depths, coagulant dosages. Efficiency of a floating media filter was to be determined by studying the resulting filtrate quality and the head variation in the filter bed; and.
- Investigate backwash methods for cleaning the filtration media.

1.4 Methodology

To develop and qualify the process of floating media filtration, a pilot plant was designed and built according to the basic principles of the filtration process obtained from literature. The mind map used to approach this study is presented in Figure 1.1.

1.5 Thesis structure

This thesis is presented in eight chapters.

- Chapter 1 includes an introduction to and the objectives of the study.
- Chapter 2 (Literature review) – The filtration process (one of the most common solid-liquid separation processes) is described. It includes the different filtration methods that have been widely used such as conventional filtration and direct filtration, and the modifications that have been made to enhance performance.
- Chapter 3 – A review of research on filtration using floating media is presented.

Design of an upflow floating media filter is included.

- Chapter 4 – The experimental work that was carried out in this study is described.
- Chapter 5 – The design of experiments carried out in this study is described.
- Chapter 6 – The results and discussion of the above experimental work are presented.
- Chapter 7 – Conclusions

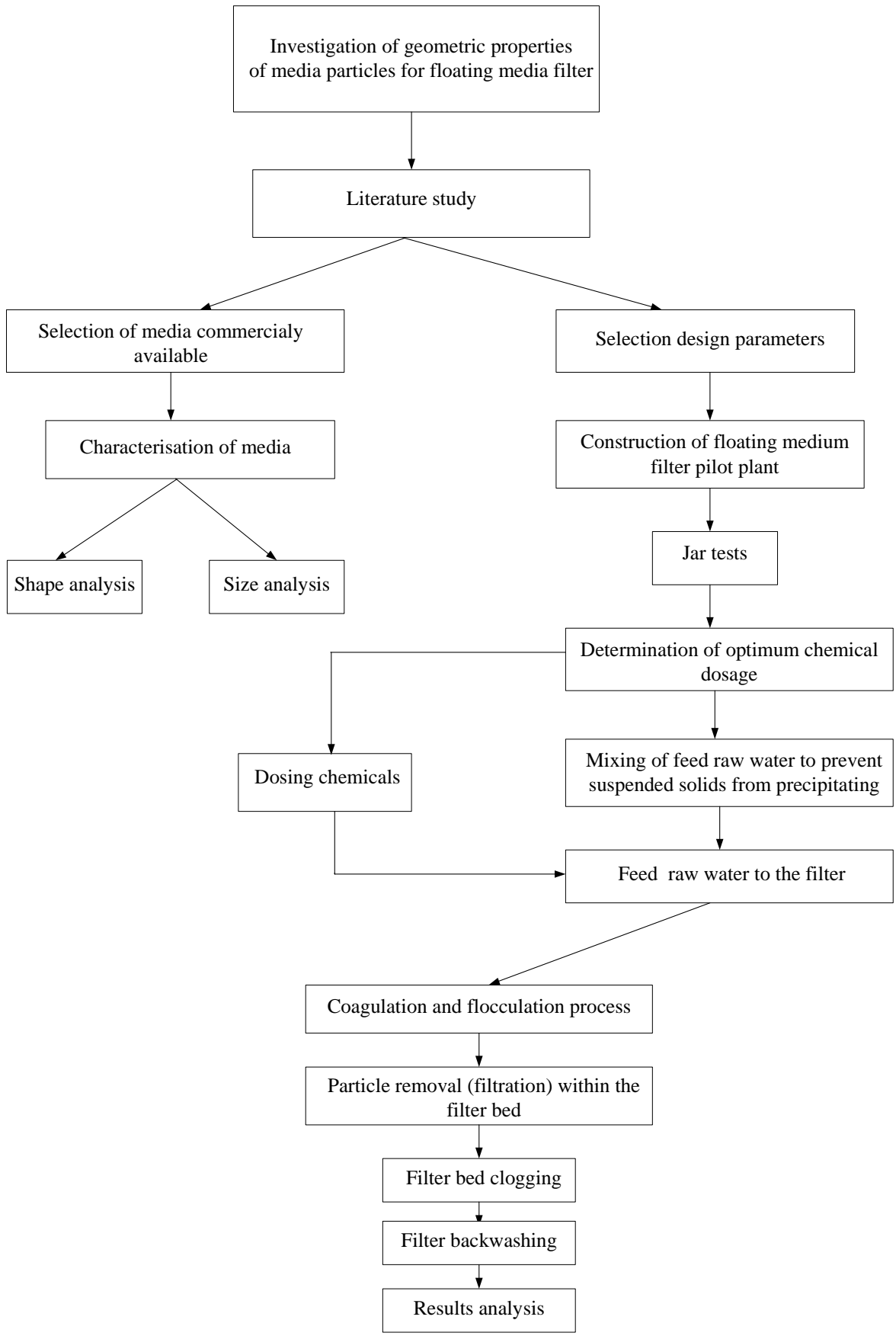


Figure 1.1: Flow diagram of the proposed study methodology.

2 Literature review

2.1 Introduction

Filtration is considered to be the most important solid/liquid separation process in water treatment as well as in most sewage (tertiary) wastewater treatment. Nowadays, due to a gradual decrease in raw water quality and in order to adhere to more strict drinking water quality standards as well as tougher pollutant content levels applied to existing tertiary wastewater treatment work, filters need to be installed in most water and wastewater treatment plants [Ngo and Vigneswaran, 1995; Souboulies *et al.*, 2002]. Filtration is also being investigated as an additional application to domestic wastewater treatment and is being considered as an alternate technology for secondary clarification of wastewater [Svarovsky, 1977; Wagener, 2000].

Granular medium filters separate solids from liquids when the feed is passed through the medium which retains the particles. Filtration through granular media is a physical process, it is based on the principle of capturing the particles rather than removing masses of solids. The main mechanisms that contribute to the removal of suspended solids include: straining, sedimentation, impaction, interception, adhesion, chemical adsorption, physical adsorption, flocculation, and biological growth [Metcalf and Eddy, 1991; Ødegaard and Helness, 1999; Zouboulis *et al.*, 2002]. Granular medium filters can be of different types and arranged in various configurations, with several different options for media type.

Filters used in water and wastewater treatment technology can be classified in several ways. They can be classed according to: (i) the direction of flow through the bed (downflow, upflow, biflow, radial flow, horizontal flow, fine-to-coarse, or coarse-to-fine), (ii) the type of filter medium (sand, coal, coal-sand, multilayered, mixed media), (iii) the number of media (monomedia, dual-media, multimedia), (iv) pressure or gravity flow, and (v) the type of system used to control the flow rate through the filter (constant rate, declining rate, constant pressure) [Culp *et al.*, 1974; Hamann and Mckinney, 1968].

2.2 Theory of filtration

2.2.1 Coagulation and flocculation

All water, especially surface water, contain both dissolved and suspended particles. These particles are usually less than 1 μm in size and are termed colloids. They have poor settling characteristics and are responsible for the colour and turbidity of water. Most solids suspended in water possess a negative charge and, since they have the same type of surface charge, repel each other when they come close together. Therefore, they will remain in suspension rather than clump together and settle out of the water. The stabilized particles can be aggregated by adding colloids having an opposite (positive) charge. These are added as chemical coagulants.

Coagulation can be defined as the process of charge neutralization of colloidal particles using the addition of a chemical reagent. Cationic coagulants provide the positive electrostatic necessary charge to reduce the negative charge of the colloids. Rapid mixing is required to disperse the coagulant throughout the liquid. The key for effective coagulation depends on the interaction of the coagulant species with colloids in the raw water [Sawyer *et al.*, 1978].

O'Melia (1972) and Dempsey (1984) identified four mechanisms that contribute to the coagulation process, namely enmeshment of particles, charge neutralization or destabilization, precipitation and adsorption. These mechanisms were categorizing as the primary reaction mechanism and they may exists either by themselves or they also may exists in combination due to the complexity of the nature of the coagulation process [Edzwald and Van Benschoten., 1990].

Flocculation is the process where small particles agglomerate to form larger particles. The essential steps in flocculation consisted of destabilization of the particles and the collisions of destabilized particles to form flocs. During flocculation, aggregation of particles occurs which results in the variation of size and number of the flocs. Large flocs required a relatively long period of mixing at a low intensity, whereas small flocs can be formed in a short period of time and a relatively high intensity [Boadway., 1978; Vigneswaran and Setiadi.,1986].

According to Weber [1972] flocculation depends on the number of particles and the probability of collisions among the particles. Collision may result from variable velocity of

suspended particles and from micro-pulsation generated by mixing. The intensity of mixing can be defined by the variation in the velocity vector of fluid motion, which is described in terms of average velocity gradient. The velocity gradient (G) is produced by the headloss developed during the passage of the suspension through the filter bed. The velocity gradient (G) and flocculation time (t_f) are the most important factors in controlling the floc size. The velocity gradient (G) can be calculated from the following equation [Schulz *et al.* 1994].

$$G = \sqrt{\frac{g \cdot \Delta h}{\nu \cdot t \cdot f}} \quad (1.1)$$

Where g = the gravitational acceleration, cm/s^2 ; Δh = headloss across the filter bed, cm ; ν = kinematic viscosity, cm^2/s ; t = detention time in filter bed, s ; and f = porosity of filter medium (dimensionless).

2.2.2 Principal mechanisms of filtration

Deep bed filtration is an effective process for removing particles that are present in water and wastewater, but it involves complex mechanisms. These mechanisms depend on the physical and chemical characteristics of the water, the particles and the filter medium. The particles to be removed from the suspension are smaller than the interstices of the medium. It follows that if particles had followed the fluid streamlines, many of the particles would not have touched the surface of a filter grain and been removed from the flow. But due to various particle transport mechanisms, particles move across the streamlines and arrive nearby to a filter grain surface. Once particles get close to a filter grain, an attachment force is to be present in order for particles to be retained on the filter grain or on the previously deposited particles. If the deposited particles are entrained again in the flow, a detachment mechanism has to be involved [Jegatheesan and Vigneswaran, 2005]. The three main mechanisms of filtration are discussed in detail in the following three sections.

2.2.2.1 Transport mechanism

In the transport mechanism the particles are transported from the bulk of the fluid within the interface close to the surface of the filter grains. Various transport mechanisms are involved in bringing the particles closer to the filter grain. These mechanisms can include the following:

- **Straining:** When particles, large enough to be significantly strained, arrive at the filter grain surface a mat will be formed and the bed will rapidly become clogged. Such surface clogging can also occur if the concentration of particles is too high.
- **Interception:** Interception occurs when a particle that is following the streamline of the fluid flow comes into contact with a filter grain. The particle touches the filter grain and is captured, thus being removed from the liquid flow. This mechanism is affected by the size of the particle.
- **Inertia:** This mechanism occurs when a particle is so large that is unable to quickly adjust to the sudden changes in streamline direction near a filter grain. The particle, due its inertia, will continue along its flow path and hit the filter grain.
- **Sedimentation:** If the particle is large enough, and has a density greater than that of water, it is subject to a constant velocity relative to the water, in the direction of gravity. Therefore it causes the particle to follow a different trajectory and settle out.
- **Diffusion:** Brownian motion is the dominant factor in the deposition of very small particles suspended in a medium. Ives (1970) found that the Brownian motion is very important in transporting the submicron size particle to the collector (filter grain). For particles greater than 1 μ m in diameter the viscous drag of the fluid limits this movement and the mean free path of the particle is, at most, one or two particle diameters, and therefore this mechanism is less important.
- **Hydrodynamic action:** The fluid flow in the filter pores is laminar, with a velocity gradient in each pore (zero velocity at the boundary of the grain surface and maximum velocity at the pore center). The velocity gradient imposes a shear field in the pore. In a uniform shear field a spherical particle will experience rotation with a consequent accompanying spherical flow field. This will cause the particle to migrate across the shear field. If the particle is not spherical, it will experience further out-of-balance forces moving it across the streamlines. The net result is that particles will exhibit an apparently random, drifting motion across the streamlines, which may cause them to collide with grain surfaces.
- **Orthokinetic flocculation:** It is also called velocity gradient flocculation. Velocity gradient is a measurement of the intensity of mixing in the flocculator. The velocity

gradient determines how much the water is agitated. And also determines how much energy is used to operate the flash mixing or flocculator. The velocity gradient (G) is produced by the headloss developed during the passage of the suspension through the filter bed while the headloss is a function of flow rate, size of medium, cross-sectional area of the bed and volume of floc retained in the bed [Schulz *et al.*, 1994].

It is unlikely that any of the transport mechanisms act individually. Particles in a flowing suspension will be subject to all mechanisms to different degrees, and their importance will depend on the fluid flow conditions, the geometry of the filter pores, and the nature (size, shape, density) of the particles [Jegatheesan *et al.*, 2005; Zamani *et al.*, 2009].

2.2.2.2 Attachment mechanism

An attachment mechanism is required as the particle approaches the surface of the filter medium. The attachment mechanism is affected by the chemical characteristics of water and the medium. The attachment mechanism may include:

- electrostatic interactions;
- chemical bridging; and
- specific adsorption

It has been proposed that the removal of suspended particles is maximum when the electrokinetic repulsive forces are minimum [Stanley, 1955; Adin *et al.*, 1979]. Adsorption of suspended particles to the surface of a medium is an important mechanism in rapid sand filtration performance. The particles can attach to the filter grain through hydrogen bonding of water molecules between their surfaces [Ives, 1961; Camp, 1964].

During filtration through deep granular filters, accumulated particles build up on the filter, and are removed from the water by one or more of the above mechanisms. The particles are held in the filter in equilibrium with the hydraulic shearing forces that tend to shear them away and wash them deeper into, or through, the filter. As the deposits build up, the velocity of the feed through the more tightly clogged upper layers of the filter increases, and hence the filter becomes less effective in terms of removal. The burden of removal passes deeper and deeper into the filter. Ultimately, there is not enough clean bed depth available to achieve the desired effluent quality and the filtration sequence might need to be terminated.

According to Adin and Rebhun (1974) the efficiency of filtration process for a specific set of hydraulic conditions depends on the attachment forces. Since the approach-velocity in high-rate filtration is kept constant, the hydraulic gradients increase because of the accumulation of particles, and hence the shear forces increase. The filtration efficiency is effectively determined by a relationship between the attachment and the shear forces. As the hydrodynamic shear forces become greater than the attachment forces, breakthrough occurs.

2.2.2.3 Detachment mechanism

There is evidence that an increase in the flow rate through a filter will detach particles, causing a more turbid filtrate. The intensity of this mechanism depends on the amount of the increase of the flow rate and the rate of change of the flow rate. If the flow rate remains constant, as in the normal mode of operation of rapid filters, opinions differ on whether detachment happens. One group of researchers considered that the structure of accumulated deposits in a filter medium is not equally strong. Under the action of hydrodynamic forces caused by the flow of water through the media with increasing headloss, this structure is partially destroyed. A certain portion of previously adhered particles, less strongly linked to the others, becomes detached from the grains, as long as new particles are being supplied [Jegatheesan *et al.*, 2007].

2.3 Conventional filters

The most common method of filtration is conventional media filtration, where filtration follows coagulation, flocculation and sedimentation. This type of filtration leads to flexible and reliable performance, especially when treating variable or very turbid source water.

Sand filtration was once thought to be a suitable treatment for rendering seawater drinkable [Baker, 1981]. Sand is the most common filtering medium used in conventional media filtration. However, other media such as crushed anthracite (hard coals), crushed magnetite, and garnet are also widely used. The medium size and its pore openings are important characteristics that affect removal. Sand filtration is a process whereby water is passed through a bed of sand and, by means of mechanical and biological mechanisms, organic and inorganic matter, bacteria and viruses is removed. Removal is highly dependent on the surface area of the media particles. Sand filters are granular medium filters, which may be packed or fluidized, downflow or upflow, single pass or recirculation that contains sand as the filtering

medium. Packed sand filters have been widely used for the removal of particulate matter [Jellison *et al.*, 2000; Arndt and Wagner, 2003].

2.3.1 Slow sand filter

Slow sand filtration is a simple and reliable process, and the most efficient treatment technology for improving water quality [Galvis, 1999]. The efficiency of the slow sand filter depends on the particle size distribution of the sand, the ratio of surface area of the filter to depth and the flow rate of water through the filter. Slow sand filtration is used to filter water at very slow rates. The typical filtration rate of 2 to 5 L/min/m² is fifty times slower than for rapid sand filtration. Due to this very slow rate, a very large amount of land is required.

Slow sand filters can provide removal of suspended solids, turbidity, and micro-organisms without the need for chemical addition or the use of electrical power. A slow sand filter consists of two or more filter beds containing 0.9 to 1.2 meter of sand placed over a gravel-supported under-drain. The filter is cleaned by scraping about 2 or 3 cm of sand from the top. This method of the cleaning is an effective process in suspended solid removal [Fogel *et al.*, 1993]. The schematic of a conventional slow sand filter is shown in Figure 2.1.

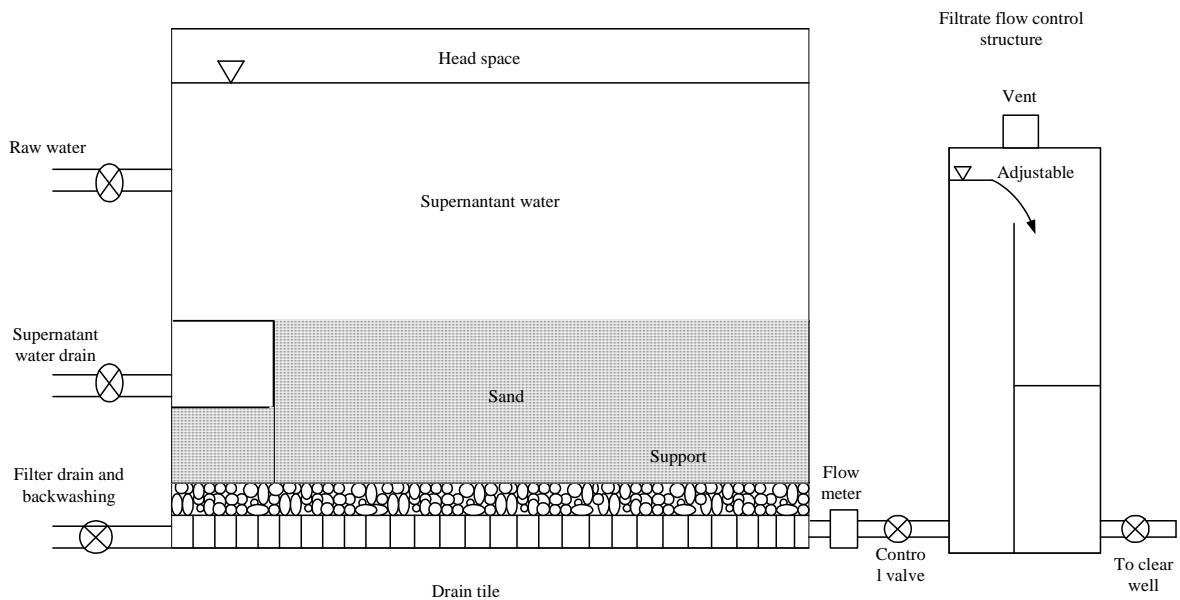


Figure 2.1: Schematic of a conventional slow sand filter [after Collins *et al.*, 1991].

The mechanisms responsible for particle removal in slow sand filtration are not well understood. Due to the fact that slow sand filter performance gradually increases with time, it

has often been assumed that the growth of biofilms is responsible for the gradual improvement in filter performance. Another theory suggested that biofilms are not responsible for significant particle removal and the most particles are removed by physical-chemical mechanisms [Weber-Shirk and Dick, 1999]. Potential mechanisms of particle removal by slow sand filters can be summarized in Figure 2.2.

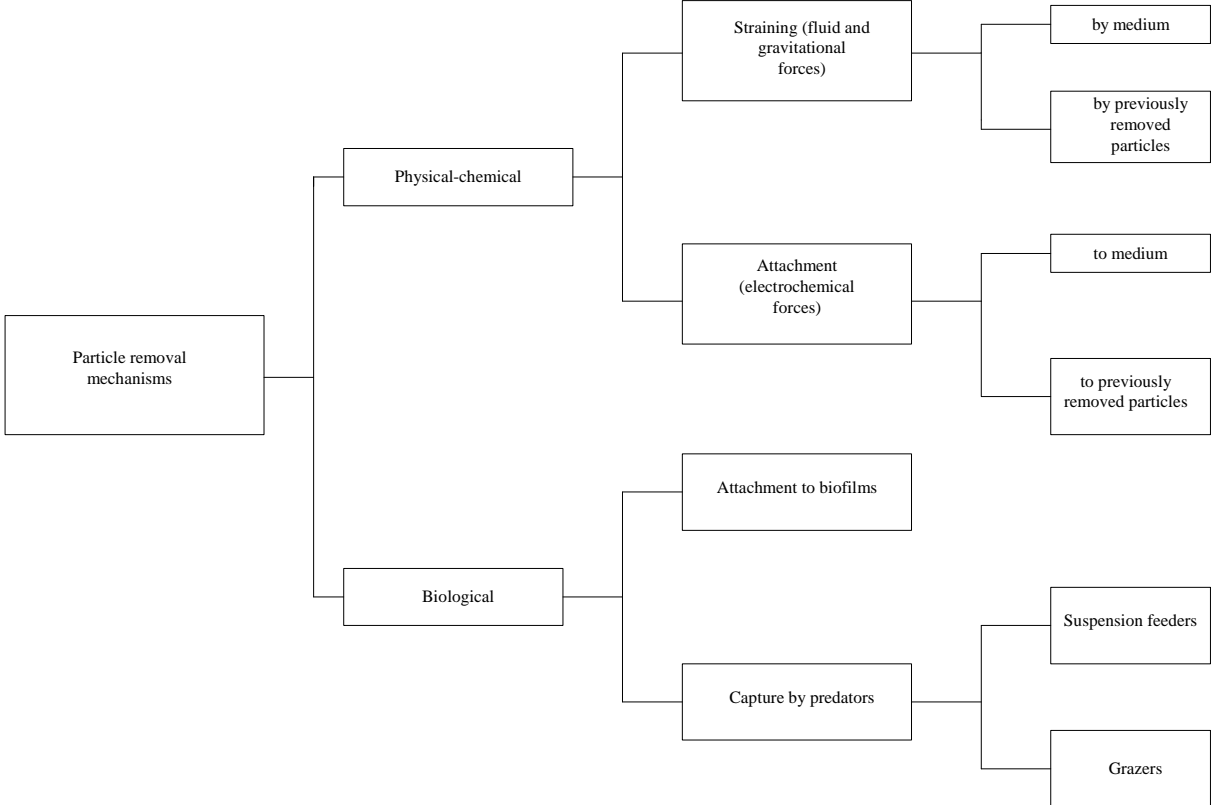


Figure 2.2: Particle removal mechanisms that potentially could be involved in slow sand filters [after Weber-Shirk and Dick, 1999].

2.3.2 Rapid sand filters

Rapid sand filters are operated at a much higher rate than slow sand filters, either via pumping or adequate head pressure, and coarser sand is used. The filtration rate in a rapid sand filter is 1 to 5 m³/(m².h) [Weber, 1972; Droste, 1997]. As a result of the high filtration rate more debris accumulates over a shorter period of time, and therefore the filter needs to be backwashed frequently. The filter bed is cleaned by flushing water in the opposite direction to the normal water flow at a sufficient velocity. This leads to fluidising the bed material and the removal of the trapped material. Cleaning occurs by scrubbing, caused by hydraulic shear forces on the media, and by abrasive scouring resulting from particles rubbing against each other. The filter requires frequent cleaning; one to three times daily [Amirtharajah, 1978;

Arndt and Wagner, 2003]. Due to its lower volume requirement (25 to 150 times less than slow sand filters) it is widely used as a final clarification unit in municipal water treatment plants. A schematic diagram of a rapid sand filter is shown in Figure 2.3.

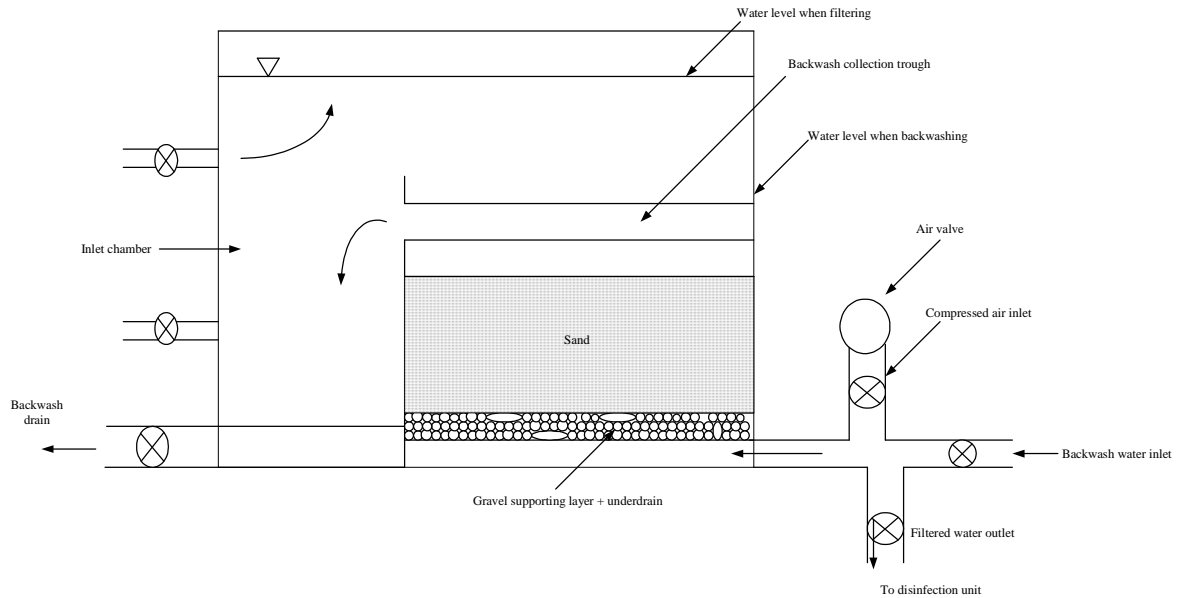


Figure 2.3: Schematic of a conventional rapid sand filter.

Particulate matters are entrapped by two mechanisms: mechanical straining, if the particle is bigger than the smallest opening through which the water flows; and physical adsorption, which refers to attachment of particulate matters to the sand media. The efficiency of both mechanisms are enhanced by coagulations, which leads to 1. the formation of bigger flocs and 2. particles with their surfaces neutralized [Culp *et al.*, 1978].

In both types of sand filters, sand is characterized by the diameter of the individual sand grains (e.g. 0.15 to 0.35 mm) and the effective size of the composite sand, the ES or d_{10} . D_{10} is defined as the sieve size in mm that permits passage of 10% by weight of the sand. The uniformity coefficient (UC) of sand is defined as d_{60}/d_{10} .

2.4 Filter modification

Extensive research has been performed over the last three decades to modify the filter, in terms of the type of filter media, the direction of flow through the bed, and the operating conditions. Some of these modifications are presented in the following sections.

2.4.1 Direct filtration

Direct filtration is a relatively simple filtration process. It is one of the unit operations used in conventional water treatment plants. This type of filtration does not include a sedimentation unit. Therefore all the solids present in raw water as well as those accumulated during treatment must be removed and temporarily stored in the filter bed. Direct filtration includes chemical addition (coagulants, such as iron or aluminum salts). The mixture is then slowly stirred to cause the micro-suspended particles to aggregate to form larger flocs. Once this process is complete the raw water is passed through the filters, so that any remaining particles attach themselves to the filter material. Direct filtration results in a significant improvement in water quality. Figure 2.4 shows different direct filtration schemes [Odira, 1985].

It is recognised that direct filtration is more suitable for use in water of low turbidity with constant flows than in high turbidity water. Direct filtration does not need sophisticated equipment or skilled labour to operate the filter. An additional advantage of direct filtration is a reduction in the capital cost of the treatment facility, since the requirements for settling basins are eliminated. Reduction in chemical flocculation dosages results in decreased sludge production and hence less maintenance is required [Ngo and Vigneswaran, 1995].

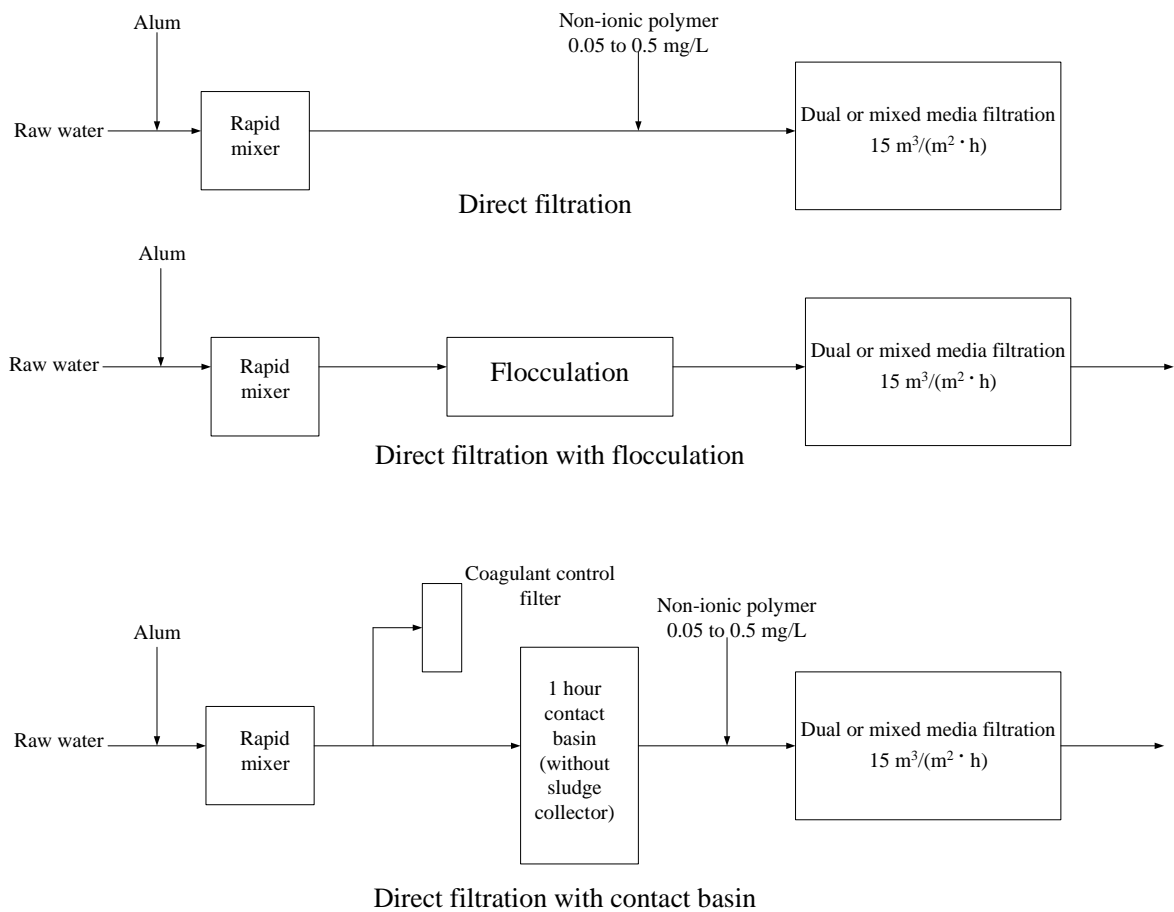


Figure 2.4: Direct filtration flow schemes [after Odira, 1985].

2.4.2 Contact flocculation-filtration

Adin and Rebhun (1974) reported that the contact flocculation–filtration process is different from the conventional volume flocculation process in that it can be accomplished at very high rates. In other words, contact flocculation–filtration is a high-rate direct filtration process through a porous bed. This leads to particle removal from dilute suspensions without the requirement for separate flocculation and settling units. Experiments have shown that addition of flocculant is necessary in contact filtration to achieve a high-quality filtrate.

Adin and Rebhun (1974) proposed three stages in the removal process in contact flocculation-filtration: a working-in stage, a working stage, and a breakthrough stage. The working-in stage can be defined by a decrease in turbidity residue with time, until a constant value is reached. The working stage is the main effective stage of the filtration. It was found that during this stage a much better effluent quality was obtained when polymer was used

compared to when alum was used. The quality of the effluent declines during the breakthrough stage. The attachment process in contact flocculation is achieved by an adsorption-bridging mechanism.

Adin and Rebhun (1974) studied the effect of alum and cationic polyelectrolytes as flocculants in contact flocculation-filtration and found that:

- contact filtration with alum alone is not effective at high rates with coarse media (the attachment forces between the removed matter and the bed are weak); and
- cationic polyelectrolytes are effective at high hydraulic loads (20 m/hr) (the polymer causes strong attachment forces).

It was observed that using polymer in contact flocculation leads to a rapid development of head loss, high filtration coefficients, and a slow penetration into the bed.

Shea *et al.* (1971) found that coarse and uniform dual-media (used in a coarse-to-fine media arrangement) is the best media to use for contact flocculation-filtration.

The main advantages of contact flocculation-filtration are that the requirements for conventional sedimentation and flocculation units are removed, and sludge handling problems are reduced. The disadvantage, however, is the short filter runs that occur as a consequence of the fact that the entire solids removal takes place within the filter bed itself [Vigneshwaran *et al.*, 1996].

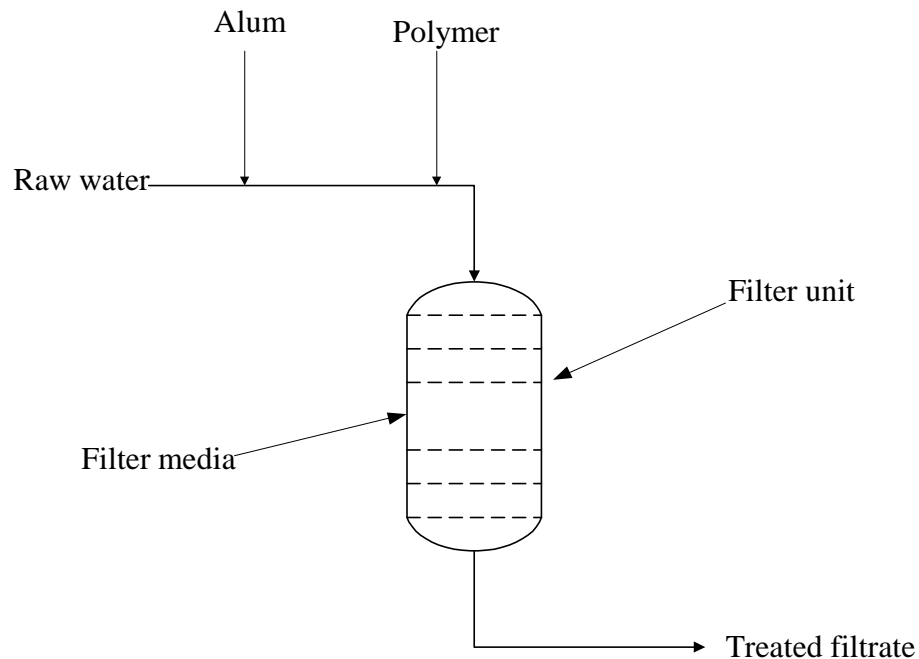


Figure 2.5: Schematic representation of contact flocculation filtration.

2.4.3 Upflow filtration

2.4.3.1 Upflow filtration with non-floating media

Upflow filtration with non-floating media has been used to remove precipitates as well as toxic metals from wastewater [Higgins, 1981; Hultman *et al.*, 1994; Peladan *et al.*, 1996]. It is claimed that upflow filtration has a definite advantage over gravity sand filtration in terms of using the entire media for suspended matter removal.

Hamann and McKinney (1967) reported that most of the early upflow filters had a common shortcoming. These upflow filters were designed to be washed by reversing the flow; the water pass downward through the filter media. This method of cleaning the filter is ineffective as it does not provide scrubbing or agitation of the media. As no expansion of the media is occurred during washing, suspended matter that had penetrated deep into the media was not completely removed. It was also found that the greater the media expansion the better the washing efficiency. A schematic diagram of this type of filter is shown in Figure 2.6.

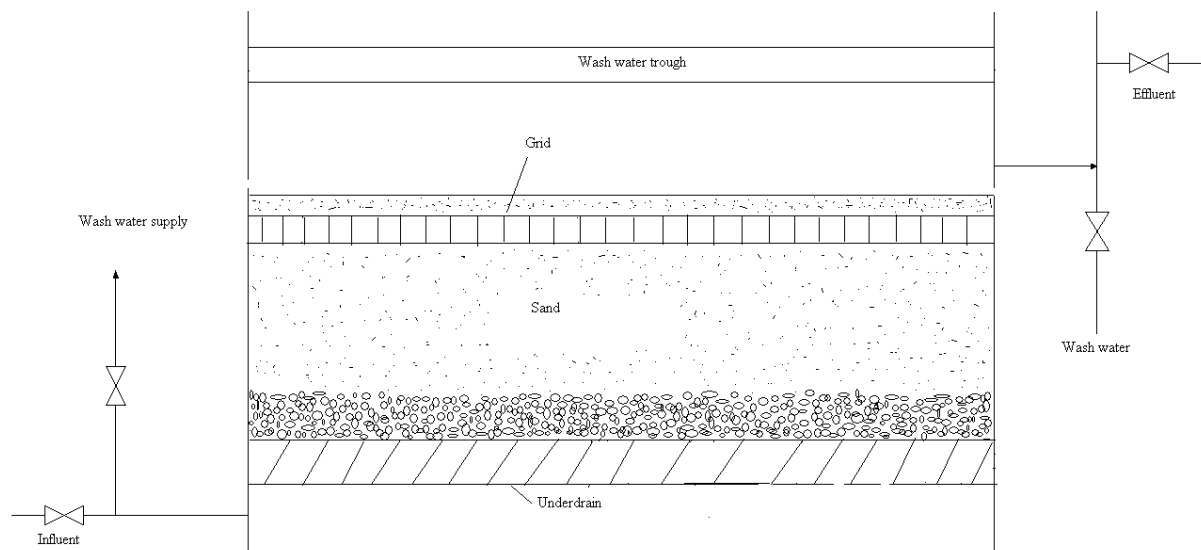


Figure 2.6: Upflow grid filter (after Hamann and McKinney, 1967).

Various combination of sand, coal, glass beads, palette paraffin were used as media for upflow filtration [Daniel and Garton., 1969]. The headloss development in upflow filtration using sand media was studied by Odira (1985). The result showed a linear variation of headloss with time. For high filter rates (above 10 m/h) the headloss development was very rapid which resulted in very short filter runs.

2.4.3.2 Upflow filtration with floating granular media

The shortcomings of an upflow filtration unit have been overcome by using a FMF. Backwashing of a FMF can be achieved with low water consumption. A FMF is considered to have higher retention capacity and lower headloss when compared to conventional sand filters [Jaccarino, 1991; Ngo and Vigneswaran, 1995; Zouboulis *et al.*, 2002].

It has been recommended that a FMF can be installed as a contact-flocculator and a pre-filter instead of using conventional processes for flocculation and sedimentation. The basic concept of a FMF involves the flow of suspension with flocculant through a packed bed of floating material to remove the flocs in the suspension. The flocculation process takes place during the contact of raw water and flocculant within the interstices of the medium, followed by the separation of particles and flocs by the filter medium [Ngo and Vigneswaran, 1995].

Tanaka *et al.* (1995) tested the performance of a FMF for the primary treatment of municipal sewage during dry weather and the high-rate treatment of combined sewer overflow during stormy weather. The medium that was used was a ring-shaped polypropylene net (diameter 2.2 cm, height 2.5 cm and mesh size 6 mm). The removal rates of pollutants were 80 to 90% of suspended solids and 44% of biological oxygen demand (BOD₅) under the following operating conditions 1000 m/day flow velocity, and 2 to 3 mg/L of cationic polyelectrolyte concentration. Figure 2.7 shows a diagram of an upflow filtration with floating media filter

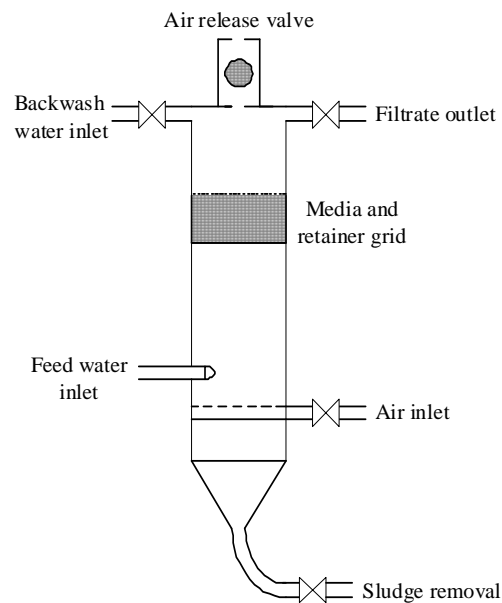


Figure 2.7: Upflow filtration with floating media filter

2.4.3.3 The Haberer process

Haberer and Schmidt were two German researchers who developed an upflow granular filtration system in which contact flocculation can also be utilised using powder activated carbon (PAC).

The Haberer process is an upflow filter design in which backwashing of the filter is done in a downward direction instead of an upward direction. Down-washing has advantages over conventional backwashing. Down-washing allows downward movement, with the force of gravity, of the dense floc formed in the upflow filter and therefore the solids are then rapidly removed from the filter bed. Backwashing, on the other hand, in a conventional filtration system has to remove solids from the filter bed against gravity and, as a result of this; a considerable amount of time and volume of water is required to clean the filter. Foamed

polystyrene beads (1 to 2 mm size and specific gravity of less than 0.1 g/cm^3) were used as filter media. The filter bed height was 1 to 1.5 m and no coagulant aids were used. The backwashing velocity was between 70 and 110 m/h, which is the same as that used by Stukenburg and Hesby (1991). Their results showed that the filter can be washed in approximately 2 min, whereas with conventional backwashing washing may take up to 8 min. They also concluded that resin beads made of foamed polystyrene are better suited for an upflow filter than either polyethylene or polypropylene because of its lower density and considerably greater buoyancy in water. An additional advantage is that polystyrene is inert and poses no health hazard. A schematic diagram of the process is shown in Figure 2.7.

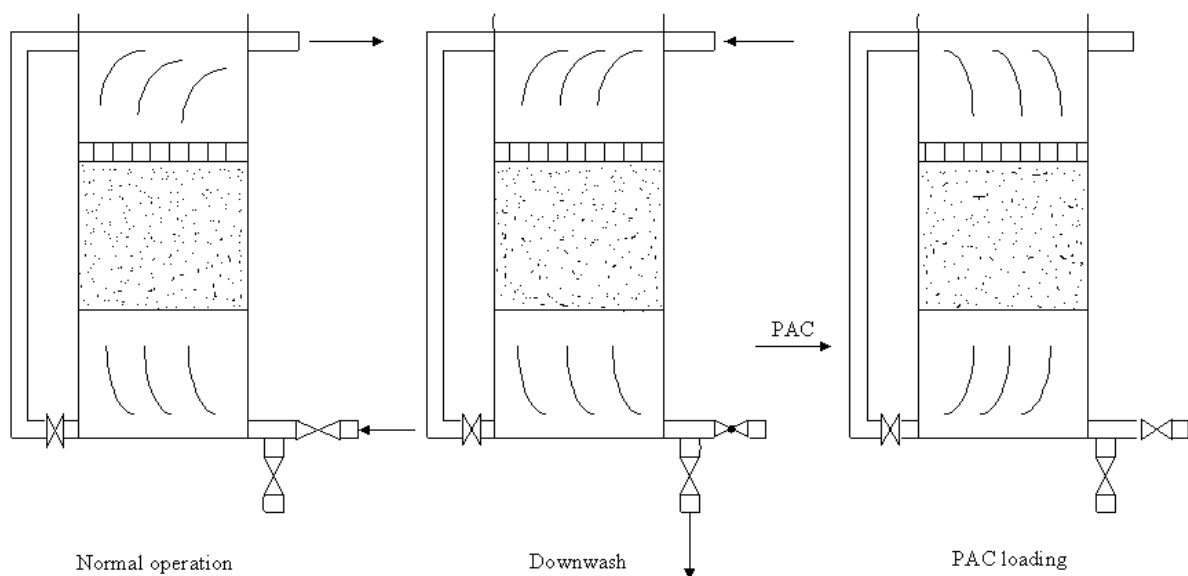


Figure 2.7: Schematic representation of the Haber process [after Stukenburg and Hesby, 1991].

2.4.4 Horizontal filter using floating media

Tanumiharja (1981) experimented with a bench-scale horizontal filter using a plastic filter medium (diameter 25 mm, specific gravity 0.26). The use of different flow rates and different raw water turbidity levels were investigated.

The experiments showed that the coarse plastic media have suspended solids removal efficiencies in the range of 30 to 60%. The flow rates utilised in the experiments were in the range of 0.5 to $1.5 \text{ m}^3/(\text{m}^2 \cdot \text{h})$, while the feed turbidity levels were in the range of 50 to 150

NTU. The main advantage of horizontal flow filtration is that when the water flows through it, a combination of filtration and gravity settling takes place, which considerably reduces the concentration of suspended solids.

2.5 Headloss development

Headloss in a filter bed is an important indicator of the filter bed condition, and can be used as an indicator to start filter washing. Headloss through the filter media is usually monitored by different pressure-cell devices that measure the water pressure above and below the filter media.

When terminal headloss is reached the filter should be washed, otherwise turbidity breakthrough may occur. One of the most practical headloss monitoring methods is to measure the headloss at points within the filter bed by installing several pressure taps at different depths of the filter bed. These pressure taps can be connected to transparent tubes, creating a piezometer board [Monk and Gagnon, 1985].

For a clean bed, the pressure drop across the filter bed is given by the Carmen-Kozeny equation [Carmen, 1937]. This equation was derived assuming that flow is laminar, filter media are uniform spheres, and the pressure drop results entirely from the form-drag loss as fluid moves around the media. The Carmen-Kozeny equation can be expressed as a change in headloss over a length of filter bed.

$$\frac{\Delta H}{L} = K \frac{\mu}{\rho} \frac{V_0}{g} \frac{(1-\varepsilon)^2}{\varepsilon^2} \left(\frac{A_c}{V_c} \right)^2 \quad (2.2)$$

Where K is an empirical constant with a value of about 5 for flow in the laminar region, ρ is the density of the fluid, ε is the variable voidage of the filter bed, g is acceleration due to gravity, ΔH is the headloss over a depth of filter bed, and A_c , V_c are the surface area and volume of the filter grain respectively. This equation predicts that the headloss should increase as a function of decreasing grain diameter, increasing superficial velocity, increasing viscosity and decreasing density of the influent.

2.5.1 Headloss development in direct filtration

It has been found the headloss increases with alum dosage. Headloss development is also affected by the media size [Hutchison and Foley, 1974]. In a study carried out by An-shu (1982) to compare direct filtration and contact flocculation-filtration it was found that direct filtration showed less headloss development per unit time than contact flocculation-filtration.

2.5.2 Headloss development in contact flocculation-filtration

Adin and Rebhun (1974) found that the headloss developed much faster with polyelectrolyte than with alum. Visvanathan *et al.* (1996) studied the headloss variation along a dual media filter and concluded that, for most of the (dual media) filter runs, the headloss development within the coarse media layer (polypropylene) was linear, while the fine media layer showed exponential headloss development.

Shea *et al.* (1971) studied contact flocculation-filtration with sand filters and found a non-linear relationship between the initial headloss and the rate of filtration. The initial headloss was 2.3 cm for a flow rate of 7.3 m/h and 14 cm for a flow rate of 22 m/h.

Narin (1994) carried out a study using dual floating media (polypropylene as coarse medium and polystyrene as fine medium), and sand (for the purpose of comparison). He found that the headloss of the dual media is less than that of the sand medium. During the floating media filter experiments, the headloss development was distributed throughout the media bed, while in sand filter experiments in upflow mode, the headloss development was mainly at the bottom layer of the filter bed. That is mainly due to the fact that sand has a lower porosity compared to the synthetic media.

Pilot scale experiments were carried out in contact flocculation-filtration using a floating media filter. Four types of filter media combinations were investigated. Some of these combinations were mixed with sand and synthetic media. Headloss development was found to be very high in the conventional rapid sand filter, whereas the headloss development was very low in the floating media filter, and the combined coarse sand and fine sand media filter. One reason for this is the larger size of the floating media [Sundarakumar, 1996].

2.5.3 Headloss development in upflow filtration

Tanaka *et al.* (1994) developed a new filtration process in which headloss and energy consumption are lower than in dual media high-rate filtration. In this particular study, bench-scale and pilot-scale upflow filter experiments were carried out in order to investigate pollutant removal rates and headloss of floating media filtration under different operating conditions. Results of the pilot plant experiment showed that the headloss of the floating media was less than 0.2 m with a filter depth of 2 m and a flow velocity of 1000 m/day. This headloss value is much lower than that of dual media high-rate filtration, as determined by Innerfeld *et al.* (1979).

Ødegaard and Helness (1999) carried out experiments on a high-rate secondary-treatment plant that incorporated a moving-bed biofilm and an upflow floating filter. They found that the headloss increased with filter run time as a result of the sludge accumulation. Figure 2.8 shows the relationship between the headloss and filter run time at different filtration velocities, and different media depths. There was also a clear relationship between the headloss development rate and sludge accumulation rate. This relationship is given in Figure 2.9.

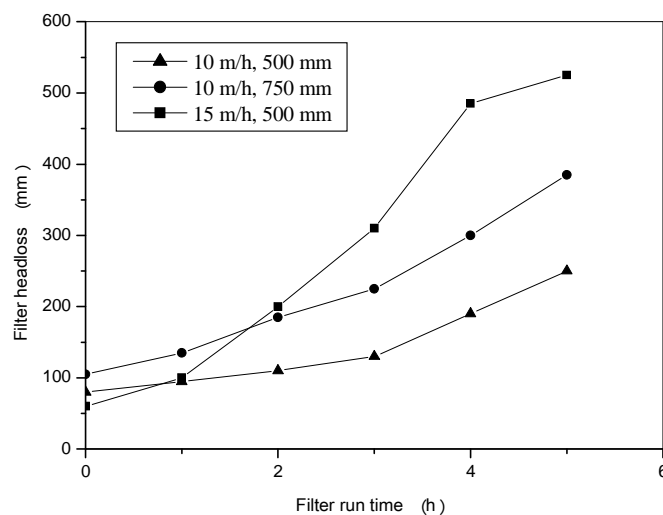


Figure 2.8: Filter headloss versus filter run time [after Ødegaard and Helness, 1999].

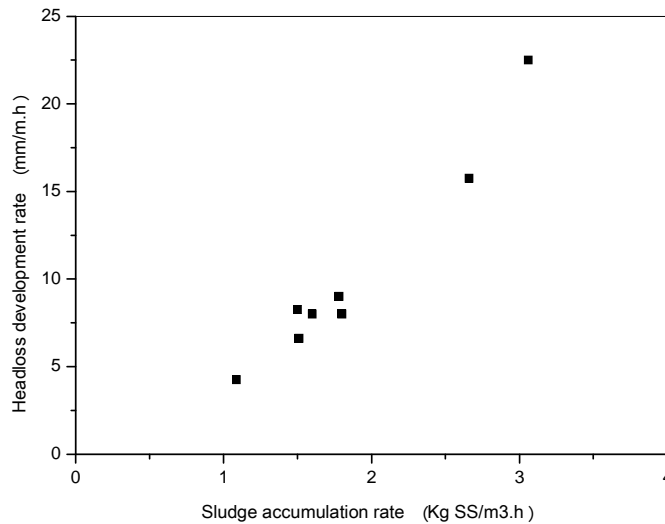


Figure 2.9: Headloss development rate versus sludge accumulation rate [after Ødegaard and Helness, 1999].

Hamann and McKinney (1968) carried out some experiments with sand filters and reported that the headloss in the upflow filter was lower than in the downflow filter. A study of headloss development patterns in upflow filtration using sand as medium and alum as coagulant showed a linear variation in headloss with time. The headloss development was very rapid for filter rates above 10 m/h.

2.5.4 Headloss development in a reverse-graded dual media filter

Reverse-graded dual media filter has been developed using two different media sizes: coarse medium on the feed side of the filter and a fine medium on the filtrate side of the filter. This allows for greater particulate distribution through the filter bed, with much of the suspended solids being removed by the coarse media. Filtration through the reverse-graded media allows a filter run up to five times longer than in the case of a conventional filter, and the headloss is much lower than in the case of a conventional filter [Weber, 1972].

2.6 Filter backwashing

Suspended particles in the raw water accumulate within the media during the filtration process. As water passes through the filter bed, more and more suspended particles will be sequestered. The filter becomes clogged as a direct result and can then no longer produce the desired quality of water. As a result of suspended solids accumulation two detrimental

situations can arise: the headloss within the filter can reach excessively high levels, or suspended solids already trapped within the filter bed will be pushed through the filter, resulting in product water turbidities that reach undesirable levels (greater than 1.0 NTU). Therefore, washing is required to clean the bed and extend the lifetime of a given filter. This filter-cleaning operation is carried out by means of a filter backwash method [Visvanathan *et al.*, 1989; Dodd and Fettig., 1998].

Backwashing is the process during which water is forced through a filter in the reverse flow direction in order to release the dirt and flocs immobilized within the media bed. There are various methods of backwashing, the most common of which is the use of a combination of air and water.

During backwashing, clean water is energetically pumped downward (in a reverse direction to the filtration direction). This action causes the bed to expand slightly, releasing the captured particulate matter and washing it out of the bed. As the bed expands the bed particles have less interference with each other and therefore settle faster. Proper backwashing requires sufficient filter bed expansion. Sufficient expansion means that the entire filter media is fluidized and all individual particles are suspended. For the purpose of cleaning the filter properly the filter bed needs to be agitated violently to eliminate sticky floc. On the other hand, insufficient filter bed expansion leads to poor filter cleaning, and might cause serious problems. The recommended bed volume expansion is 30 to 50%, however a 15 to 20% expansion volume is practical [Visvanathan *et al.*, 1989; Schwarzkopf, 2006].

Backwashing with water alone is considered a weak cleaning process due to limited particle collision. Therefore air scouring is recommended in order to enhance the water backwash, either used alone prior to the fluidizing water wash or in combination with a low rate water wash [Amirtharajah, 1978; Fitzpatrick, 1998].

The use of compressed air was found to be essential during backwashing of a filter to clean the bottom layers of sand and gravel [Hamann and McKinney, 1968]. Air scouring provides an effective cleaning action, especially if used simultaneously with a water wash. Use of air scouring can significantly reduce the volume of water required to backwash filters.

Based on some studies, it was found that a typical method to backwash granular media filters includes air scouring, water scouring and surface washing.

According to Hamann and McKinney (1968) all the early upflow dense-media granular filters were designed to be washed by reversing the flow (passing the water downward through the filter bed). This method of cleaning the filter is however inefficient, resulting in no scrubbing or agitation of the media. The net effect is that particulates that had penetrated deep into the media were not entirely removed.

Sundarakumar (1996) carried out experiments on a sand and floating media filter and studied the effect of the backwashing system using two types of backwashing water alone and air followed by water. In his sand filter the clean water was sent upward for 14 min at the rate of 12 m³/h. As a result of this backwashing process some mud balls were precipitated at the surface of the bed after backwashing. When using air followed by water, air was first sent upward for 4 min at the rate of 4 m³/h, and then the clean water was sent upward for 14 min at the rate of 12 m³/h. The amount of mud balls on the top of the sand bed was less than in the first case. The expansion of the sand bed was about 30% in both cases. The volume of water required for air followed by water backwashing was less than that of backwashing with water only.

Sundarakumar (1996) studied filter performance using upflow floating media. In the first case backwashing involved water only, whereas air, followed by water was used in the second study. In the first case, water was sent in the down-flow direction for 14 min at a rate of 8 m³/h. In the second study air was initially sent at the rate of 4 m³/h for 4 min, followed by down-flow water at different flow rates (6, 8, 10 and 12 m³/h) for 10 minutes. The required volume of water for backwashing with air followed by water was less than that of backwashing with water only, since most of the entrapped suspended solids were detached from the media during air backwashing. The media expansion was 50 % in the case of using water alone and in the 60 to 90% range in the case of using air followed by water.

2.7 Effect of physical parameters on filtration performance

2.7.1 Filtration rate

Hamann and McKinney (1968) found that in upflow granular filters the effluent turbidity increases as the flow rate increases. Visvanathan *et al.* (1996) found that a dual-floating media of polypropylene (PP) and polystyrene (PS) beads afforded a good quality filtrate and high water production rates when using filtration rates of 10 and 12.5 m/h. They also found that

both sand and floating media filters performed well at filtration rates lower than 7.5 m/h. When using a rate of 5 m/h a much better effluent quality was achieved. This filtration rate is similar to the filtration rate of a conventional rapid sand filter.

Chiemchaisri *et al.* (2003) developed a floating plastic media filtration system for water treatment and wastewater reuse. They found that for its use in water treatment a filtration rate of 5 m/h was suitable. Application of floating plastic medium and a coarse sand filter as a direct filtration system required an optimum filtration rate of 5 m/h, with an appropriate media depth of 60:20 cm of plastic medium: coarse sand. For contact flocculation-filtration it was found that a filtration rate of 1 m/h and media depth of 50:30 cm of polypropylene bead: zeolite bed gave the best results.

Sundarakumar (1996) studied several media combinations and found that the optimum filtration rate was 5 m/h. The filtration rate of 7.5 m/h gave fairly good results in terms of filter run time, water production and headloss development. At low filtration rates the amount of suspended solids captured within the media is lower than at the high filtration rates. Therefore the headloss development is very slow. Figure 2.10 shows the relationship between the headloss and filter run time at different filtration rates of one of the media combinations that were used.

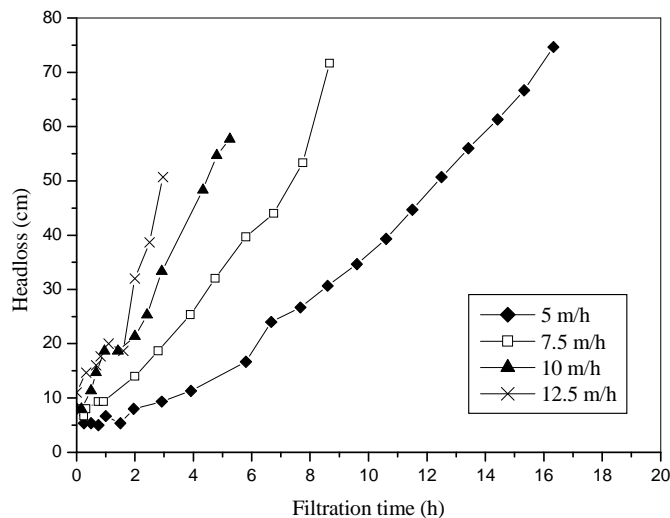


Figure 2.10: Headloss vs. filtration time at different filtration velocities (polypropylene & polystyrene media, downflow filtration) [after Sundarakumar, 1996].

2.7.2 Filter media

The filter medium removes the particles from the water and is therefore a very important part of the filter. Selection of a suitable medium is therefore very important to the operation and performance of the filter. Suitable media selection and filtration rates will improve solids capture in granular medium filters [Deshpande *et al.*, 2004].

A filter medium is, by nature, non-homogeneous; pores are non-uniform in size, irregular in geometry, and unevenly distributed across the surface and in the bulk of the medium. Selection of the medium is dependent on the particular filtration technique and intended application. Different filter media are used. Sand is the most common medium, but other media such as crushed anthracite (hard coals), diatomite, and inert synthetic media are also used.

In the case of FMFs, various types of synthetic media such as cylindrically shaped plastic media, PS foam, cylindrically shaped plastic net media, and cluster particles made from textile fibers have been used. The filter medium is generally 1 to 15 mm (mean diameter) in size [Ødegaard and Helness, 1999].

The successful performance of filters is affected by the physical characteristics of their media, such as specific surface area, porosity, size, shape, and specific gravity [Bellelo, 2006]

Deshpande *et al.* (2004) carried out a study in which different commercially available media were investigated. Media that were smaller and spherically shaped were found to capture higher percentages of fine particulates.

Werellagama (1993) carried out experiments to determine the performance of the filter with respect to the size and shape thereof, as well as different media combinations. He found that the smaller size coarse media gave better results (in terms of effluent turbidity) than the larger size media. The headloss development was found to be less in the fine media. Regarding the media shape, the angular fine media performed comparably with the spherical fine media but the headloss development was more rapid in the case of the angular media. The results of this particular study indicated that spherical PS performs better than angular PS (under the conditions used in this study).

It has been proved that bed behaviour is also affected by density and voidage of the media, especially during the backwashing process. During backwashing, media properties affect flow rates required for water wash and combined air and water wash. Some media characteristics such as grain size distribution and porosity, might be changed during the life of a filter and therefore affect its performance [Fitzpatrick, 1998].

Iwai and Kitao (1994) reported that granular media capture suspended solids more effectively and in greater amounts than other shaped media. The mechanism of solids capture in a FMF is mostly physical in nature and is common to all types of granular medium filters [Ahmed, 1996]. Different shapes of plastic media used for capturing solids are shown in Figure 2.11.

Ahmed (1996) indicated that suspended solids removal increases with a decrease in size of individual media. The key to selecting a proper media depends on the treatment technology. For example, the first and the fourth media (from top to bottom) shown in Figure 2.11 is recommended for evaluation of carbonaceous biological demand (CBOD₅) and total suspended solids removal.



Figure 2.11: Shapes of plastic media that have been used in floating media filter to date [Wagener, 2000].

2.7.3 Chemical dosage

Different coagulant chemicals (both organic and inorganic) have been used in water treatment plants. When added to water in an optimum dosage they lead to particle destabilization. The most commonly used materials are alum, ferric salts, lime, and cationic organic polymers.

Floc formed by adding alum are light and fragile, and are therefore too weak to endure high shear forces and quite difficult to settle, unlike flocs formed by ferric salts that are better settling flocs, hence may be more effective in removing natural organic matter (NOM). On the other hand, polyaluminum chloride often produces a better-settling floc in colder waters, and very often low dosages are required, thereby producing less sludge than when alum and ferric salts coagulants are used [Adin and Rebhun, 1974; Delphos and Wesner, 2005].

A study was carried out using a floating medium and coarse sand filter to treat surface water using four different types of coagulants, namely alum, ferric chloride, polyaluminum chloride and a cationic polymer. Ferric chloride gave slightly better results performance in terms of colour removal, whereas alum and polyaluminum chloride gave lower turbidity and suspended solids removal [Chiemchaisri *et al.*, 2003].

It is claimed that the crosslinked polyelectrolytes produce a very strong floc and that overdosing with these polyelectrolytes is difficult. Laboratory experiments carried out by Gray *et al.* (1998) have shown that increasing the flocculant dose leads to increased performance, by increasing the shear resistance of the floc, and thereby decreasing floc break-up in the filter.

The characteristics of the floc are affected by the polyelectrolyte type. It has been found that linear polyelectrolytes with low charge density and high molecular mass, produce floc of higher shear resistance, and afford lower total suspended solids in the filter effluent, than do the high charge density, high molecular mass, crosslinked polyelectrolytes [Gray *et al.*,]

Benedek and Bancsi (1977) report that the polyelectrolyte giving the best results in terms of floc formation and settling velocity was an anionic polyacrylamide with a molecular mass greater than 8.0×10^6 .

3 Development of a pilot floating media filter

3.1 Scope of this chapter

The chapter includes a literature review of the latest progress made in pilot plant development of a FMF using low density particles as medium. This information was accommodated in the filter designed and constructed for this work.

3.2 Background

It has been shown that conventional granular filtration does have some disadvantages, such as a limited retention capacity, a high backwash water requirement and unsuitability of operation during periods of high turbidity [Ngo and Visuanathan, 1995]. Over the past few years there has been much focus to develop improved filtration processes. Several process modifications such as upflow filtration, biflow filtration and mobile bed filtration have been evaluated for their ability to enhance the filtration performance [Ben Aim *et al.*, 1996].

Upflow filtration has a definite advantage over gravity sand filtration because the entire bed is used for the removal of suspended matter. The capacity for storage of solids is such that conventional flocculation, sedimentation and filtration can, in some cases, be replaced by upflow filtration [Hamann and McKinney, 1968]. Upflow filtration can be operated as a primary filter in order to remove suspended solids, and turbidity [Darby *et al.* 1994].

The use of an upflow floating media filter could be an alternative method to overcome the shortcomings of a conventional granular filter. In the upflow filtration, the process liquid is pumped into the bottom of the filter chamber and it flows vertically upwards through the bed [Ngo and Visuanathan, 1995]. An upflow filtration unit, however, also has some shortcomings, which can be overcome by using floating filter-media. An additional benefit of a FMF is that the backwashing of the filter can be achieved with a minimum volume of water and at a much lower backwash velocity than that used in a conventional granular filter [Jccarino, 1991; Ngo and Visuanathan, 1996].

The use of synthetic floating media is an innovative technology that can be successfully used for surface water treatment. Several laboratory-scale studies have shown that a higher turbidity removal per unit headloss can be achieved by using a FMF compared to sand filters. The use of a synthetic floating media could contribute to the cheaper design and operation of filters because of the lighter mass and more reasonable cost of media compared to that used in a conventional filter [Visvanathan *et al.*, 1996].

3.3 Literature review of recent research on upflow filtration using floating media

The latest progress in this field, as described by eight other researchers, is summarized in the ensuing.

Ngo and Vigneswaran [1995] experimented with a FMF in water and wastewater treatment in a contact flocculation-filtration arrangement. In their study, raw water from a water treatment plant intake point and effluent from a secondary treatment unit of a wastewater treatment plant were used as the feed water for the FMF. Polypropylene beads (diameter 3.8 mm, density 0.87 g/cm³) were used as filter medium. A filter media depth of 200 and 400 mm and a filtration rate of 5 and 9.9 m/h were used in the water treatment study, while filtration rates of 2.5 and 5.4 m/h were used in the wastewater treatment study. Alum was used as flocculant. The optimum dose was 40 to 50 mg/L.

After each experiment the filter media was washed using compressed air at a pressure of 35 to 70 kPa for 1 to 2 min, followed by backwashing with water at a rate of 6 L/m²s for 2 to 5 min. These were, however, not the optimum backwash conditions. Filter performance was determined in terms of buildup of headloss as well as the removal of suspended solids, turbidity, and colour. It was noted that removal efficiencies improved slightly with filtration time. A use of a filter media depth of 400 mm and filtration rate of 5 m/h resulted in a reduction in turbidity of 80% in the water treatment experiment. Similarly, use of a filtration rate of 2.5 m/h resulted in a good reduction in turbidity of up to 90%.

You and Kim [2001] utilised an upflow FMF. Their pilot scale setup comprised a 3 m x 1 m x 6 m high steel tank divided into two equal independent operating cells in which the media depth was 2 m. The space on the top of each tank was for filtrate storage. There was therefore

no need for a backwash pump or a separate clean water reservoir. The stored filtrate provided enough head to backwash the media bed. In this unit a strainer plate was installed at the bottom of the storage tank to separate the treated water and the packed media in the filter. A volume of 3 m³ of expanded floating PP beads (size 3 to 5 mm, density 80 kg/m³) was packed in the filter below the strainer plate (70 strainers per filter, 0.8 mm openings). Space for backwashing was provided below the packed bed because the bed expands during the backwash operation. Air was introduced at the bottom of the filter. An aeration grid with (120 x 1.5 mm) sparge holes was provided in both tanks (filters). From the wastewater (feed) tank, above the effluent storage tank, influent was introduced separately into the bottom of the filters by gravity flow. Each filter contained a wastewater distribution grid of (60 x 10 mm) holes. Wastewater flowed through the packed bed before being filtered. The wastewater then passed the strainer and was discharged by overflow of the effluent storage tank. Figure 3.1 shows a schematic diagram of the plant configuration that You and Kim [2001] used in their study.

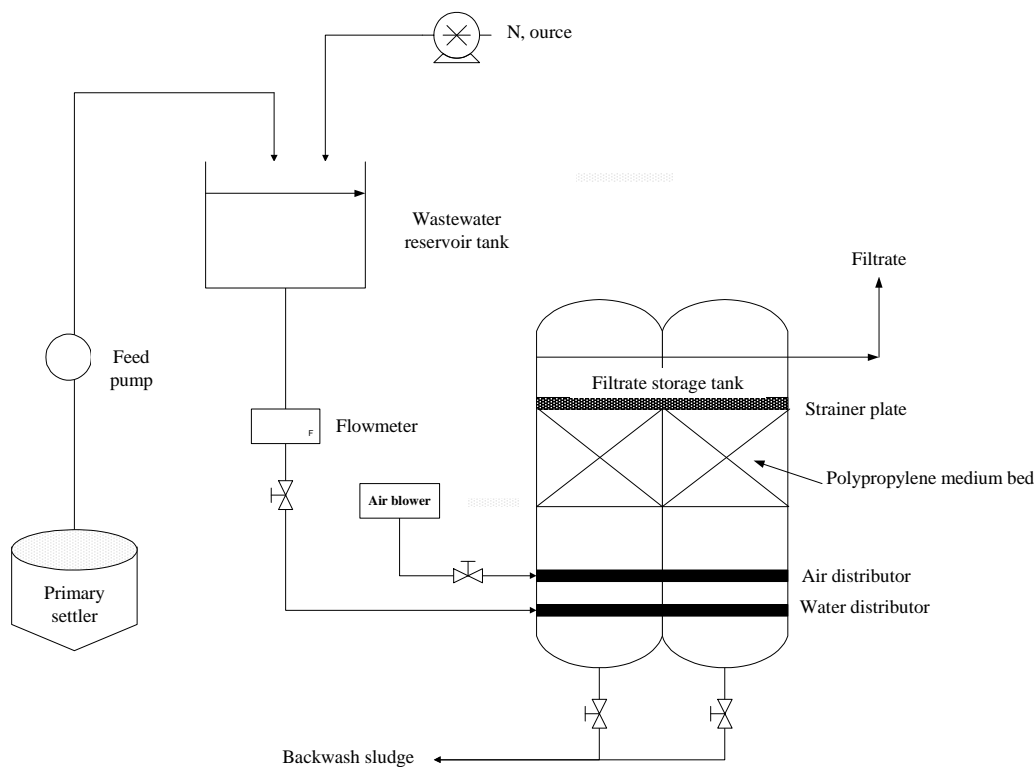


Figure 3.1: Schematic diagram of an upflow system filtration system in which floating media are used [after You and Kim, 2001].

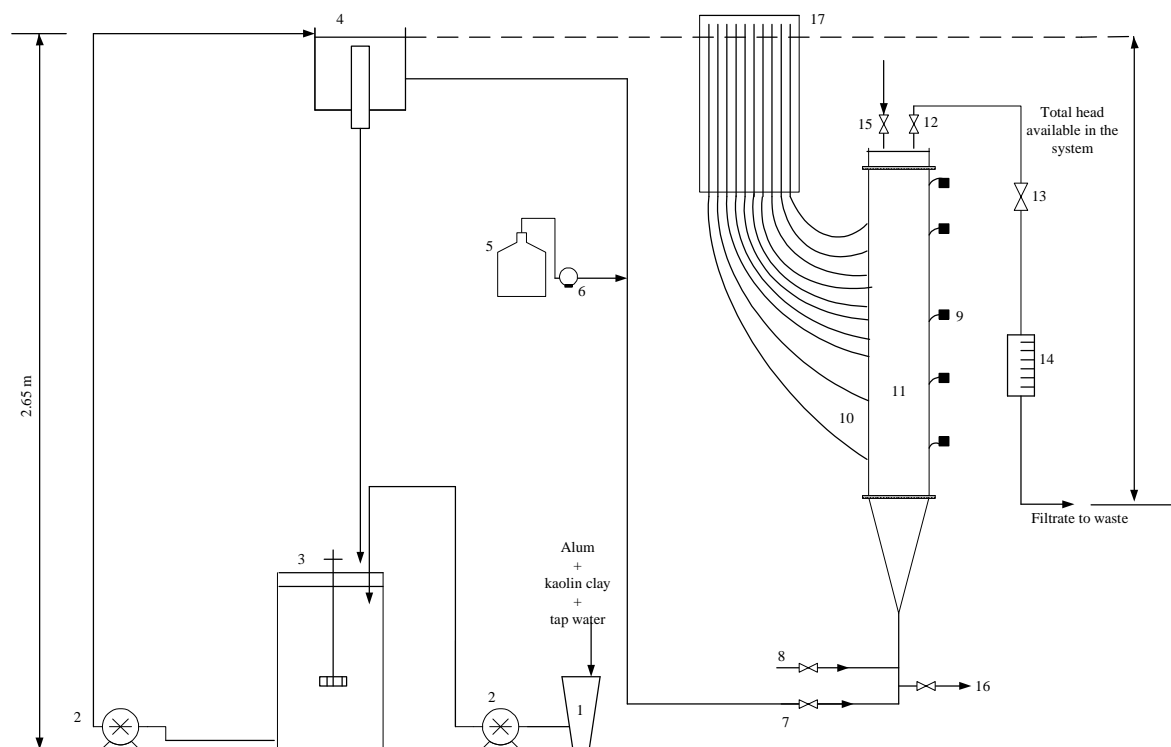
In the same study, the floating media unit was backwashed every 24 h using the treated wastewater and air. Upon opening and regulating the drain valve, the stored filtrate flowed downward to expand the media bed. During backwashing with water, and as the packed media bed was expanded and loosened, the sludge was removed. Backwashing with air was used to fluidize and mix the expanded media to be washed effectively. The air has two functions: (1) air moves upwards through the bed causing the media to rub against each other, whereby the dirt is removed from the particles, and (2) the air accumulates at the top of the column, increasing in volume and thereby forcing the water downward. Then backwashing takes place. The experiments were carried out over a five month period, for paper wastewater treatment. An average removal efficiency of 88% for suspended solids and 78% for chemical oxygen demand were maintained.

Visvanathan *et al.* [1996] described an upflow filter in which the main components were the raw water feeder system, a chemical dosing system, filter column, filter media and backwash air/water feeder system. The raw water, which contained an artificial suspension of kaolin clay, was prepared in a 50 L tank. Once the required water quality was ensured, the raw water was pumped from this tank to the raw water tank using a small centrifugal pump. The raw water was stored in a 290 L tank, which allowed a 5 h filter run without refilling. During the filter runs that were longer than 5 h the raw water tank was refilled periodically from the solution preparation tank. The raw water tank had a stirrer, which continuously stirred the suspension to prevent the suspended solids from precipitating. The raw water was fed by a centrifugal pump to the constant head tank, where the level was kept constant by an overflow arrangement. The excess water was again recycled from the overhead tank to the raw water tank. A dose of 20 mg/L alum [$\text{Al}_2(\text{SO}_4)_3 \cdot \text{H}_2\text{O}$] was added to the 50 L solution preparation tank. The required dosage of the coagulant (polyelectrolyte) was introduced continuously near the inlet of the filter. The use of a polyelectrolyte was recommended. The polyelectrolytes offer the characteristic of a small floc volume [Adin and Rebhun, 1974; Hutchison, 1975; Quaye, 1991].

The filter was a 1-m-high acrylic column with a 64 mm internal diameter. Media used in this study were granular polypropylene and polystyrene, both of which have densities lower than that of water. The filter contained eight piezometer taps in the top 600 mm, with four piezometer holes for each media layer. There were five sampling ports in the column: only one point (near the media interface) was used to measure the water quality. The filter was

fixed vertically with raw turbid water entering from the bottom. The filter bed was a 0.6 m deep. A retaining mesh was placed on the top and bottom of the filter to prevent the loss of media during operation. The flow rate was controlled by a pinchcock clamp, which was frequently adjusted to maintain the required filtration rates of 15, 12.5, 10, 7.5 and 5 m/h.

For backwashing purposes air was compressed in the upflow direction at 100 m/h for 2 min, followed by a downflow water wash for 3 min at 50 m/h. A 65% expansion of the filter bed was achieved. Valve 8 and valve 12 (Figure 3.2) served as inlet and outlet for the air backwash, while valve 15 and valve 16 served as inlet and outlet for the water backwash. A schematic diagram of the experimental setup that was used in this case is shown in Figure 3.2



1. Solution preparation tank 2. Feed pump 3. Raw water tank with stirrer 4. Constant head tank
 5. Flocculant stock bottle 6. Dosing pump 7. Raw water inlet valve 8. Backwash air inlet 9. Sampling points
 10. Pressure tapping 11. Filter column 12. Filtrate/backwash air outlet 13. Flow rate control valve
 14. Rotameter 15/16. Backwash water inlet/outlet valves 17. Piezometer panel

Figure 3.2: Experimental setup of an upflow filter [after Visvanathan *et al.*, 1996].

The best results in terms of filtrate production per unit area and less headloss were obtained with 2.57 mm polypropylene and 1.54 mm spherical polystyrene when operating at 5m/h, and 3.66 mm polypropylene and 1.54 mm spherical polystyrene when operating at 12.5 m/h. The turbidity removals obtained were about 90%.

Tanaka *et al.* [1994] carried out experiments with the upflow filtration of sewage as feed. Figure 3.3 shows a schematic diagram of the bench scale and pilot scale upflow filter that they used.

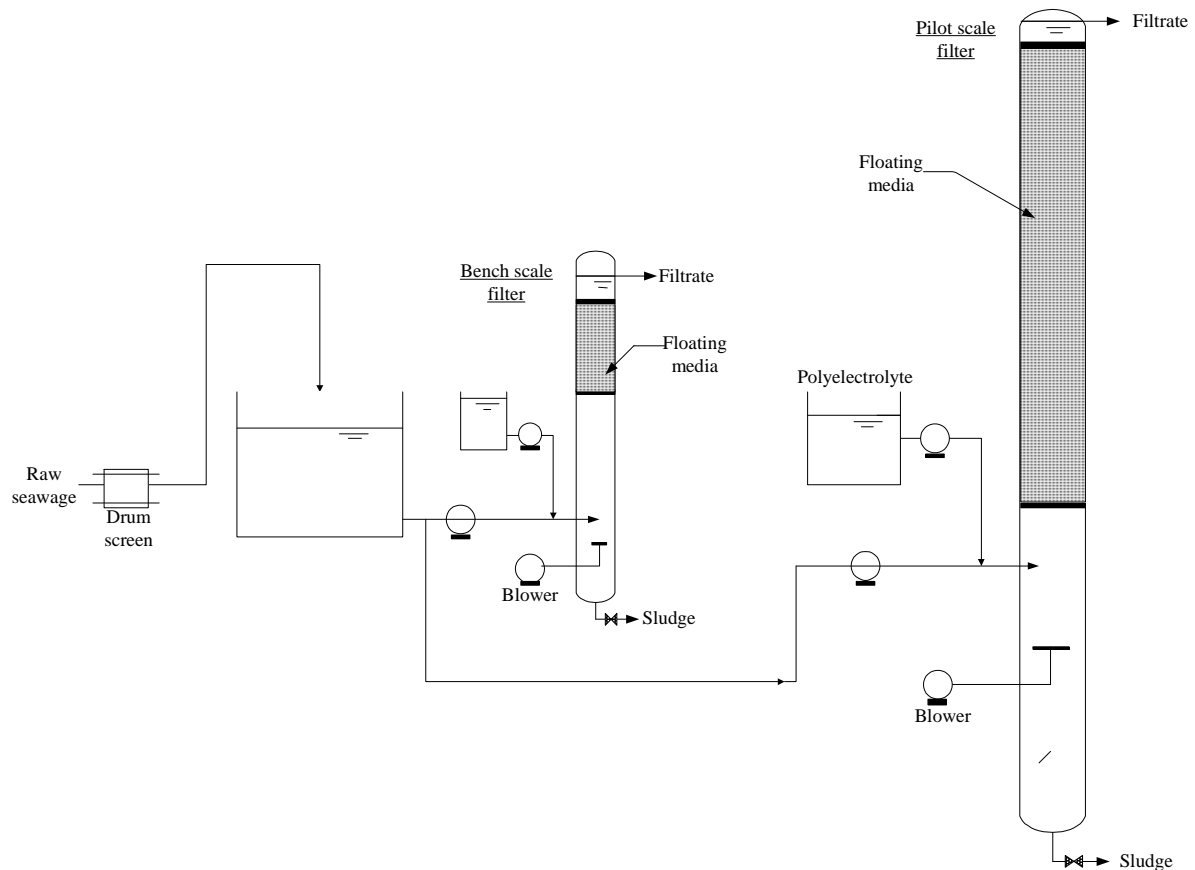


Figure 3.3: Flow diagram of bench-scale and pilot-scale floating media filter [after Tanaka *et al.*, 1994].

Raw sewage was pumped from a grit chamber of a waste water treatment plant and fed to a drum screen with 5 mm openings. After screening, the sewage was stored in a 6 m³ reservoir tank and slowly aerated to prevent suspended solids from settling. The stored sewage was used as feed for each series of bench scale experiments that were carried out to determine the effects of operational conditions, using the same quality of influent. Polyelectrolyte was added to the influent at the outlet point of an influent feeding pump. The polyelectrolyte used was selected by jar tests as the most suitable one among several types of cationic polyelectrolytes.

The bench scale filter was 150 mm in diameter, 500 mm in media depth, and 600 mm in length from the inlet point to the bottom of the media layer. The pilot scale filter was 330 mm in diameter, 2 m in media depth, and 300 mm in length from the inlet point to the bottom of the media layer. The media used for filtration was a ring-shaped polypropylene net (22 mm in diameter, 25 mm in length) with a 6 mm mesh size, which typically has a high voids ratio (90%) and low specific gravity (0.93).

The filter bed was backwashed with air, at a flow rate of 100 to 120 Nm/h, for 1 min, and then the slurry was drained from the bottom of the column with continuous aeration. The filter was again backwashed using tap water and drained after aeration. The media was completely clean after three successive backwashing cycles.

Experiments using bench scale and pilot scale filters showed that the removal rates of the pollutant were 80 to 90% for suspended solids under operating conditions of 1000 m/day flow velocity and 2 to 3 mg/L cationic polyelectrolyte addition. Mass capture reached 7 to 10 kg/m³ with a low headloss (less than 0.2 m), with a media depth of 2 m. A high removal rate of suspended solids and low headloss are the main advantages of the process.

Ødegaard and Helness [1999] carried out numerous experiments on a high-rate secondary sewage treatment plant that incorporated a moving-bed biofilm and floating filter (Figure 3.4). Crude sewage, after straining, was pumped (1) to a constant head tank (2), from where it was introduced into the aerated moving-bed biofilm reactor (3). The effluent from the bioreactor, after passing through a carrier sieve, was pumped (4) to a column (5) where the headloss can be observed as the difference between the water level in the column and that in the filter outlet. Then the sewage was fed to the upward-flow floating filter bed (6). A perforated plate was placed on top of the filter bed (7) to keep the filter media in place, and the treated water was either discharged through a perforated pipe (8) or via an overflow weir at the top of the column (9). The filter column was 380 mm in diameter and 2.4 m in length, and the filter bed depth was either 500 mm or 750 mm. A perforated pipe-grid aerator (10) was used for washing the filter. The slurry (biomass) was then drained from the filter column (11).

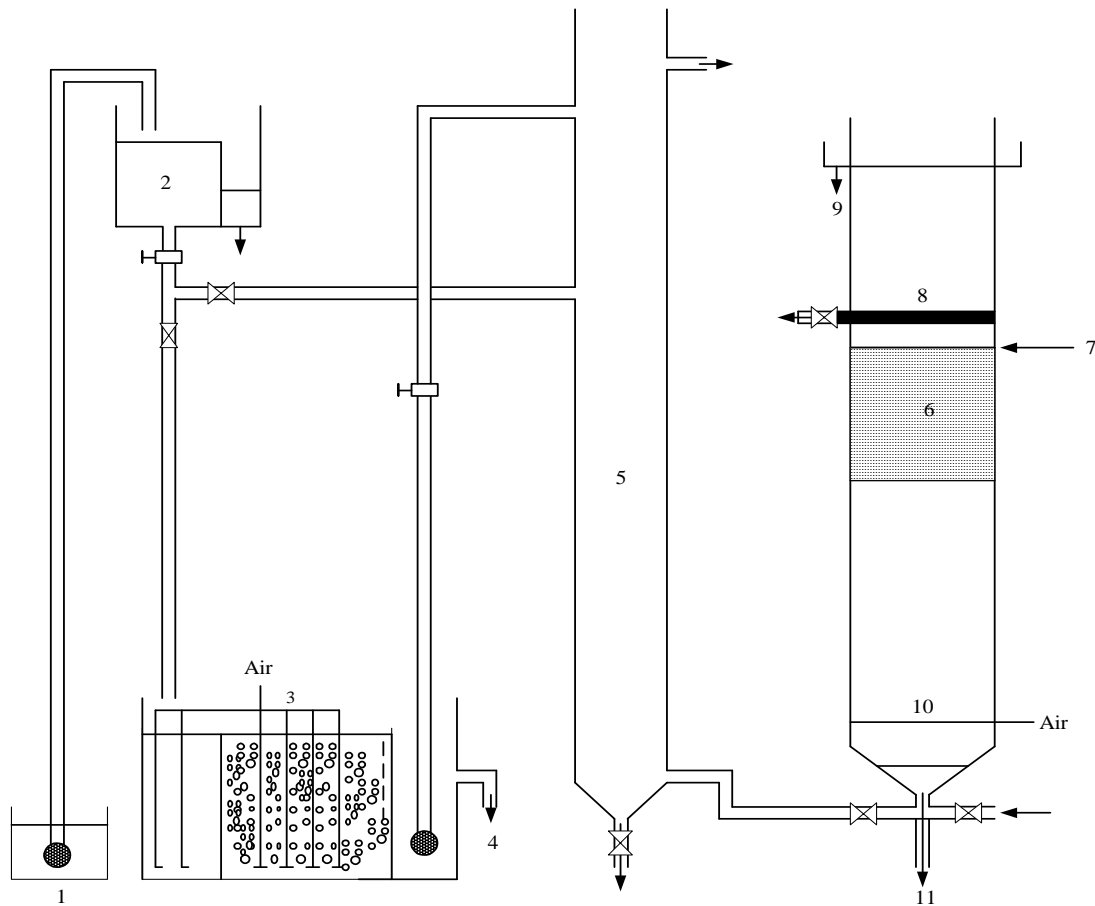


Figure 3.4: Experimental pilot plant [after Ødegaard and Helness, 1999].

A filter run lasted for 5 to 7 h, the duration of which was determined either by when maximum headloss was reached or by an intended stop of the run. Air was blown into the column through the air-distribution pipe (10) after each run. After vigorous mixing by air for 4 min (in order to release the suspended matter from the medium) the entire liquid volume of the filter column was drained out through the valve (11). This process (filter-bed washing by air) was repeated three times. The final two washings were done with clean water.

Ødegaard and Helness [1999] drew the following conclusion from their results: up to 85% suspended solids were removed and the headloss was low. A typical filter bed depth was 1.0 m and a typical design headloss would then be 500 mm through the filter-bed itself. The suspended solids loading ($\text{kg SS/m}^2\cdot\text{h}$) is the key design parameter. At a suspended solids loading of $1 \text{ kg SS/m}^2\cdot\text{h}$, a filter run time of 10 h can be expected in a 1 m deep filter bed, while increasing the suspended solids loading rate to $3 \text{ kg SS/m}^2\cdot\text{h}$ reduces the filter run time to about 5 h.

Fitzpatrick [1998] conducted some experiments to investigate the effect of media properties on upflow filter performance and backwashing. The experiments were carried out using a pilot column of 1.8 m length and 80 mm internal diameter, and bed depth 0.6 m. Different types of media were investigated in order to study their effects on the filter performance and backwashing. A schematic diagram of the experimental setup is shown in Figure 3.5. Backwash air and water entered the column through a single nozzle and passed up through the media. Fitzpatrick [1998] reported that during backwashing the media properties affect the flow rates required for both the water wash and combined air/water wash. Some properties, such as grain size distribution and porosity, could change during the filter life and affect its performance. Unsuitable backwashing can cause many problems, e.g. filter media loss due to attrition, mudball formation, reduced filter run times and poor filter performance.

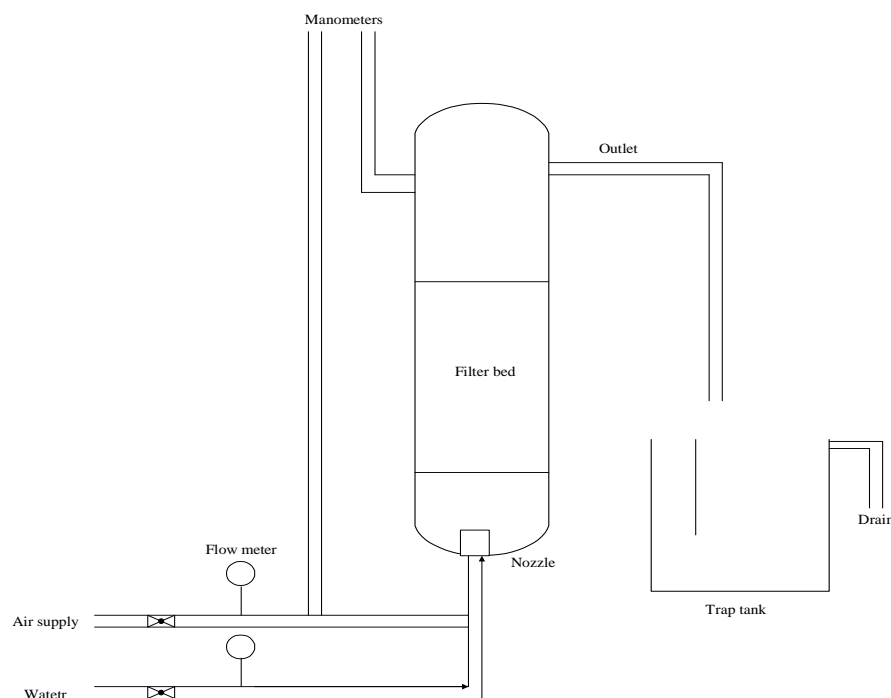


Figure 3.5: Schematic of a backwashing apparatus [after Fitzpatrick, 1998].

Verster [2005] carried out a laboratory scale experiment on FMF. The feed solution that was used was prepared by adding a concentrated bentonite solution to tap water in the feed tank in order to create specific turbid feed water. A stainless steel mixer was used to stir the concentrated solution before introducing it to the feed tank. A centrifugal recycle pump was used to keep the bentonite in suspension and also to serve as a mixer, by adding energy to the feed water. Once the feed water solution was homogeneous the feed water was pumped to the

filter by means of a positive displacement pump with a variable speed drive. The coagulant, which was a highly charged liquid cationic polyelectrolyte, was also added to the feed water before it entered the filter.

The filter column used by Verster [2005] was made of polyethylene, it had a diameter of 430 mm and a total height of 1.5 m. A manometer was connected to the filter column. A flexible helicoidal tube was connected after the discharge side of the feed pump to assist the flocculation process. The clarifier assisted by increasing the volume of the flocs before they entered the filter. Four different particle shapes were used as floating media. A schematic diagram of the FMF pilot plant that was used here is shown in Figure 3.6

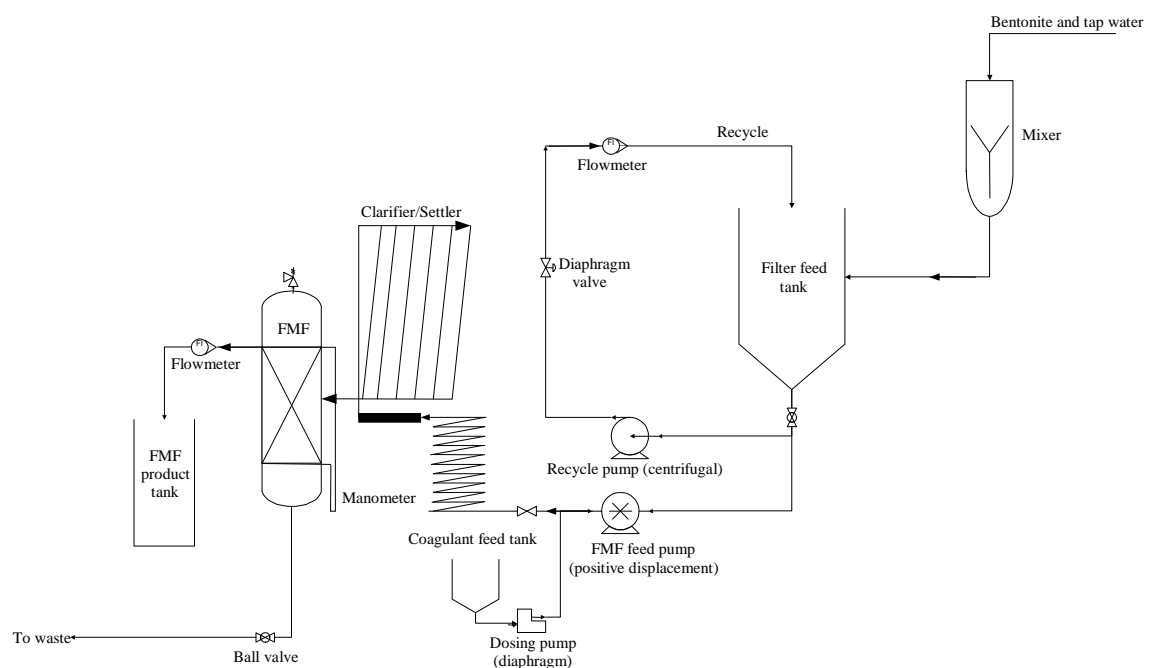


Figure 3.6: Schematic diagram of floating media filter [after Verster, 2005].

Verster (2005) studied the effects of several factors that may have significant effects on the performance of the floating media filter: (1) floating media geometry, (2) velocity through the filter, (3) concentration of suspended solids in the feed water, and (4) bed depth of the floating media. He recorded that all of these four factors have significant effects on the performance of the FMF.

Zouboulis *et al.* [2002] investigated the use of upflow filtration with a floating filter medium for the removal of toxic metals from wastewater. The experimental pilot-scale filtration unit

(Figure 3.7) consisted of a feed tank (40 L volume), containing the waste solution to be treated. The content of the tank was stirred for a period of 1 h to allow the metal precipitates to form. The wastewater was fed to a filtration unit by means of a Watson-Marlow peristaltic pump. The filtration unit consisted of two Perspex columns in series, contained the filter media (polystyrene beads), supported by a plastic grid in the upper section of the device.

Headloss was controlled by a mechanical manometer. The filter was washed by downflow backwashing of the media, using the treated water that was collected in the upper part of the unit. Samples of water were collected from the influent and from the effluent of the filtration unit in order to analyze them for residual turbidity and zinc content.

Zouboulis *et al.* [2002] noticed that a filter operating with a higher bed depth and lower filtration velocity led to greater turbidity removal ($\geq 95\%$ of the initial turbidity was removed at filtration rates of around $10 \text{ m}^3/\text{m}^2 \text{ h}$). He showed that upflow column filtration, applied in a semi-batch recirculated mode, is an effective treatment process for the separation/removal of toxic metal precipitates.

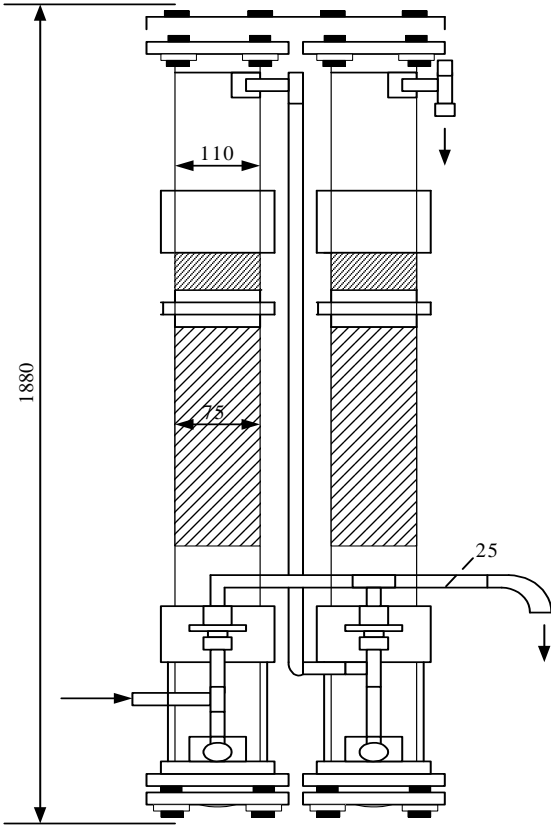


Figure 3.7: Schematic diagram of the upflow filtration unit [after Zouboulis *et al.* 2002].

3.4 Summary and discussion of pertinent aspects of the literature study

A FMF is primarily different from other filters due to its floating bed. Several types of synthetic (buoyant) plastic media, with specific gravity < 1 , are used in this type of filter. Floating media filter design and operations should be kept as simple as possible. There are a few main parameters that should be taken into consideration before creating a design:

3.4.1 Backwashing system

Two types of backwashing system have been reported in the literature,

only water backwashing, and

air backwashing followed by water backwashing.

FMF are operated in upflow mode. When backwashing with water only, the clear (clean) water is pumped in a downflow direction for a finite period of time, at a specific rate. When backwashing with air, followed by water, air is initially released below the bed for a specific period and rate of flow. After that the clean water is sent in a downflow direction for a period that is longer than the duration of the air backwashing. Backwashing with air followed by water, overall, requires less water than backwashing with water only. Air backwash agitates the media very well and most of the captured suspended solids are detached from the media during the air backwash. The bed will be vigorously agitated by air backwash because of the low density of the media. This leads to much of the captured suspended solids becoming detached and dropping down from the media during air backwashing.

According to Amirtharajah [1978], backwashing with water alone is a weak cleaning process due to the limitations in particle collision. The backwashing performance is considered in terms of water required for the backwashing. A FMF bed is easily expanded at low backwash velocity because of the low relative density of the floating media. Furthermore, the suspended solids captured within the media will be pushed down in the direction of gravitational force in a FMF [Sundarakumar, 1996].

3.4.2 Filter column

The use of various lengths and diameters of filter columns has been investigated (lengths ranged from 1 to 6 m and diameters from 60 mm to 1.5 m). The use of smaller columns is not recommended because there is an excessive sidewall-to-surface ratio, which results in significant variance in headloss build-up [Lang *et al.*, 1993]. The most common materials used for the construction of filter columns are clear polyvinyl chloride (PVC) and Perspex because they allow the operator to inspect the bed visually while it is in operation. Visual inspection can help identify the level of the media, formation of mud particles, media expansion during backwash and excessive floc accumulation on the surface of the media. Columns can be constructed in one section, or in short sections with flanges that are bolted together [Robert *et al.*, 2005].

According to Stukenberg and Hesby (1991) the filter medium can be at any depth. A depth of approximately 1200 mm has been frequently used. A retaining mesh is required above and below the media to prevent the loss of media during operation [Visvanathan *et al.*, 1996].

3.5 Design of the major components of the plant

According to the literature study on FMF pilot plants, the main components of the pilot plant are the following:

1. raw water feeder system;
2. chemical dosing system;
3. filter column and the filter bed; and
4. backwash air/water feeder system.

Accordingly, the following are the more important components of the design that were modified to suit the purpose of this study.

Raw water feeder system

To maintain a homogeneous raw water supply, it was decided to circulate the feed water by means of a centrifugal pump rather than a stirrer in the feed tank. It was also decided to use a

positive displacement pump to ensure constant feeding velocity, to allow control of the feed rate.

Chemical dosing system

In order to achieve contact flocculation a coagulant needs to be added continuously at the influent end of the filter. The suitability of different coagulants has first to be determined by jar testing. Jar testing is a laboratory technique for determining the most effective coagulant, chemical dosage, and operating pH for coagulation and flocculation. A standard dosing pump was used to feed the raw water with a coagulant.

Filter unit

(a) Filter column

The filter length could be in the range 1 to 3 m and the diameter 200 to 400 mm. The filter body material of construction was clear PVC. The transparent column allows observation of the media as the filtration process is in progress.

(b) Filter bed

The volume of the filter bed was calculated based on the quantities of the materials (media) to be used as well as the filter cross-sectional area.

(c) Headloss measurement

The piezometer tubes were connected to the pressure taps using flexible plastic tubes.

(d) Flow pattern and control

FMF experiments were conducted in the upward flow direction at different flow rates. The flow rate was controlled by using electronic flowmeters in conjunction with a variable-speed pump.

Backwash feeder system

Filter backwashing facilities was provided to clean the filter at the end of a filter run. Backwashing using air, followed by water, was adopted in this study.

3.6 Final design and installation

A significant amount of time was spent on designing the upflow floating media pilot plant, obtaining the required quotes, procuring the relevant items, constructing the pilot plant and then commissioning it.

An upflow pilot FMF was constructed on a scale to overcome the limitation of bench-scale equipment noted in literature. The pilot plant also had to comply with a few other requirements.

1. The pilot plant was to be constructed as economically as possible. The simplest, most viable and economical solution was always preferred and used where possible.
2. The pilot plant had to be flexible in design. Flexibility in design allows the operator to connect and disconnect unit processes and make any required modifications. It also had to be flexible in operation. All the operating processes and backwash operations were controlled by PLC (programmable logic control).
3. The pilot plant had to comply with all relevant safety regulations. Most of the equipment, including the filter column and piping, was installed on a framework. Only the feed water tank and the product tank protruded from the framework. The framework, measuring 950 x 1100 mm was constructed entirely from 304 stainless steel. The framework was designed based on the measurements of a trailer available for transporting of the pilot plant.

3.6.1 Process description

The sequence of process steps used to treat raw water to obtain clean water is presented in Figure 3.8. A schematic diagram of an upflow FMF pilot plant is shown in Chapter 4, Figure 4.1.

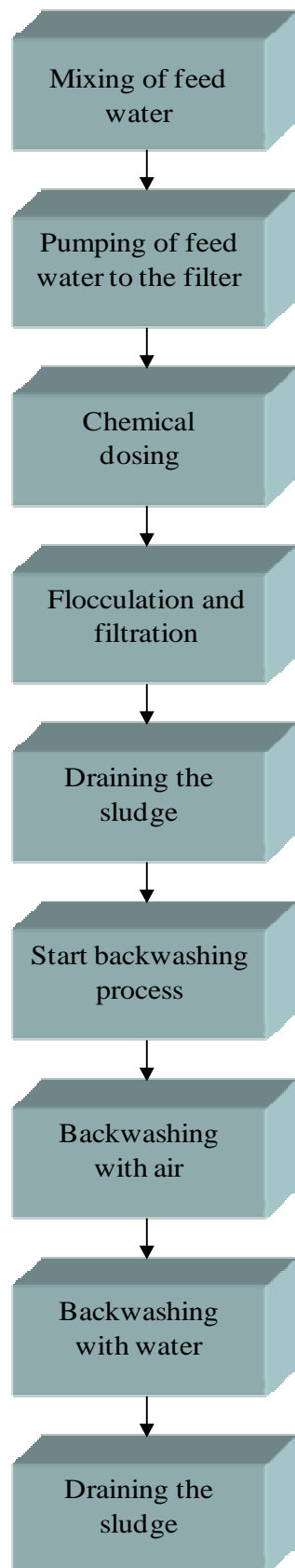


Figure 3.8: Simplified flow diagram for water treatment in this study using floating media with flocculation.

3.6.2 Construction materials

PVC pipes are commonly used in the water treatment plants. PVC pipes prevent contamination of the water. It does not affect the taste or odour of water and does not chemically react with even the most aggressive water. PVC is therefore the best cost-effective choice for piping systems. PVC pipes (diameter 25, 32, and 40 mm) were used. All fittings used were PVC fittings. Normal ball valves and actuated ball valves were used.

The basic specifications and the detailed pilot plant design drawings are included in Appendix A. The data sheet of the equipment is provided in Appendix F.

3.6.3 Ancillary equipment

To ensure a constant water flow from the feed tank to the filter, as well as ensuring a suitable air flow, a mono pump and an air blower with a variable speed drive were selected. Programmable logic control (PLC) hardware with a small screen was fitted in the control panel. The PLC consists of a central processing unit containing processor, executive memory and application memory, input and output interfacing modules, which are directly connected to the field I/O devices. The program controls the PLC so that when an input signal from an input device is turned on, the appropriate response is made. The response normally involves turning on or off an output signal to some sort of output devices. The input modules convert the high-level signals that come from the field devices to logic-level signals that the PLC's processor can read directly. The logic solver reads these inputs and decides what the output states should be, based on the user's program logic. The output modules convert the logic-level output signals from the logic solver into the high-level signals that are needed by the various field devices. The program loader is used to enter the user's program into the memory or change it and to monitor the execution of the program.

The control logic hardware was selected to ensure that the pilot plant could be operated manually or in a set sequence.

A PVC water tank (capacity 1500 L) was installed next to the pilot plant to feed the raw water to the plant. A tank of 200 L was also installed to collect the product / treated water.

As the filter column was relatively high a step ladder, with a small horizontal platform at the top, was used. It was located at the back of the pilot plant. The platform ladder allowed the operator to easily charge and replace the filter media.

Figures 3.9 to 3.11 show the pilot plant as finally installed.



Figure 3.9: The floating medium filtration pilot plant.



Figure 3.10: Piezometer panel.



Figure 3.11: Feed water tank and platform ladder.

3.6.4 Conclusion

The design of a FMF is one of the objectives of this study. The design must be based on the best knowledge available in the literature and from theoretical considerations of the shortcomings of existing conventional filters. For the purpose of this study, specifically, the design must also be able to be modified.

The pilot plant was therefore configured to allow the evaluation of the overall performance of contact flocculation filtration system using media of different size and shape.

Details of the experimental work and data that were gathered during the course of the project are described in the following chapters.

4 Experimental

4.1 Introduction

The previous chapter summarized a literature review on FMF and how the available information led to the design and construction of the pilot plant for this study. This chapter is closely related to the previous chapter. This chapter is dedicated to a detailed description of the main components of the FMF pilot plant used. The last section of this chapter presents the methodology that was accommodated to characterise the media that were used in this study.

4.2 Experimental setup

The FMF pilot plant was designed and then constructed. The filter column was made at Emplast Engineering Company (Cape Town, South Africa) according to the design specifications. The filter column was then connected to the rest of plant, and the entire unit then installed at the Department of Process Engineering (University of Stellenbosch). A schematic diagram of the experimental setup is shown in Figure 4.1. The main components of the pilot plant are the following:

1. raw water mixing and feeding system;
2. chemical dosing system;
3. filter unit; and
4. backwashing system.

4.2.1 Raw water mixing and feeding system

An artificial suspension of bentonite clay (Protea Chemicals, South Africa) and tap water (concentration 250 mg/L \approx 60 NTU) was first prepared in a 20 L tank using a stainless steel high rate mixer. The mixture was stirred for 30 minutes and then the suspension was transferred from this tank to the raw water tank (1500 L). The raw water in the feed tank was

continuously stirred using a centrifugal pump (2.5 L/s capacity) while the pilot plant was in operation to prevent the suspended solids from settling.

A centrifugal pump, with a capacity of 12 m³/h, was used to mix the raw water into the feed tank in order to obtain a homogeneous solution. A mono pump, with a capacity of 900 L/h, was used to pump the raw water from feed tank into the plant for treatment. A flow meter (0–1000 L/h) was used to measure the water flow in the FMF.

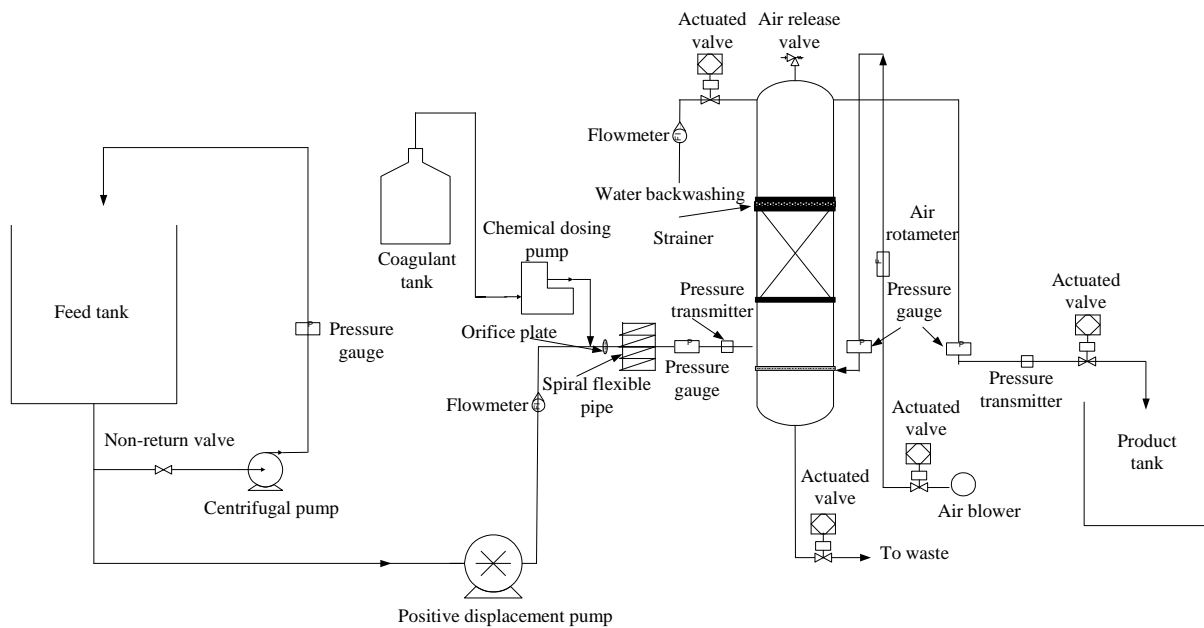


Figure 4.1: Schematic diagram of the upflow floating media filtration unit designed for use in this study.

4.2.2 Chemical dosing system

Chemical additions were dosed in-line. Ferric sulphate was used as a coagulant. The coagulant was pumped by using a dosing pump (capacity 8 L/h) on-line to the system from the 20 L capacity storage tank. The coagulant dosing pump has two pulse volumes and the pulse rate can be adjusted from 0% to 100%. Pumping dosage data were not available, hence the dosing pump had first to be calibrated. The dosage capacity at different settings was measured (using a stopwatch). This data is shown in Appendix C.

Suitable coagulant dosages were selected after carrying out jar tests. Different coagulant concentrations and pH ranges were used to determine which one produces the most

satisfactory results at the lowest cost. The optimum ferric sulphate dosage was 23 mg/L, at pH 5.5. The required dosage of ferric sulphate was introduced near the inlet of the filter. Calcium oxide (lime) was used to adjust the pH to 5.5. The lime was mixed with the raw water in the feed tank in order to increase the feed water pH. Results of the jar test are given in Appendix C.

Immediately after the point of coagulant addition an orifice plate (diameter 12.5 mm) was installed in order to create a turbulent mixing flow. Thus it served the purpose of a flash mixing device. A simple arrangement was provided for mixing at less turbulent condition by using a 25 mm diameter and a 9.5 m long flexible pipe in a spiral arrangement. This simulated the same principles described for the jar testing procedure, rapid mixing at maximum turbulence for a very short period of time at the orifice point (1 second) to effect coagulation and then slow mixing for a longer period of time at the spiral flexible pipe to initiate the flocculation process. The total contact time between coagulation to when the suspension reached the filter was 1.7 min for a filtration rising velocity of 2 m/h and 54 seconds for a filtration rising velocity of 4 m/h.

4.2.3 Filter unit

The filter column was made of clear PVC and had an inner diameter of 300 mm and a height of 2.8 m. The filter consisted of three sections. The column cross-sectional area was 0.07065 m² and the volume was 0.164 m³, for a water height of 2.32 m. The transparency of the column allowed observation of the media as the filtration process was in progress. The filter unit was connected to pressure gauges in the influent and effluent lines of the filter, in order to measure the headloss through the filter media. Details of the filter column design are described in Appendix A.

4.2.4 Backwashing system

At the end of most of the experimental runs backwashing was conducted with air, followed by water. In some cases, for the purpose of comparison, backwashing was conducted with water only.

In the case of air backwashing followed by water backwashing, the backwashing process begins by introducing air, using an air blower (60 m³/h at 350 mbar), from the bottom of the

filter column at a rate of 13.95 to 15.3 m³/h for 2 min through the air-distribution pipe that is designed to distribute air evenly across the bottom of the filter. Expansion of the media permits entrapped particles to become released and flushed downward, and out of the media. Backwashing water is introduced into the top of the filter by gravity flow. Water flows down at the rate of 0.6 to 0.63 m³/h for about 15 min. Both backwash air and water flow rates were measured using rate indicators. The air rotameter used had a range of 1.98 to 19.8 m³/h at 0.5 bar and 20 °C and the water flowmeter used had a range of 100 to 1000 L/h. The backwash performance was measured by determining effluent quality of the backwash water.

4.3 Pilot plant preliminary experimental runs

In order to verify whether the design meets the requirements of the facility, the pilot plant had to be commissioned. Commissioning also verifies that the plant performs as designed. Therefore the experimental runs were conducted to determine the operating conditions required for best performance.

4.4 Measurements

The pilot plant performance was assessed by determining the filtrate quality and the efficiency of the filter bed. The filtrate quality was measured in terms of turbidity removal, while the efficiency of the filter bed was examined by determining the headloss development along the filter bed.

4.4.1 Turbidity

The feed turbidity level was kept nearly constant, in the range of 60 to 65 NTU. The feed, filtrate, and feed water backwash, were measured using a turbiquant 1100 IR Turbidimeter (Merck Chemicals) which has a measuring range of 0.01–1100 NTU. Samples of the filtrate were collected after 30 min, and then hourly, until turbidity breakthrough occurred. The turbidimeter had to be calibrated regularly in order to avoid errors that could interfere with readings.

4.4.2 Headloss development

Headloss at the times that samples were taken for analysis, the headloss at these times were read from the piezometer. The filter column had 10 piezometer taps at different levels. Headloss was calculated as the difference between the head at each tap and the initial head.

4.5 Filter media classification

The objective of this study was to determine whether the floating media particle size and shape have a significant effect on the performance of a FMF. Therefore floating media of different sizes and shapes were investigated. The following sections define how the media that were used in this study were classified. The purpose of characterising the media is to obtain some indication of the size and shape of the media.

In order to obtain a better understanding of the effect of the geometric properties of floating media beads on the performance of the FMF, the floating media was classified in terms of size and shape analysis.

4.5.1 Size analysis

The particles were classified using sieve analysis. Sieving using woven wire sieves is a simple and inexpensive method of size analysis, and suitable for particle sizes greater than 45 μm . The sieve size is given as the size of the aperture measured perpendicular to the wires through the centre of the opening [Fernlund, 1998].

Four different types of media were mechanically sieved using sieve sizes of 4.75, 4.00, 3.35, 2.80, 2.36, 2.00, and 1.70 mm. In the actual mechanical sieving the particles were rotated in all directions to see if they would pass through the sieve opening. Sieve analysis was done in order to obtain median grain size (d_{50}). Cumulative curves were constructed based on mass percent for each sample. Based on the cumulative curves d_{50} was obtained. The sieving data and the cumulative curves are reported in Appendix B.

4.5.2 Shape analysis

Characterisation of the media shape was carried out according to the method of Lees (1964), and Barksdale and Itani (1989). The shape is characterized by the flatness ratio and the

elongation ratio. The flatness ratio (p) is the ratio of the short length (thickness) to intermediate length (width). The elongation ratio (q) is the ratio of the intermediate length to the longest length (length). By combining the flatness and elongation ratios, the shape of the particles can be described by a shape factor (F) and the sphericity (ψ). The shape factor is the ratio of the elongation ratio and the flatness ratio (equation.1).

$$F = \frac{p}{q} \quad (4.1)$$

A spherical or cubical shape will have a shape factor equal to 1. If the shape factor is less than 1, the particle is more elongated and thin. A blade-shaped particle will have a shape factor greater than 1. The shape of the media can also be described by the sphericity (ψ), which can be expressed by the flatness and elongation ratios as shown in equation 2. The sphericity varies from values close to 0 to values close to 1 for perfect spheres [Uthus *et al.*, 2005].

$$\psi = \frac{12.8 \left(\sqrt[3]{p^2 q} \right)}{1 + p(1 + q) + 6\sqrt{1 + p^2(1 + q^2)}} \quad (4.2)$$

The flatness and elongation ratios, and the shape factor and the sphericity, are combined in the diagram below (Figure 4.2). In the diagram the particles can be classified as disc, blade, cubic or rod [Lees, 1964; Janoo, 1998].

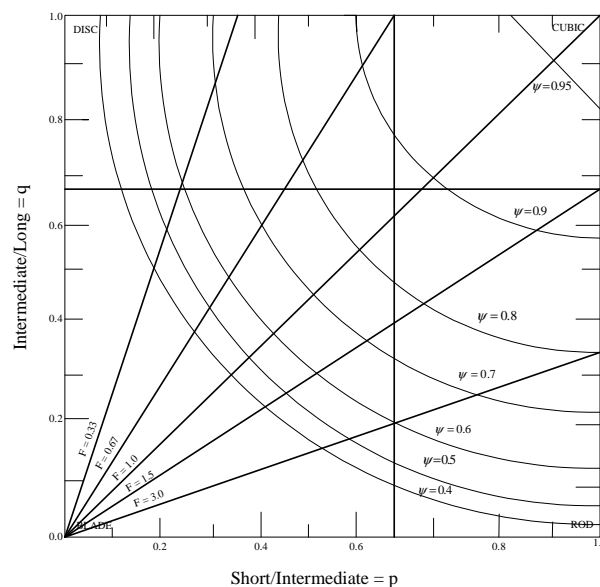


Figure 4.2: Particles classification chart [adapted from Lees, 1964; Janoo, 1998].

Shape measurements were done using venire caliper for 150 beads of each medium. This number was chosen based on some statistical analysis that showed no significant decrease in the standard deviation for sample size more than 150 beads. Filter medium particle analysis in terms of shape analysis is presented in Table 4.1

Table 4.1: Summary of filter media particle analysis

Sample	Short length (mm)	Intermediate length (mm)	Longest length (mm)	Flatness ratio (p) (-)	Elongation ratio (q) (-)	Shape factor (F)	Sphericity (ψ)
Medium i	2.81	3.60	4.22	0.78	0.85	0.91	0.93
Medium ii	3.06	3.44	4.79	0.89	0.74	1.24	0.93
Medium iii	2.25	4.96	5.34	0.45	0.93	0.49	0.82
Medium iv	1.82	2.26	2.89	0.81	0.79	1.10	0.92

Photographs of the floating media used in this study are shown in Figure 4.3. In this study two different shapes of floating media (cubic and disc) were used to evaluate the performance of the filtration unit. Although, the aim of the study was to investigate more than two shapes of floating media with the same size. The unavailability of these materials in the market limited the choice. Polypropylene beads were used because this polymer is commercially available in South Africa. Cubic polypropylene was obtained from Sasol Polymers and disc polypropylene was obtained from Pelmanco Pty Ltd (South Africa).



Figure 4.3: Different sizes and shapes of plastic media that were tested in this study. From left to right: smooth cubic (medium i), large cubic (medium ii), disc (medium iii), and small lace-cut cubic (medium iv).

4.6 Filter media properties

Granular filter media used in water treatment have a range of physical properties. Filter media are usually selected on the basis of size, but flow through filter media (bed) can also be affected by other properties such as density and voidage of the media. Therefore few relationships were used to calculate some parameters for all floating media that were used in this study.

4.6.1 Voidage in the FMF

First, the density of the different floating media was determined experimentally using a liquid displacement method according to the Archimedes' principles which states that every solid body immersed in a fluid apparently loses weight by an amount equal to that of the fluid it displaces. As the mass of media, the height (depth) of packed bed and the area of FMF column is known from measurements, the voidage in the FMF can be calculated as follows:

The mass of media in the FMF is:

$$m = AL(1 - \phi_{FMF})\rho_s \quad (4.3)$$

Rearranging equation (3) gives:

$$\phi_{FMF} = 1 - \left(\frac{m}{AL\rho_s} \right) \quad (4.4)$$

Where:

ϕ_{FMF}	bed voidage in the FMF column	$[m^3/m^3]$
m	mass of floating media in FMF column	$[kg]$
A	cross-sectional area of FMF column	$[m^2]$
L	height of packed bed	$[m]$

4.6.2 Particle size

The term size normally means the diameter. The particle diameter can be defined in different ways, and one should be aware which one is used in a given context. The volume equivalent diameter is the diameter of a sphere with the same volume as the actual particle.

By knowing the density of the particle (medium), the volume of a certain amount of particles can be calculated. 1 gram of particles has a volume of:

$$V_p = \frac{w}{\rho_s \times 1000} \quad (4.5)$$

Where:

V_p volume of 1 gram of floating media particles [m³]

w mass of particles [g]

ρ_s solid density of floating media particle [kg/m³]

The number of floating media particles in 1 gram, (n) was counted many times and then the average was considered. One particle has an approximate volume of

$$V_{particle} = \frac{V_p}{n} \quad (4.6)$$

Where: $V_{particle}$ has units of [m³/particle].

The volume of a sphere is defined as follows:

$$V_{sphere} = \frac{\pi d_{eq}^3}{6} \quad (4.7)$$

Where

V_{sphere} volume of a sphere [m³]

d_{eq} equivalent diameter [m]

Equations (6) and (7) can then be equated and solved to obtain d_{eq} for the particle.

Geometric properties of the polypropylene plastic beads are summarised in Table 4.2.

Table 4.2: Floating media particle characteristics

Media	Solid density (kg/m ³)	Bulk density (Kg/m ³)	Voidage (-)	Particle diameter (mm)	Particle equivalent diameter (mm)	d ₅₀ (mm)
Medium i	920	592	0.356	3.21	3.68	3.03
Medium ii	890	571	0.358	3.25	3.69	3.30
Medium iii	960	583	0.393	3.60	4.02	4.07
Medium iv	890	611	0.313	2.04	2.67	2.28

4.6.3 Reynolds Number

The Reynolds number gives an indication of whether the flow through the porous media is laminar or turbulent. According to Rhodes [2003], fully laminar flow exists for Reynolds number less than 10 and fully turbulent flow exists at Reynolds number greater than 2000. For the purpose of this text Reynolds number is determined to describe the flow through the packed bed. Reynolds number Re_p can be defined as follows:

$$Re_p = \frac{D_p V_s \rho}{(1 - \varepsilon) \mu} \quad (4.8)$$

The various symbols appearing in the above equation are defined as follows:

D_p	equivalent spherical diameter of particle	[m]
ρ	density of fluid	kg/m ³
μ	dynamic viscosity of the fluid	kg/(m·s)
V_s	Superficial velocity ($V_s = \frac{Q}{A}$ where Q is the volumetric flow rate of the fluid, and A is the cross-sectional area of the bed)	[m/s]
ε	Void fraction of the bed (porosity)	[-]

4.6.4 Flocculation in filter beds

In the floating medium filter bed, the increased particle contact within the pores promotes flocculation. The velocity gradient (G) in filter beds can be calculated from the following equation [Schulz *et al.* 1994].

$$G = \sqrt{\frac{g \cdot \Delta h}{v \cdot t \cdot f}} \quad (4.9)$$

Where:

g	the gravitational acceleration	[cm/s ²]
Δh	headloss across the filter bed	[cm]
v	kinematic viscosity	[cm ² /s]
t	detention time in filter bed	[s]
f	porosity of filter medium	[-]

5 Design of experiments

5.1 Introduction

Design of experiments (DOE) is a theoretical important method to identify the important factors in a process, identify and correct any problems in a process, and also identify the possibility of improving the performance of a manufacturing process. It also has extensive application in the development of new processes.

The DOE is a statistical technique that helps to study many factors and their variables concurrently and most economically. By studying the effects of individual factors on results, the best factor combination can be determined. The technique can also be used to solve scientific problems, whose solution lies in the proper combination of ingredients (factors or variables) rather than innovations or a single identifiable cause [Roy, 2001].

5.2 Factorial experiments

Factorial design is one tool that can be used in research to design experiments. An experiment using factorial design allows the experimenter to examine, simultaneously, the effects of multiple independent factors and their degree of interaction [Trochim, 2006].

It is stated that when several factors are of interest in an experiment, a factorial experimental design should be used. Furthermore, factorial experiments are the only way to discover interaction between variables [Montgomery and Runger, 2003].

The effect of a factor is defined as the change in response produced by a change in the level of the factor. It is called a main effect because it refers to the primary factors in the study.

5.2.1 Two-level full factorial design

Two-level full factorial designs are designs that test all the two-level combinations of the factors involved. A two-level full factorial design with k factors requires 2^k experimental trials to cover all possible combinations of the input factors.

5.2.1.1 The 2^3 design

The 2^3 design is a two-level factorial experiment design with three factors (A, B and C). This design tests three ($k=3$) main effects, A, B and C; three-two factor interaction effects, AB , BC , AC ; and one-three factor interaction effect, ABC . The design requires eight treatment combinations per replicate. The eight treatment combinations corresponding to these runs are: (1), a , b , ab , c , ac , bc and abc . The treatment combinations are written in such an order that factors are introduced one by one, with each new factor being combined with the preceding terms. This order of writing the treatments is called the standard order. The 2^3 design with three replicates at the center point of the design included is shown in Table 5.1 (a). The design matrix for the 2^3 design is shown in Table 5.1 (b). The design matrix can be constructed by following the standard order for the treatment combinations to obtain the columns for the main effects and then multiplying the main effects columns to obtain the interaction columns.

Table 5.1: The 2^3 design: (a) the design matrix, and (b) the algebraic signs for calculating effects

(a)

Treatment combination	Factors		
	A	B	C
<i>(1)</i>	-1	-1	-1
<i>a</i>	1	-1	-1
<i>b</i>	-1	1	-1
<i>ab</i>	1	1	-1
<i>c</i>	-1	-1	1
<i>ac</i>	1	-1	1
<i>bc</i>	-1	1	1
<i>abc</i>	1	1	1
<i>centre point</i>	0	0	0
<i>centre point</i>	0	0	0
<i>centre point</i>	0	0	0

(b)

I	A	B	AB	C	AC	BC	ABC
1	-1	-1	1	-1	1	1	-1
1	1	-1	-1	-1	-1	1	1
1	-1	1	-1	-1	1	-1	1
1	1	1	1	-1	-1	-1	-1
1	-1	-1	1	1	-1	-1	1
1	1	-1	-1	1	1	-1	-1
1	-1	1	-1	1	-1	1	-1
1	1	1	1	1	1	1	1

The 2^3 design can also be represented geometrically using a cube, with the eight treatment combinations lying at the eight corners, as shown in Figure 5.1.

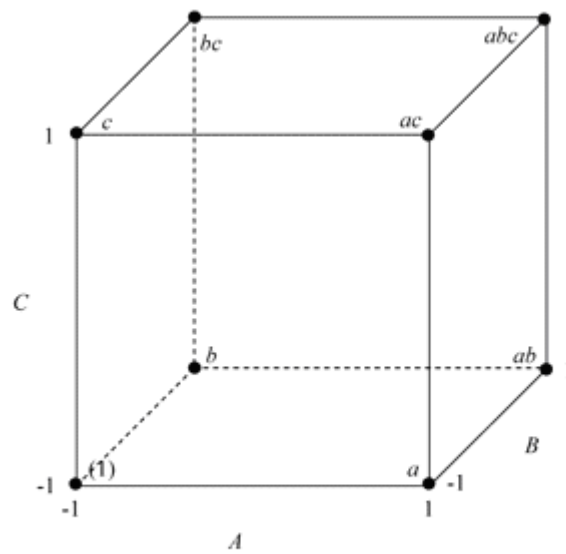


Figure 5.1: Geometric representation of the 2^3 design.

5.2.1.2 Addition of center points to a 2^k design

An assumption made in the use of two-level factorial designs is that the response function is approximately linear between the levels of factors selected. However, there is a method based on the idea of replicating some of the runs in a factorial design. The method involves adding center points to the 2^k design. These consist of n_c replicates run at the point $x_i = 0, i = 1, 2, \dots, k$. One important reason for adding the replicate runs at the design center is that center points do not impact on the usual effects estimates in a 2^k design [Montgomery, 1997].

Adding center points permits the user to check the goodness-of-fit of the planar two-level factorial model. The average response value from the actual center points is compared to the estimated value of the center point that comes from averaging all the factorial points. If there is a curvature of the response surface in the region of the design, the actual center point value will be either higher or lower than predicted by the factorial design points.

A 2^3 full factorial design with one single replicate was used in this study. Three replicates at the center of the design were investigated to allow for an independent estimation of the experimental error and to check the linearity of the factor effects.

5.2.2 Process of designing an experiment

5.2.2.1 Determination of design factor

Factors affecting the filtration performance of particular importance to this study include filtration rising velocity, media depth and coagulant dosage. These factors were selected because their effects on the performance of the filtration process are very noticeable.

Table 5.2 tabulates the three factors that were used in this study, along with the details of their levels. A high level is indicated by (+), a low level by (-), and the central point is indicated by (0).

Table 5.2: Factors and details of the levels for the treatment combinations in the 2³ design

Design of experiment			
Factor	Factor details	Level	Level values
A	Filtration rising velocity (m/h)	-	2
		0	3
		+	4
B	Media depth (mm)	-	200
		0	400
		+	600
C	Chemical dosage (mg/l)	-	11.5
		0	17.25
		+	23

Experimental facilities (feed tank volume) constrained the experimental design. This only allowed a maximum of 312 L /h (filtration rate) of feed water to be pumped to the filtration system. In addition; any rate above this value would not have allowed an effective assessment of all other parameters involved; considering the associated reduction in the operational period. The limited experimental materials (floating media) dictated the choice of the levels of media depth. The available materials only allowed a maximum depth of 600 mm. In the case of chemical dosages the highest level (23 mg/l) was obtained from Jar testing as the optimum coagulant dose for the feed water used in this study.

5.2.2.2 Determination of design response

The main design response in this study is the turbidity; the turbidity value should be as low as possible. According to the WHO (World Health Organization) the turbidity of drinking water should not be greater than 5 NTU, and should ideally be below 1 NTU.

5.2.2.3 Generation of experiment list

Upon completion of the determination of the design method and all its related parameters, a list of experiments that need to be carried out will be generated as shown in Table 5.3. A total of 11 experiments (include three replicates at the central points) needed to be conducted in random order for the three different media studied (medium i, medium ii, and medium iii).

Table 5.3: Experiments generated from DOE

Experimental trial	Treatment combinations	Factors		
		A: Filtration rising velocity (m/h)	B: Media depth (mm)	C: Chemical dose (mg/l)
Trial 1	(1)	2	200	11.50
Trial 2	<i>a</i>	4	200	11.50
Trial 3	<i>b</i>	2	600	11.50
Trial 4	<i>ab</i>	4	600	11.50
Trial 5	<i>c</i>	2	200	23.00
Trial 6	<i>ac</i>	4	200	23.00
Trial 7	<i>bc</i>	2	600	23.00
Trial 8	<i>abc</i>	4	600	23.00
Trial 9	<i>centre point</i>	3	400	17.25
Trial 10	<i>centre point</i>	3	400	17.25
Trial 11	<i>centre point</i>	3	400	17.25

6 Results and discussion

6.1 Introduction

This chapter presents the results of experiments that were conducted as described in Chapters 4 and 5. The data obtained throughout the experiments were analyzed and interpreted. First, definitions of filter efficiency and turbidity breakthrough are presented as they are essential to the understanding of the results. Summaries of results are presented in tables and figures. Typical graphs of experimental results are provided in this chapter, while all tables of raw data and complete results relating to the experiments conducted are shown in Appendix D.

6.2 Filter efficiency

The main objective of the filtration operation is to efficiently remove particles from the feed water. Therefore, the filtrate quality was considered as one of the most important parameters for characterizing the filter efficiency. In this study filter efficiency was defined in terms of the filtrate turbidity. Volume of filtrate water production to turbidity breakthrough is considered as another indication of filter efficiency.

6.3 Turbidity breakthrough

Generally, suspended solids and colloidal particles in the water are attached to the filter grain surface. As time progresses the interstices will be saturated and there will not be any retainment capacity left within the interstices. This causes turbidity breakthrough (an increase in filter effluent turbidity). Another theory is that attached particles can start to detach after some time causing breakthrough. The breakthrough was generally accompanied by an increase in headloss.

In most of the experiments, when the turbidity breakthrough was reached, this was regarded as the maximum possible filter run time and the experiment was terminated. Some experiments were terminated due to the feed water tank being emptied.

6.4 Results obtained from preliminary plant experiments

Preliminary experiments were performed on the FMF pilot plant for three main reasons. First, was to commission the plant, second, to become familiar with aspects of the pilot plant equipment in terms of operating and adjustment and third, to observe the filtration and flocculation that takes place in practice.

The experiments were carried out with feed turbidity in range of 60 to 65 NTU. Most of the experiments were carried out with 60 NTU feed turbidity. The experiments to do the commissioning and select the operating conditions were carried out using polypropylene medium with a smooth surface (media i in Figure 4.2). The operating conditions of these experiments are presented in Table 6.1. A summary of the results are presented in Table 6.2. In Table 6.2 the following applies: turbidity measurement is taken at the point at which samples were collected for analysing, water production is the accumulative volume of filtrate water produced up to the point where the lowest turbidity was achieved.

Table 6.1: Operating conditions of the preliminary experiments

Experimental run	Filtration velocity (m/h)	Medium depth (mm)	Chemical dosage (mg/L)
1	2	400	17.25
2	4	400	11.50
3	4	400	17.25
4	4	400	23.00
5	3	400	17.25
6	3	400	23.00
7	3	400	28.75
8	2	400	23.00
9	3	400	17.25
10	2	200	23.00
11	4	200	11.50
12	4	600	23.00

Table 6.2: Summary of preliminary experiments

Experimental run	Breakthrough time (h)	Lowest turbidity achieved (NTU)	Water production (L)	Reason for termination of the experiment
1	4	1.30	550	Turbidity breakthrough
2	2	7.30	310	Poor removal
3	3	1.49	620	Turbidity breakthrough
4	2	0.90	310	Turbidity breakthrough
5	4	0.51	470	Turbidity breakthrough
6	5	0.41	700	Turbidity breakthrough
7	3	0.50	470	There was not enough coagulant
8	6	0.39	470	Turbidity breakthrough
9	4.1	0.56	940	Turbidity breakthrough
10	3	0.75	310	Turbidity breakthrough
11	2	5.40	310	Poor removal
12	3.5	0.56	940	There was not enough raw water

After the plant was commissioned some modifications such as adding a plastic pipe in a spiral arrangement before the FMF, and some PVC piping fittings (elbows, unions) were removed. This was done to improve the energy mixing required for flocculation and to obtain an increase in the floc size, rather than the floc breaking up because of the PVC piping fittings.

6.5 Results obtained from actual experimentation

The following operational parameters were investigated:

- a- filtration rising velocity;
- b- synthetic media type (size and shape);
- c- medium depth;
- d- coagulant dosage; and
- e- filter backwashing

The results of the actual experiments conducted based on the list generated by a full 2^3 factorial design (Table 6.3) with one single replicate and three replicates at the center of the design was analyzed. A total of 33 experiments were conducted at different operating conditions such as filtration rising velocity, media depth, and chemical dosage. These operating condition were applied on four different types of media. The summary of selected results of different media is shown in Table 6.3 and the detailed results of all the experimental trials are shown in Appendix D.

Table 6.3: Summary of results

Medium	Experimental trial	Breakthrough time (h)	Lowest turbidity achieved (NTU)	Maximum headloss at breakthrough (mm)	Water production (L)	Water used for backwash (L/run)
Medium i	Trial 2	2	1.73	11.3	312	103.54
-	Trial 4	3	0.83	41.5	624	124
-	Trial 7	6	0.25	42	780	155
-	Trial 8	3	1.03	34.5	624	120
Medium ii	Trial 1	3	1.66	16.5	312	103.54
-	Trial 3	6	0.64	31.3	780	106.88
-	Trial 5	4	0.79	11	468	102
-	Trial 7	7	0.32	40.2	936	105
Medium iii	Trial 1	4	1.34	15.5	312	207
-	Trial 3	6	0.84	35.3	780	124
-	Trial 4	3	1.44	57.5	624	103.54
-	Trial 7	7	0.48	36.2	936	105.21
Medium iv	Trial 2	2	1.14	65.2	312	100.20
-	Trial 4	3	0.57	109	624	120
-	Trial 5	5	0.42	48	624	103.54
-	Trial 7	7	0.40	85.2	936	103.54

6.6 Effects of physical parameters

6.6.1 Filtration rising velocity

Two different filtration rising velocities, as mentioned in Table 6.1 (2 and 4 m/h), were tested for all types of media in this study. The variation of filtrate quality at different filtration velocities is shown in Figures 6.1 (a and b).

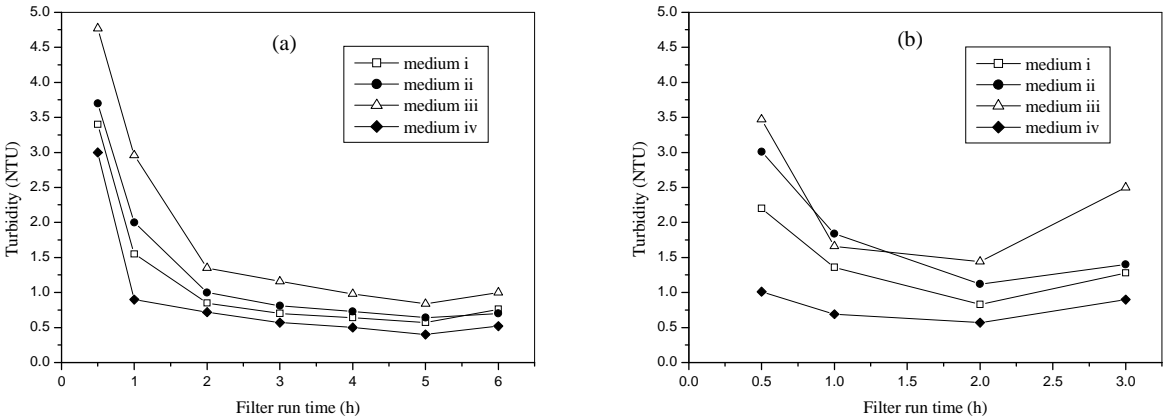


Figure 6.1: Effect of filtration rising velocity on filtrate turbidity for all media. Medium depth: 0.6 m; chemical dose: 11.5 mg/L; filtration velocity: (a) 2 m/h, (b) 4 m/h.

During the course of filtration, the accumulation of deposited particles/flocs within a filter initially increases with time. As incoming particles attach to previously deposited particles, the filter’s ability to remove particles is improved. As a result, the filtrate turbidity varies with time.

As filtration continues there may be a period in which turbidity of the filtrate does not change considerably. As can be observed from Figure 6.1 (a) there was no significant improvement in turbidity between 3 and 5 hours for medium i, ii, and iv.

Figure 6.1 (a and b) demonstrates that filtration rate has an influence on the particle removal. Many studies reported that good removal in the filters was achieved at low filtration rate [Boller, 1993].

The higher flow rate forces the particle/flocs to permeate deep into the channels. Since the interstitial velocity is higher, the shear forces experienced by collected (attached) particles are greater. Hence, particle detachment is much more likely, leading to an early breakthrough time. This could be seen in Figure 6.1 in which turbidity breakthrough occurred at the third hour at the higher flow rate (4 m/h), while at the lower flow rate (2 m/h) turbidity breakthrough occurred at the sixth hour of operation.

It was visually observed that at the increased filtration rate (4 m/h), particles/flocs penetrated deeper into the bed. This results in decreased filter efficiency. This visual observation can be fully supported by the results shown in Figure 6.1, where the overall filtrate turbidity for all media was not as good as it was in the case of lower filtration rate (Figure 6.1 a). One possible reason for the increase in the filtrate turbidity is the shorter retention time corresponding to higher filtration rate. In addition, the higher filtration rate results in greater fluid shear forces at the media surfaces. Increased shear would likely result in a decrease in the attachment efficiency because of the greater fluid drag on particles near the media surface. It was also observed that there was a good distribution of particles loading throughout the bed at low filtration rate (2 m/h). These findings are consistent with those of Wegelin., *et al* (1986) which showed the same trend.

6.6.1.1 Implication for filter operation

As expected, the filter run times were significantly lower for the higher loading rates, thus the volume of water produced per filter run was less than that produced with lower loading rates. The cumulative water produced at the lower loading rate ($36.8 \text{ L/m}^2 \cdot \text{min}$; 2 m/h) was 780 L, whereas the cumulative water produced in the higher loading rate ($73.6 \text{ L/m}^2 \cdot \text{min}$; 4 m/h) was 624 L for all media. These results are consistent with the findings that indicate that improved cumulative removal efficiency is typically correlated to longer filter runs. [Wegelin, 1986; Collins, 1994]

The results showed that an average reduction of 60 percent in the total filter run time occurred as a result of the increase in the flow rate from 36.8 to $73.6 \text{ L/m}^2 \cdot \text{min}$ for all medium sizes tested. This was expected because at the higher flow rate, the filter is loaded with higher particles/flocs content in a shorter period of time.

At both flow rates, the filter using smaller medium (medium iv, $d_{50} = 2.28 \text{ mm}$) produced the best filtrate quality ($\leq 0.5 \text{ NTU}$). However the difference between the maximum filter run times of all media decreased as the flow rate was increased (Figure 6.1).

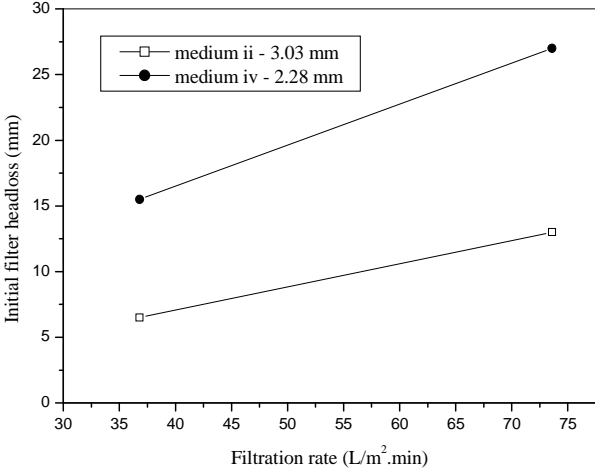


Figure 6.2: Effect of filtration rate on initial filter headloss.

Measured clean filter headloss across the filter media as a function of filtration rate is shown in Figure 6.2. When water passes through a clean granular medium, energy losses occur due to both form and drag friction at the surface of media grains. Furthermore, energy losses or pressure drops occur due to continuous contraction and expansion experienced by the fluid as it passes through interstitial spaces between the media grains.

As shown in Figure 6.2, initial headloss at a flow rate of $36.8 \text{ L/m}^2 \cdot \text{min}$ is 6.5 mm of water for medium ii (3.30 mm). This initial value increases to a value of 13 mm of water at a flow rate of $73.6 \text{ L/m}^2 \cdot \text{min}$. Similarly, initial headloss increases from 15.5 to 27 mm of water when the filtration rate is increased from 36.8 to $73.6 \text{ L/m}^2 \cdot \text{min}$ in the case of medium iv (2.28 mm). Based on this result one can conclude that the effective size of a filter medium and the flow rate are the two major factors influencing the initial headloss. Other factors may also affect the headloss but their contribution is less. Clearly this result is in accordance with the well established behavior as expected from the Carmen-Kozeny equation [equation 2.2].

6.6.2 Medium size

6.6.2.1 Plastic beads

The effect of medium size (d_{50}) on removal of turbidity is shown in Figure 6.3. In this figure, the results of three different sizes (d_{50}) of medium (2.28, 3.03, and 3.30 mm) are presented. In this comparison medium (iii) was excluded since it had a different shape (it has a disc shape).

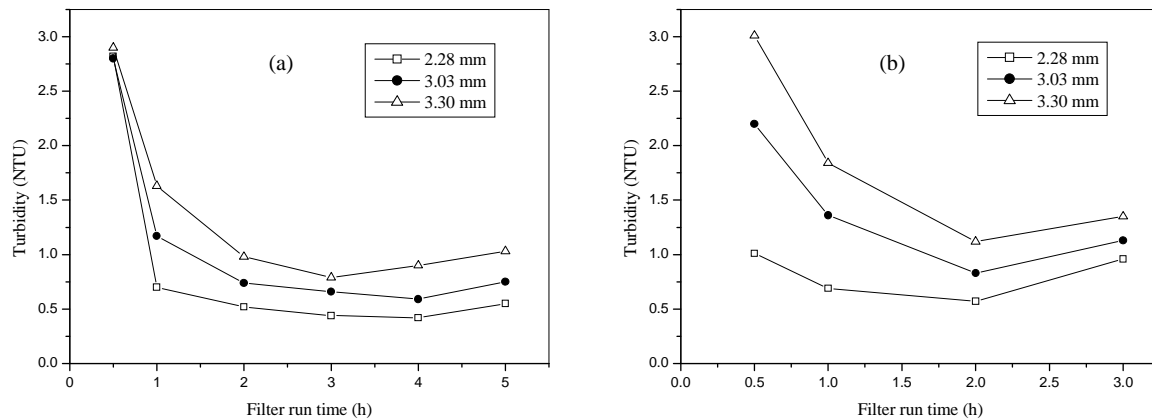


Figure 6.3: Effect of medium size on filtrate turbidity. Filtration velocity: (a) 2 m/h, (b) 4 m/h; medium depth: (a) 200 mm, (b) 600 mm; coagulant dose: (a) 23 mg/L, (b) 11.5 mg/L.

From Figure 6.3 under the normal operating conditions, medium iv which has a size of 2.28 mm was able to produce filtrate with a minimum turbidity of 0.6 NTU and to provide a turbidity of less than 1 NTU for 2.5 hour of operation at the conditions indicated in the figure. However, for the media with effective size of 3.03 and 3.30 mm the filtrate turbidity was more than 0.6 NTU but still within the recommended limit set by WHO for drinking water which is 1.0 NTU (WHO, 2004).

The same filter run time was achieved by the three different medium sizes, but this differed with the flow rates. For instance, the filter run at a flow rate of $36.8 \text{ L/m}^2 \cdot \text{min}$ (2 m/h) was constant for sizes of 2.28, 3.03, and 3.30 mm and the run time was 4 hours. In the case where a filter rate was at $73.6 \text{ L/m}^2 \cdot \text{min}$ (4 m/h) the sizes were comparable with 2 hours.

It was visually observed that when the smaller medium (2.28 mm) was used, the majority of turbidity profiles indicated that only part of the filter was being utilized for particle (turbidity)

removal. The main active depth was the first 200 mm and in the most extreme case, only the first 300 mm of the filter bed removed turbidity before the turbidity level stabilized (Figure 6.3). A greater proportion of the filter bed was used for particle/turbidity removal in the FMF using the larger medium (3.0 and 3.30 mm). This suggested that particles/flocs penetrated deeper into the filter that contains the larger media (3.0 and 3.30 mm) and therefore, more solids (particle) would be retained. Thus, a FMF that contains the smaller medium (2.28 mm) would actually utilise a portion of the deeper filter depth to remove particles. However, it may be possible to obtain similar performance using the larger sized medium, by increasing the medium depth.

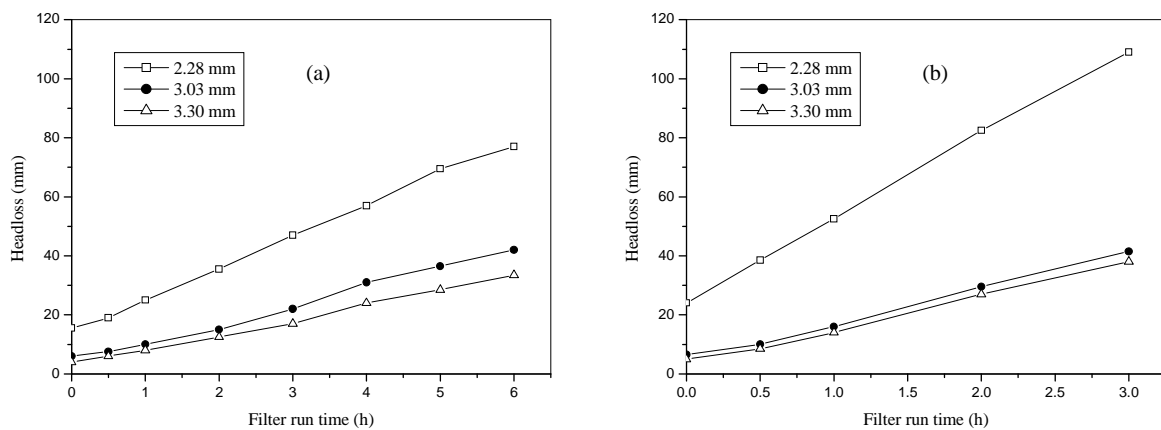


Figure 6.4: Filter headloss as a function of filtration time. Filtration velocity: (a) 2 m/h, (b) 4 m/h; medium depth 600 mm; chemical dose 23 mg/L.

As expected, headloss increases with time during the operation of a filter [Ives, 1970]. As the filtration process progresses, particle/flocs retained in the voids lead to a decrease in the filter bed voidage. The resistance of the bed to the water flow will increase due to the size reductions of the interstitial spaces between media grains. Increasing resistance with time increases the headloss.

For all medium sizes (except for $d_{50} = 2.28$ mm), the rate of increase in headloss was gradual with filtration run time. In the case of medium iv ($d_{50} = 2.28$ mm), the rate of increase in headloss was greater with the filtration run time. According to Tobiason and Vigneswaran 1994, headloss development is typically linear with filter run time. The fact that headloss increases linearly with filtration velocity for any medium shown in Figure 1.13 is an indication that the flow regime through the filter is laminar [Ergun, 1952].

As shown in equation 2.2, the headloss of a clean bed is proportional to the negative square of the grain size; thus, a clean filter with larger grains will give a lower headloss. This was observed experimentally with medium ii (3.30 mm, Figure 6.4). However the results also confirmed that a medium with smaller particle size (medium iv, 2.28 mm) causes more headloss per unit mass deposited, as was also stated by Tobiasson and Vigneswaran (1994).

Besides the medium size, the flow rate also affected the headloss: the higher flow rates resulted in a greater headloss as it contributed to a higher solid loading.

Generally, flow resistance relates closely to interstitial spaces between medium grains or the voidage of the filter bed. Filter bed voidage is one of the key parameters that directly affect filtration performance. Based on the results shown previously (Figures 6.3 and 6.4) it can be observed that the filtrate quality (turbidity removal) is dependent on the voidage of the filter bed. The results indicate that the lower the filter bed voidage the better the filtrate quality. This was observed with the smaller medium (medium iv, 2.28 mm) which had the lowest voidage (0.313). Increase in the voidage of filter bed resulted in a lower filtrate quality and lower rate of headloss build up.

6.6.2.2 Linear low density polyethylene powder

Plastic beads (medium i, ii, iii, and iv) are not porous material and particles can mostly be retained within the interstitial spaces between the grains in the filter bed, so smaller particulate matter can more easily drain through the plastic beads and escape in the filtrate water. Therefore medium in a smaller size will retain smaller particulate matter (micro-particles) as the void spaces are smaller.

In order to confirm the effect of media size on the FMF performance, linear low density polyethylene (LLDPE) powder ($d_{50} = 600 \mu\text{m}$) was used. Since inter-grain powder void spaces are smaller, particles in water will be forced to come close to the filter medium particles. The closer they come, the more effective the attachment forces they become. The performance of LLDPE powder as filter medium is shown in Figure 6.5.

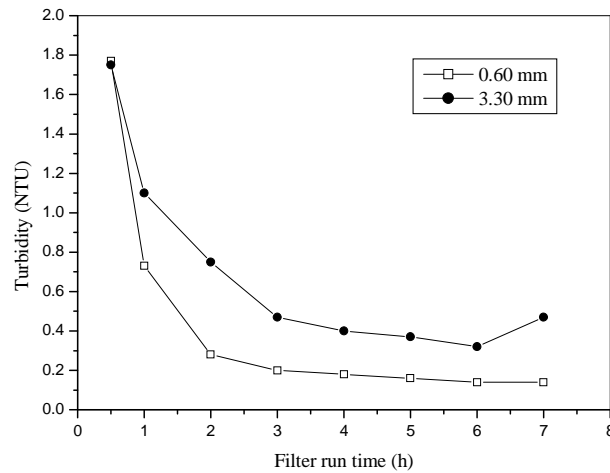


Figure 6.5: Effect of medium size on filtrate turbidity. Filtration velocity: 2 m/h; medium depth: 600 mm; coagulant dose: 23 mg/L.

Figure 6.5 shows the performance of LLDPE powder ($d_{50} = 600 \mu\text{m}$) in comparison with the performance of plastic beads (medium ii, $d_{50} = 3.30 \text{ mm}$). It can be clearly seen, the removal efficiency is excellent with a long filtration run when LLDPE powder was used. LLDPE powder produced the lowest turbidity (0.14 NTU) with cumulative water of 1092 L, while, plastic beads (medium ii, $d_{50} = 3.30 \text{ mm}$) produced a turbidity of 0.32 NTU with cumulative water of 936 L.

It was visually observed that the particles were not captured within the media path in the deep bed. The particles were captured within the first few centimeters, leading to the formation of a cake layer, which caused a large increase in headloss. This indicates that the FMF acts as a surface filter when LLDPE powder ($d_{50} = 600 \mu\text{m}$) is used. The thickness of the cake, however, consistently increases in surface filtration, and in the long run the cake itself acts as a filter layer.

Despite the fact that LLDPE powder gave the best filtrate quality, the headloss development was very high (more than 400 mm) compared to 85 mm, which was obtained when the smallest synthetic beads (medium iv, $d_{50} = 2.28 \text{ mm}$) was used.

It was not observed that any particles/flocs penetrated deep into the filter bed since the top layers of the filter bed remained clean. This can be supported as no turbidity breakthrough occurred even after 7 hours of operation (Figure 6.5).

6.6.3 Medium shape

The shape of the filter medium is another important factor affecting filter performance. The shape of the media affects the bulk porosity (voidage) of the bed, which is strongly related to the increase in headloss that results from deposits in the filter. The media shape has a fairly strong relationship with the ability of the filter media to remove particulates [Trussell *et al.*, 1980].

The shape of media particles leads to various particle-packing, which changes the liquid flow through the filter bed. The more compacted the filter bed the, is the less the voidage, the better the particle removal.

Figure 6.6 shows the results of some experiments conducted using two medium shapes. One medium was a cubic, angular-shaped particle (medium ii, 3.30 mm). The other medium was a disc-shaped particle (medium iii, 4.08 mm). One other difference between the two media with respect to their shapes is that, medium ii has sharp edges with a rougher surface, while medium iii has a smoother surface. The Figure compares the two media (cubic-shaped and disc-shaped) at two filtration rates (36.8 and $73.6 \text{ L/m}^2 \cdot \text{min}$), giving the time to turbidity breakthrough, the filtrate turbidity over filtration time.

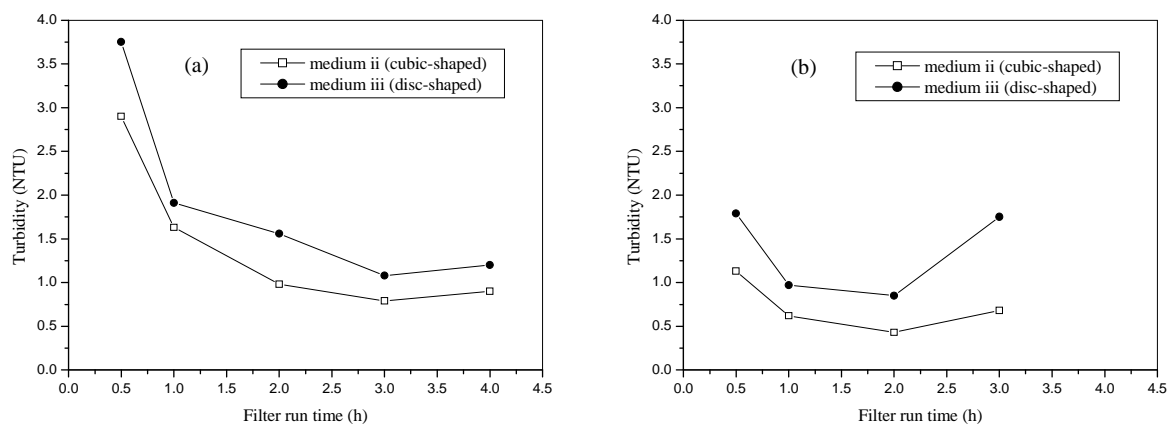


Figure 6.6: Effect of medium shape on filtrate turbidity. Filtration rate: (a) $36.8 \text{ L/m}^2 \cdot \text{min}$, (b) $73.6 \text{ L/m}^2 \cdot \text{min}$; medium depth: (a) 200 mm, (b) 600 mm; coagulant dose: 23 mg/L.

It can be seen that use of the cubic-shaped medium with sharp edges results in an improved performance with respect to filtrate turbidity. At low flow rate and lower media depth (Figure

6.6 a) a cubic-shaped medium with sharp edges could produce filtrate at low turbidity of 0.79 NTU, whereas, a disc-shaped medium produced filtrate with turbidity of 1.1 NTU. Similarly, at high flow rate and higher media depth (Figure 1.5 b) cubic-shaped medium outperformed disc-shaped medium by producing filtrate with turbidity of less than 0.5 NTU. However, turbidity breakthrough occurred at the same time with the two media shapes.

In part, this variation in filter performance might be due to the fact that medium (ii) has sharp sides. This, in combination with medium grains compaction, gives a bed that is different from that of the disc-shaped medium. Compaction of medium grains can be further assessed through voidage measurements. The voidage of sharp-edged cubic medium (medium ii) is 0.36, while the voidage of disc-shaped medium (medium iii) is 0.39. Therefore, one can deduce that the combination of sharp sided compacted medium results in superior filtration as compared to disc-shaped medium (medium iii).

A further reason for a better removal quality with sharp-edged cubic medium (medium ii) that can be stated here is the difference in the surface properties between the two media. Surface properties are one of the key factors affecting particle removal in filtration.

Figure 6.7 shows the SEM micrographs of a cubic-shaped medium (medium ii) and a disc-shaped medium (medium iii). Medium (ii) has a rough surface, while medium (iii) appeared to have a smoother surface. Rough surfaces provide a large specific area for particle deposition. The smooth surface of the filter medium (medium iii in this study) could be a reason for the less effective in the removal of particles.

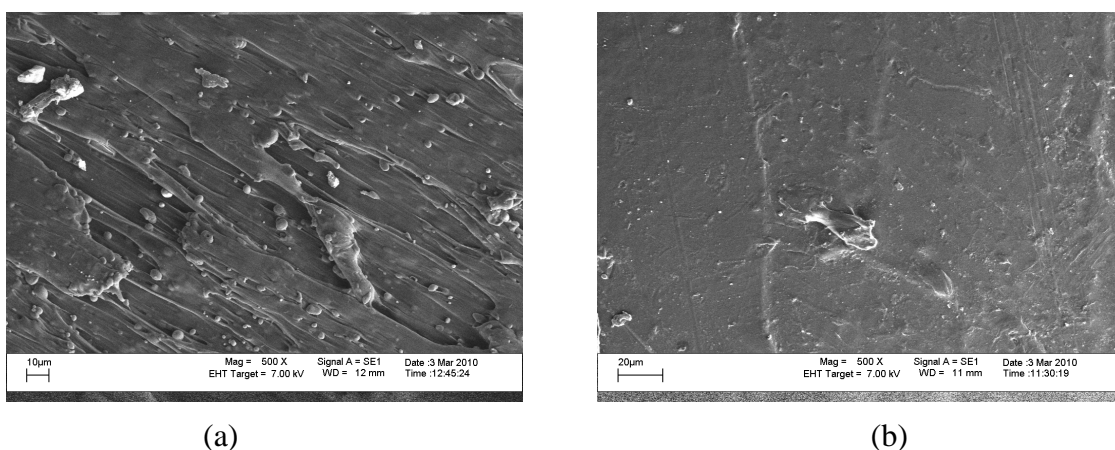


Figure 6.7: SEM images showing the surface morphologies of (a) a cubic-shaped medium; and (b) a disc-shaped medium.

Apart from the shape difference between these two media (sharp-edged cubic and disc-shaped), medium size should also be considered. These two media are different in size. Medium (ii) has d_{50} of 3.30 mm, while medium (iii) has d_{50} of 4.07 mm. Aforementioned results in section (6.6.2) showed that the smaller the size the better the performance. Medium (iv) with a cubic shape and d_{50} of 2.28 mm gave the best performance in terms of turbidity removal. Therefore, one can not state definitively that shape alone improved the filtrate quality since media size was inconsistent.

6.6.4 Medium depth

The media depths tested were 0.2, and 0.6 m. Figure 6.8 (a and b) present the influence of the media depth on the filtrate turbidity at effective sizes of 3.03 mm (medium i) and 4.07 mm (medium iii). Performance of the deeper medium (0.6 m) for both media improved when compared to the shallow media depth (0.2 m). Medium i (3.03 mm) produced a filtrate turbidity of 0.58 NTU after 2 hours vs. 0.59 NTU after 4 hours. While the deeper bed of medium iii (4.07 mm) produced a filtrate quality of 1.1 NTU after 1 hour vs. 1.08 NTU after 3 hours with the shallow bed.

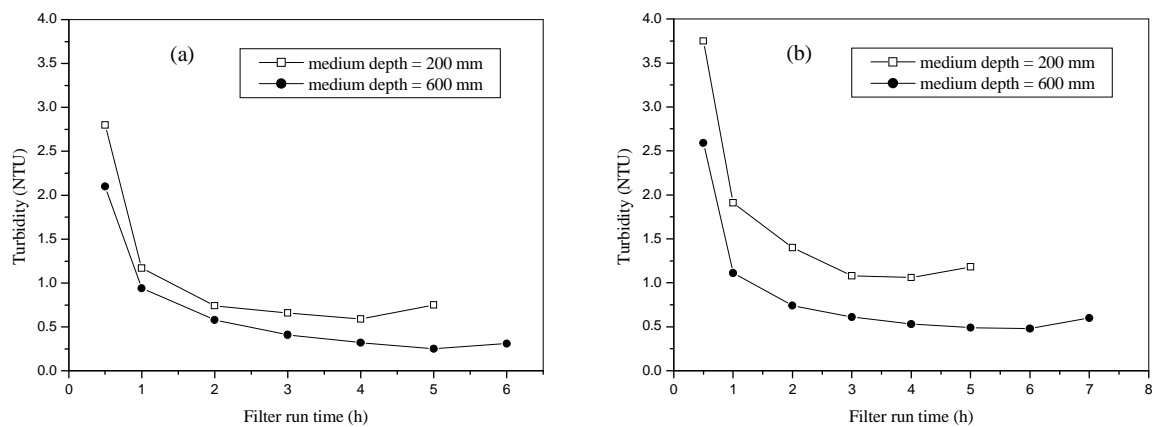


Figure 6.8: Effect of medium depth on filtrate turbidity. Filtration velocity: 2m/h; chemical dose: 23 mg/L; medium: (a) i, (b) iii.

Deeper beds have more medium grains and, therefore, can remove more particles from raw water. The more tortuous path at greater medium depth, aids in better filtration efficiency, with regard to turbidity. The larger water production is found with greater media depth because of the larger filter volume.

Figure 6.8 (a and b) illustrate that turbidity breakthrough occurred earlier when the bed depth was 200 mm compared to that when the filter bed was 600 mm. This could be explained by the fact that particles in water had the opportunity to potentially interact with more medium grains, and hence the chance for particle attachment to a media grain is greater.

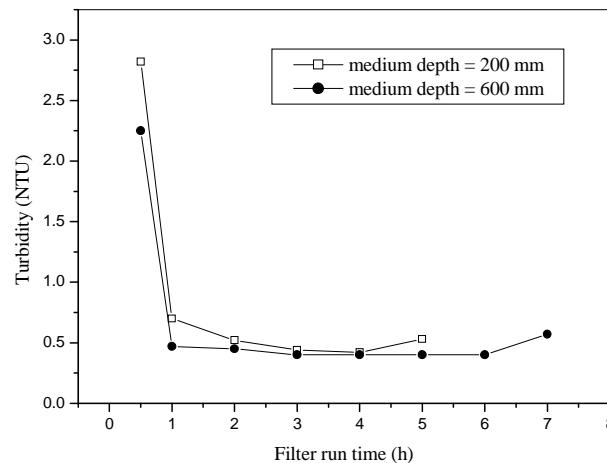


Figure 6.9: Effect of medium depth on filtrate turbidity. Filtration velocity: 2m/h; chemical dose: 23 mg/L; medium: medium iv.

Visual observation indicated that for some media (such as medium iv; 2.28 mm), the lower part of the filter bed (the first 200 mm of the 600 mm bed depth) was the main active bed for particle removal. This was clearly observed as there was a big difference between the colour of the two sections (lower and upper). The lower section of the filter bed was darker than the upper section. As the filtration process proceeded, more particles trapped into the filter bed resulted in an increased intensity of the colour of the first section of the filter bed.

The abovementioned observation can be supported with analysis of the headloss profile along the filter bed (Figure 6.14). This figure showed that there was no considerable difference in the headloss profiles above point 6 (the start of the upper section). The same behavior can also be observed from the results shown in Figure 6.9 as the turbidity removal did not improve and remained nearly constant after the third hour of operation. It was also observed that the lower section of the filter bed was full of particle/flocs after approximately three hours of operation.

Based on the previous interpretation of the results as well as visual observation, one can conclude that the bulk of the particle removal (capture) takes place in the first section (200 to 300 mm) of the filter bed when the smaller medium (medium iv; 2.28 mm) were used.

Generally, it can be said that the effective depth reduces with reduction in effective sizes. For instance, the effective depth for effective size of 2.28 mm was in the range of 200 to 300 mm, whereas the effective depth for larger effective sizes (3.03, 3.30 and 4.07 mm) was greater than 300 mm.

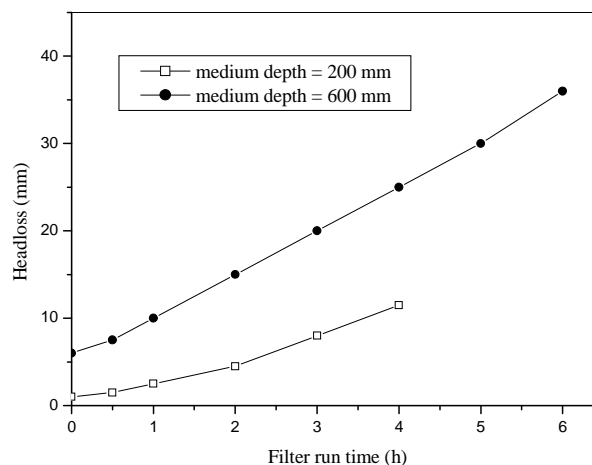


Figure 6.10: Headloss development as a function of filtration time. Filtration velocity: 2 m/h; chemical dose: 23 mg/L; medium: medium i.

Comparing the headloss development of the two depths of medium i ($d_{50} = 3.03$ mm) in Figure 6.10, it can be observed that the deeper filter (0.6 m) reaches a headloss of 10 mm after 1 hour, while the shallow filter (0.2 m) reaches the same headloss after 4 hours.

Increasing the bed depth leads to an increase in friction force of the bed because of increasing surface area, and this cause an increase in headloss values (Figure 6.10).

6.6.5 Coagulant dosage

The performance of a FMF was examined using two different coagulant doses of 50% and 100% of the optimum dose (11.5 and 23 mg/L) obtained from the jar tests. This was to determine the degree of flocculation required in the contact-flocculation process.

The filtrate turbidity profiles for medium i ($d_{50} = 3.03$ mm) and medium ii ($d_{50} = 3.30$ mm) are illustrated in Figure 6.11 (a and b), where the lowest turbidity was obtained with a higher coagulant dosage. For both presented media, the addition of a small dosage of coagulant (corresponding to 11.5 mg/L) resulted in a filtrate water quality of about 2.0 NTU. However, the addition of a higher dosage of coagulant (corresponding to 23 mg/L) resulted in a better quality of filtrate of less than 1.0 NTU.

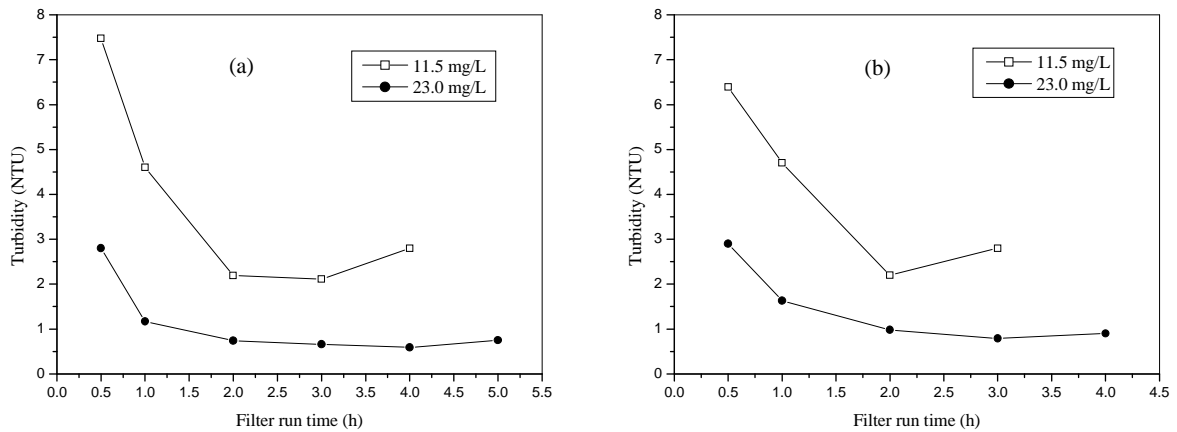


Figure 6.11: Effect of coagulant dose on filtrate turbidity. Filtration velocity: 2m/h; medium depth: 200 mm; medium: (a) i, (b) ii.

The results shown in Figure 6.11 (a and b), indicate that at a lower coagulant dose (11.5 mg/L) turbidity is reduced over time but not enough to meet the required standards. This suggests that insufficient coagulant is being used, whereas, at optimum coagulant dose (23 mg/L) an acceptably low level of turbidity is achieved with longer filter run length. The same trends as indicated in Figure 6.11 were also obtained for the two other media types, as can be seen in Appendix D.

Figure 6.12 shows the variation of the headloss across the filter bed with medium i (3.03 mm) and medium ii (3.30 mm) at a filtration rate of $73.6 \text{ L/m}^2 \cdot \text{min}$, media depth of 600 mm and coagulant dosage of 11.5 and 23 mg/L. The headloss increases with the coagulant dosages. The reason for this is, as the particles/flocs accumulate within the bed and since the number of flocs associated with coagulant dose of 23 mg/L is larger than that associated with 11.5 mg/L, the void space available for flow decreases, and the interstitial velocity increases. Consequently, more energy is required to overcome the friction loss within the filter, and headloss through the

bed increases. The other two media types showed the same trend. Results may be found in Appendix D.

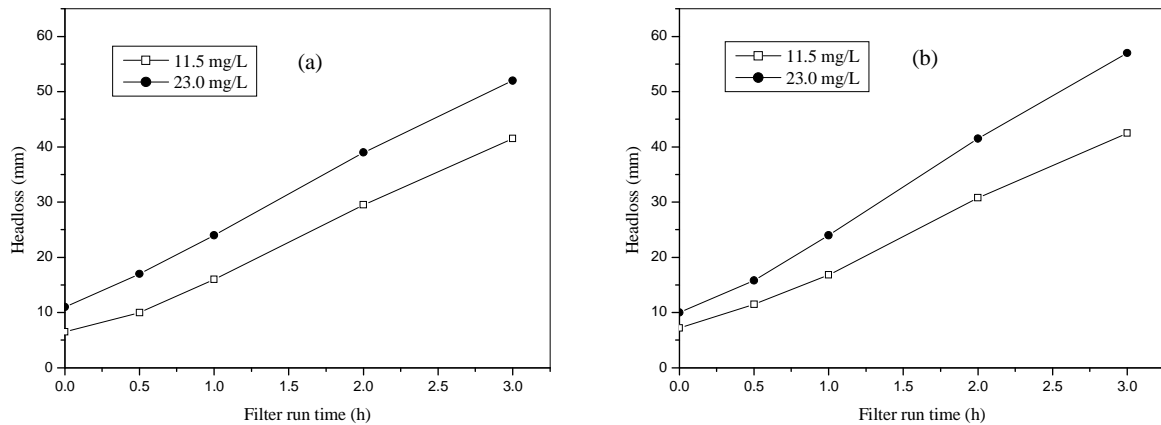


Figure 6.12: Headloss development as a function of filtration time. Filtration velocity: 4 m/h; medium depth: 600 mm; medium: (a) i, (b) ii.

6.6.5.1 Flocculation time and mixing intensity

It should first be mentioned that the flocculation unit, which consists of flash mixing device (orifice plate) and helicoidal (spiral flow) tube, was provided to create coagulation and flocculation; design was not optimised. It is felt that the turbulence created by the orifice and the configuration of the mixing unit did not provide enough mixing to form large flocs. It was observed that flocs continued to increase in size as feed water proceeded into the filter column and in some experiments, flocs were formed within the filter bed.

The influence of flocculation time was examined by visual observation of floc size along the filter column. No consistent, significant difference was observed in terms of floc size for all media tested under the same operating conditions. However, there was a clear difference in floc size when the two coagulant dosages (11.5 and 23 mg/L) were compared.

The influence of flocculation time on filtrate turbidity indicated that the lowest turbidity level was achieved with longer time within the filter bed. This suggests that floc size continued to increase, thus, being more effectively captured within the filter bed. The sinuous flow of water through the interstices of medium provided repeated contacts among the small particles/flocs to form compact settleable flocs. As a result, a portion of the agglomerated flocs attached to the

surface of and within the interstices of medium, which further helped in removing finer particles as they came into contact with the settled flocs.

Visual observation showed that the number of aggregates (flocs) increases as the flocculation process was continued for longer time intervals (in this study, time ranging between 10 and 32 minutes). Observation also indicated that increasing the flocculation time to 20 minutes or longer resulted in sufficient growth of flocs to cause their removal in the subsequent filtration step. A flocculation period of 20 minutes or longer provided a filtrate with turbidity ranging between 0.5 and 1 NTU, given the same flocculation time.

Flocculation depends on the number of particles and the probability of collisions among the particles. The number of collisions between particles is directly related to the velocity gradient [Weber, 1972]. The intensity of velocity gradient (mixing) contributes to floc formation in the filter bed. Therefore, velocity gradient (G) in the filter bed was calculated [Equation 4.9].

A velocity gradient of 59 s^{-1} with coagulant dosage of 23 mg/L gave a considerably better result of filtrate turbidity (0.25 NTU) than with 11.5 mg/L of coagulant dosage at the same velocity gradient (0.84 NTU). It was visually observed that floc size decreases with increasing velocity gradient or mixing intensity, as can be expected. This observation is in agreement with the findings of Bache and Rasool (2001). The previous observation can be further supported by the results of filtrate turbidity in which indicated that, turbidity removal continued to improve with decreasing velocity gradient. Samples of some selected results for all media are shown in Table 6.4.

Table 6.4: Summary of calculated parameters at bed depth of 200 mm

Media	Filtration velocity (m/h)	Detention time in filter bed (min)	Reynolds number in filter bed (-)	Velocity gradient (G) (s^{-1})	Lowest turbidity achieved (NTU)
Medium i	2	2.13	2.97	69.93	0.59
Medium i	4	1.10	5.93	111.19	1.73
Medium ii	2	2.14	3.37	51.77	0.79
Medium ii	4	1.07	6.75	85.50	2.79
Medium iii	2	2.40	3.47	68.40	1.06
Medium iii	4	1.20	6.95	134.84	2.35
Medium iv	2	2.00	2.30	119.91	0.42
Medium iv	4	1.00	4.60	197.63	1.14

From the results, it is clear that the lowest turbidity achieved was at the lower velocity gradient for each medium, as expected. At lower filtration velocities, the interstitial velocity and mixing intensity are lower and the residence time is longer. One can expect that shear forces which would remove attached flocs would be less in this case, and hence a greater solids retention could be achieved.

Table 6.4 also shows that the flow conditions within the filter bed are laminar even at higher flow velocity as described by the Reynolds number (Re). Removal efficiency increases with decreasing Reynolds number, which is also a linear function of filtration rising velocity. The Reynolds number is a function of the type of media and therefore it appears as if the medium that will provide for the lowest Reynolds number will be the most effective medium in removing turbidity. In this study and as shown in Table 1.1 medium iv (2.28 mm) provided the lowest Reynolds number (2.30) and lowest turbidity. Analysis of the effect of the effective size was done previously.

6.7 Headloss development

Headloss development in a filter is just as important as filtrate quality (turbidity) to evaluate the filtration performance. At the start of a filter run the water flows through the clean bed, with the headloss only dependent on the media properties and flow velocity [Smith *et al.*, 1996].

The headloss development across the filter bed was discussed in the previous sections. The results presented in the previous sections confirmed what was expected, in which a medium with smaller particle size cause higher headloss. Flow rate also showed a great influence on headloss development; the higher the flow rate the greater the headloss as they contributed to higher solid loading. Similarly, increasing coagulant dosage increased headloss as the number and size of flocs formed with a high coagulant dose is larger than that formed with a low coagulant dose. In the following section, headloss development along the filter bed is discussed.

To study the headloss variation along the filter bed, a number of piezometer tapping points were placed at different positions along the filter bed. The headloss development along the filter media is shown in Figures 6.13 to 6.14 at different conditions. The ordinates show the position of the piezometer tapping points in the filter. In the case of medium depth of 200 mm, piezometer points 8 and 9 were connected to the filter bed, while, piezometer points 7 and 10

were connected below and above the filter bed respectively. In the case of medium depth of 600 mm, piezometer points 4 to 9 were connected to the filter bed, while, piezometer points 3 and 10 were connected below and above the filter bed respectively.

Piezometer points

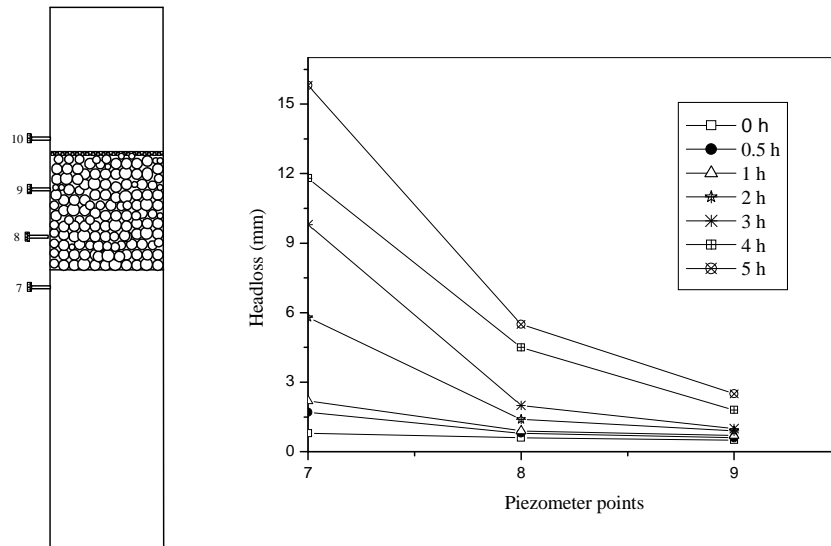


Figure 6.13: Headloss variation along filter bed at given time. Filtration velocity: 2 m/h, medium depth: 200 mm, chemical dose: 23 mg/L, medium: iii.

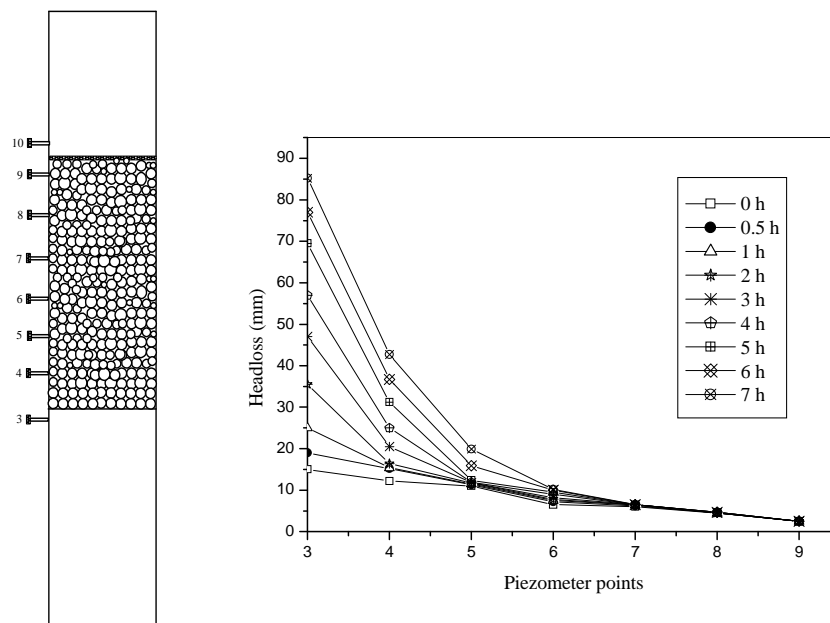


Figure 6.13: Headloss variation along filter bed at given time. Filtration velocity: 2 m/h, medium depth: 600 mm, chemical dose: 23 mg/L, medium: iv.

Figure 6.13 demonstrates that, the particle removal process occurred in the entire filter bed. However, a greater portion of the removal was achieved in the bottom layer (below point 8) and that can be deduced from the observed higher headloss difference between point 7 and point 8 in comparison with the headloss difference between point 8 and point 9. In the case of medium depth of 600 mm and when the smaller medium (medium iv, 2.28 mm) was used, most of particles was removed in the first 200 to 300 mm of the filter bed. Figure 6.14 shows the headloss development along the 600 mm filter bed depth when medium iv (2.28 mm) was used. It can be observed that the headloss development between point 3 and point 6 is remarkable, while the headloss development between point 6 and point 9 is no noticeable. This indicates that particle removal took place in the area between point 3 and point 6 which represents the first 200 to 300 mm of filter bed with no or very little penetration of particles/flocs in the upper layers (above point 6) as headloss seemed to be stabilized in this area. Results of headloss development along the filter bed of the other media can be found in Appendix D.

6.8 Backwashing

When the filter bed gets clogged, it needs to be cleaned before further use. The backwashing system used in this study is illustrated in Section 4.2.4. The effluent backwash water quality was monitored by measuring turbidity and the backwashing performance was also observed visually through the filter column. It must be noted that the backwashing was simply to clean the filter bed; the air rate and water backwash rate were not the optimum backwash conditions.

6.8.1 Backwashing of plastic media

In most of the experimental runs using plastic granules, backwashing was done by air backwash followed by water backwash. The procedure of filter backwash is discussed in Chapter 4. The total media expansion was 100 %. It was observed that all the plastic granular used in this study were well agitated during backwashing. This leads to a very high amount of detachment of the captured particles which drops down from media during air backwashing.

It was also observed that backwashing with water only did not agitate the media. As a result of that a small amount of contaminants were released from the media. That caused the backwashing process to take longer with very poor quality. The performance of filter backwash

for different media is presented in Table 6.5. Figure 6.15 shows the relation between backwashing time and backwash water turbidity. The ratio of water used for backwashing to filtrate produced water was calculated (Table 6.5).

Table 6.5: Details of backwashing

Experimental trial	Medium	Filtration velocity (m/h)	Air backwashing		Water backwashing		Volume of backwash water used (m ³ /run)	Total water produced (m ³ /run)	Water consumption (%)
			Flow rate (m ³ /h)	Time (min)	Flow rate (m ³ /h)	Time (min)			
Trial 5	Medium ii	2	14.88	2	0.61	10	0.102	0.468	21.8
Trial 2	Medium ii	4	14.50	2	0.60	10	0.100	0.312	32.05
Trial 7	Medium ii	2	14.50	2	0.63	10	0.105	0.936	11.22
Trial 1	Medium iii	2	-	-	0.62	20	0.207	0.468	66.35
Trial 5	Medium iii	2	15.30	2	0.60	12	0.120	0.624	19.23
Trial 6	Medium iii	4	13.95	2	0.62	10	0.104	0.312	33.33
Trial 7	Medium iii	2	14.88	2	0.63	10	0.105	0.936	11.22
Trial 8	Medium iii	4	-	-	0.61	25	0.254	0.312	65.70
Trial 5	Medium iv	2	14.50	2	0.62	10	0.104	0.624	16.67
Trial 2	Medium iv	4	14.50	2	0.60	10	0.100	0.312	32.05
Trial 7	Medium iv	2	14.50	2	0.62	10	0.104	0.936	11.11

The percent total water consumption for backwashing the FMF, as summarized in Table 6.5 was computed using the following expression:

$$\text{Water consumption \%} = \frac{W_b}{W_f} \times 100$$

Where:

W_b = water used for backwashing the filter (m³), and

W_f = total filtered water (m³)

A typical backwash percent for most conventional filter is between 6 and 15 % [Tchobanoglous and Burton, 1991].

Using the abovementioned criterion, the amount of water used for backwashing in this study is relatively high. It should be pointed out that the high amount of backwash water used in this

study was due to very high suspended solids (250 mg/L) containing in raw water. Conventional sand filters are usually not applied for direct filtration. Conventional sand filters are usually preceded by sedimentation unit in order to reduce the suspended solids load on the filter which is not the case in the floating media filter used in this study. Therefore, the floating media backwash results [Table 6.5] can not be compared to that used in the normal down-flow filters since the concentration of suspended solids in raw water is not the same.

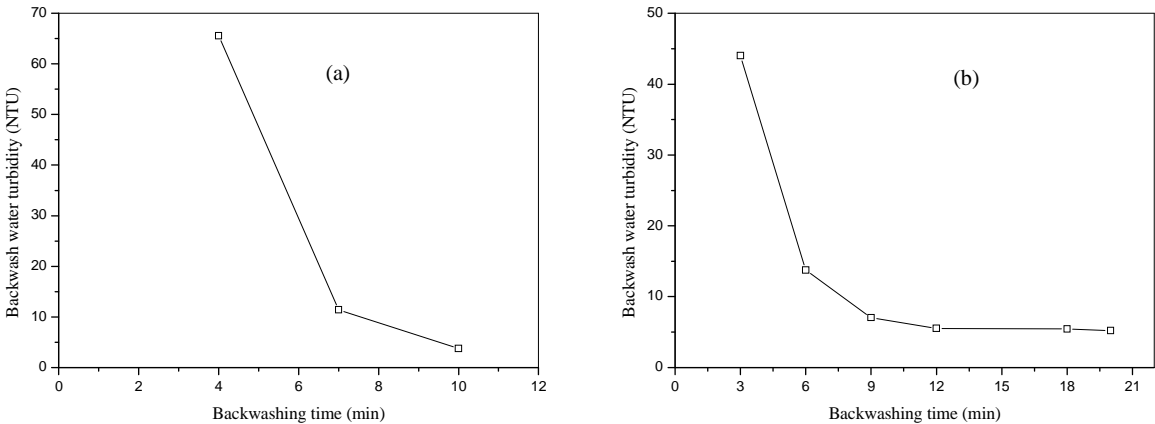


Figure 6.14: Time vs. backwash water turbidity for media iii. Backwash method: (a) air + water, (b) water only.

The backwashing performance is compared in terms of water required for the backwashing. The criterion for the backwash performance is that the turbidity of the effluent water should be as close to the influent water as possible. As can be concluded from Table 6.5 and Figures 6.15 (a and b) mentioned above, backwash with air followed by water required less water than backwash with water only, because most of the captured flocs were detached from the medium during the air backwash. This phenomenon was visually observed during the air backwash. A further observation is that in some of backwashing runs were done in this study backwash with air followed by water required half the amount of water than that used in backwash with water only to achieve the same backwash effluent quality.

6.8.2 Backwashing of combined media and LLDPE powder

It was a difficult task for the operator to do the backwashing when the media were combined (granular and fine powder) and when the medium were completely fine powder. The backwash procedure seemed not to be flexible and easy as it was in the case of plastic granular. The medium was neither agitated nor expanded well even with air backwash. Therefore air

backwash had to be done in three 2-minute periods to obtain a proper medium agitation. Water backwash was performed after each air backwash. Another major difficulty associated with combined media and fine powder backwash was the loss of the fine medium (LLDPE powder). There was actually no way of disposing sludge without losing some fine material. In this kind of backwashing, the operation was continued until the operator felt that there was a balance between cleaning the media and not losing a lot of it. This indicates that this backwashing method could not achieve 100% cleaning in combined media and fine powder.

6.9 Experimental design

A factorial experimental design was used to conduct the experiment. The three factors (filtration rising velocity, media depth, and chemical dose) and their levels are presented in Section 5.2.2.1. The experiments were carried out on three different media. The objective of the experiment was to assess the effect of the factors on the turbidity removal. Once the experiment started, the turbidity (NTU) was measured over filter run time (in hours). Figures 6.16 to 6.18 show the relationship between turbidity and filter run time for the whole experiment for each of the medium (i-iii) respectively.

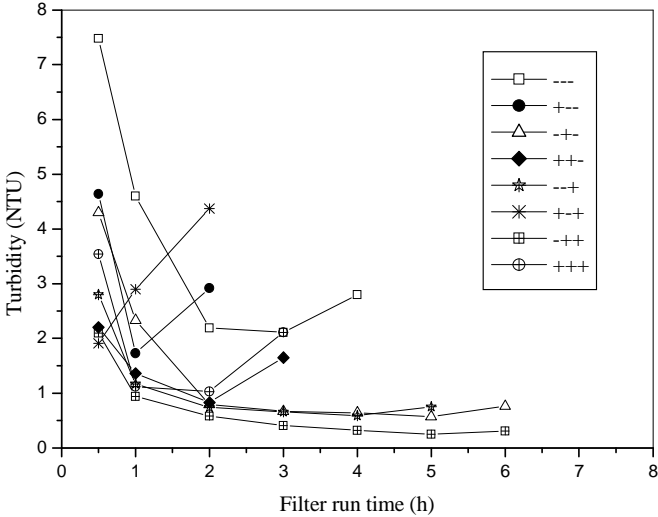


Figure 6.16: Factorial experimental trials conducted with medium i.

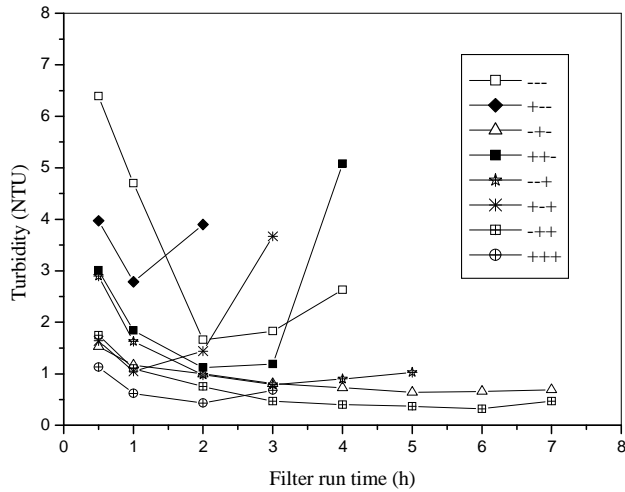


Figure 6.15: Factorial experimental trials conducted with medium ii.

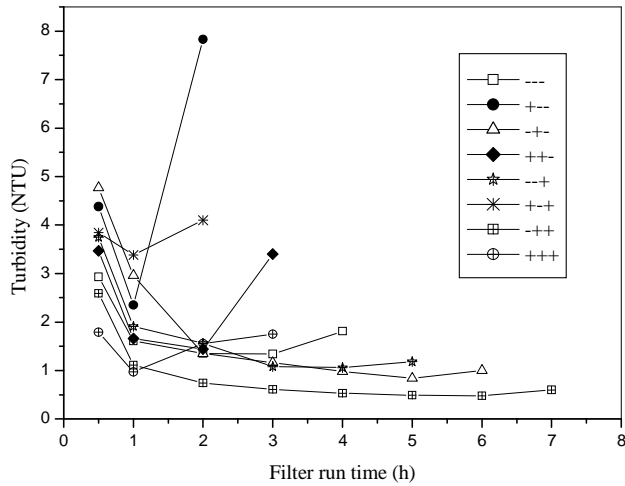


Figure 6.16: Factorial experimental trials conducted with medium iii.

It can be seen from the Figures above that there is a small difference between the three media. Experimental trial 7 (Table 5.3) which was coded as (-++) appears to be the best combination of factors since the maximum turbidity removal was achieved. This maximum corresponds to a low level for filtration rising velocity and high level for media depth and the chemical dose. On the other hand, experimental trial 2, which was coded as (+--) appears to be the worst combination of factors since the minimum turbidity removal was achieved here. The figures also reveal that the filter run time was the longest for high levels of media depth and chemical dose and for a low level of filtration rising velocity.

6.9.1 Statistical analysis

The results of the experiment were subjected to a statistical analysis. In Figures 7.16 to 7.18 the minimum turbidity over filter run time was taken as the response (dependent) variable in the analysis. The analysis was performed using the Design-Expert software (Version 7.1.6). Using the three factors (Filtration rising velocity = A, Media depth = B, and Chemical dose = C) as independent variables. For our discussion of the statistical results in Section 7.10.2 we will make use of only medium (ii) results. The data for medium (i) and (iii) are given in Appendix E. Results of the 2^4 factorial design where medium shape was included as a factor are presented in Section 6.9.3.

6.9.2 Discussion of the 2^3 factorial design results for medium ii (3.30 mm, sharp-edged cubic medium)

6.9.2.1 Factor significance using t-test

The importance of each factor is shown in the Pareto Chart (Figure 6.19), which graphically displays the magnitudes of the effects from the results obtained. The effects are sorted from largest to smallest.

Design-Expert® Software
Turbidity

A: Filtration rising velocity
B: Media depth
C: Chemical dose
■ Positive Effects
■ Negative Effects

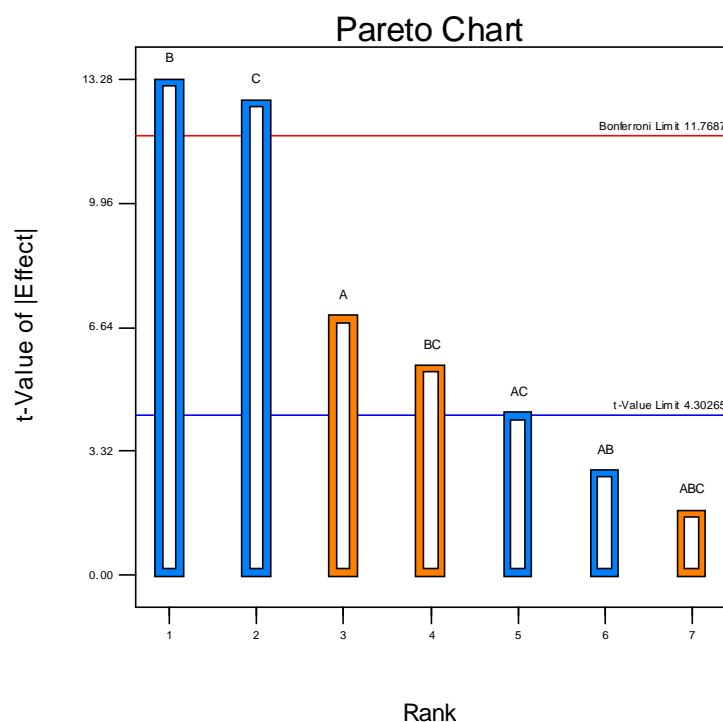


Figure 6.17: Pareto chart.

The Pareto chart clearly shows that media depth (factor B) is the most important factor affecting the removal of turbidity followed by chemical dose (factor C), and filtration rising velocity (factor A) when a t-value limit of 4.30265 adjustment is done. The conclusion from this figure is also supported by the ANOVA in the next section.

6.9.2.2 Analysis of variance

ANOVA is a widely used statistical technique to test the significance of factors and their interactions. According to the ANOVA (Table 6.6), the F values for all regressions were higher. The large value of F indicates that most of the variation in the response can be explained by the regression equation. The associated p value is used to estimate whether F is large enough to indicate statistical significance. If $p > F$ value is lower than 0.05, then it indicates that the model is statistically significant at the 95% level.

Table 6.6: Reproduced summary of ANOVA.

Source	Sum of squares	df	Mean square	F value	p-value (Prob > F)
Model	4.54	7	0.65	63.97	0.0155
A-Filtration rising velocity	0.49	1	0.49	48.36	0.0201
B-Media depth	1.79	1	1.79	176.25	0.0056
C-Chemical dose	1.64	1	1.64	161.65	0.0061
AB	0.08	1	0.08	7.89	0.1068
AC	0.19	1	0.19	18.97	0.0489
BC	0.32	1	0.32	31.58	0.0302
ABC	0.031	1	0.031	3.08	0.2212
Curvature	0.5	1	0.5	48.92	0.0198
Residual	0.02	2	0.01		
Lack of Fit	5.05	10	0.65		
Pure Error	4.54	7	0.49		
Cor Total	0.49	1			

The ANOVA results show the F -value to be 63.97, which implies that the terms in the model have a significant effect on the response. The probability p (~ 0.0155) is less than 0.05. This indicates that the model terms are significant at 95% of probability level. Any factor or interaction of factors with $p < 0.05$ is significant.

Based on the ANOVA results, the final mathematical equation (regression model) in terms of coded factors (confidence level above 95%) as determined by Design-expert software is given below:

$$\text{Turbidity} = 1.1 + 0.25 A - 0.47 B - 0.45C - 0.15 AC + 0.2 BC \tag{6.1}$$

Where:

- A filtration rising velocity [m/h]
- B media depth [mm]
- C chemical dose [mg/L]

Figure 6.20 and 6.21 show response surface plots for the relationship between filtration rising velocity, media depth and chemical dose on the removal of turbidity.

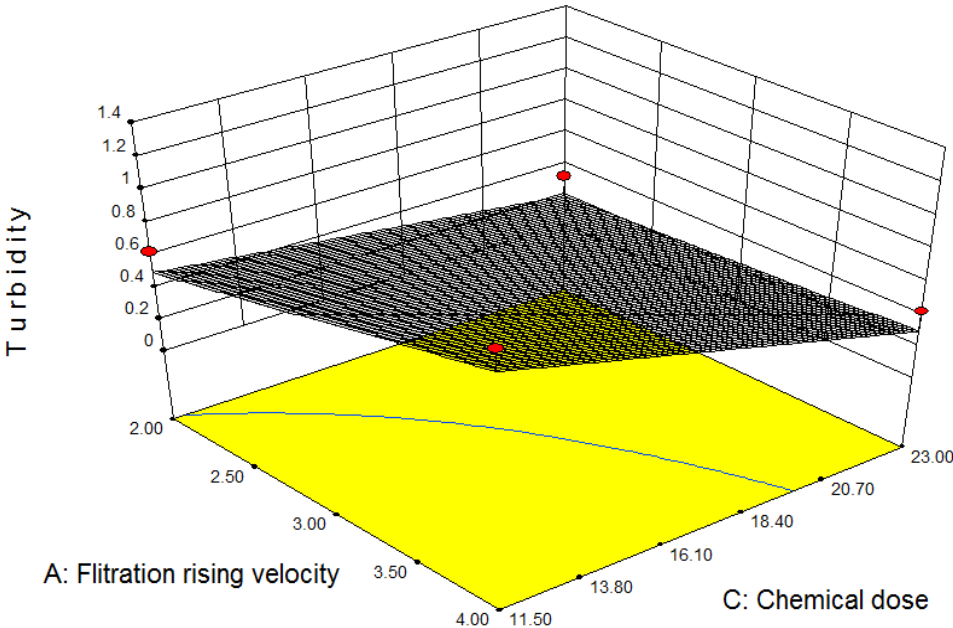


Figure 6.18: 3D response surface graph for turbidity removal vs. filtration rising velocity and chemical dose

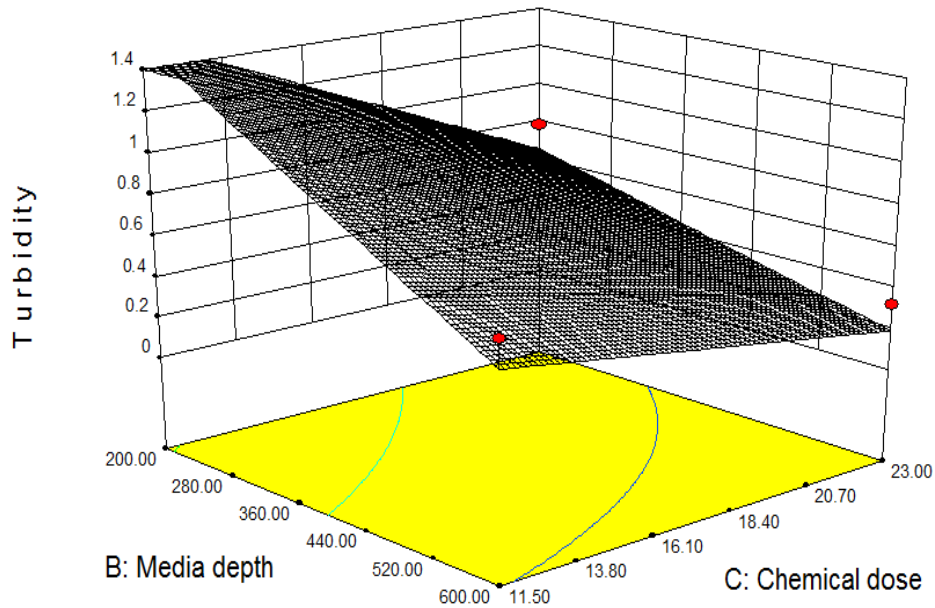


Figure 6.19: 3D response surface graph for turbidity removal vs. media depth and chemical dose.

As can be seen in Figure 6.20 at lower filtration rising velocity of 2 m/h, the chemical dose value needed for maximum turbidity removal was at 23 mg/l (high level). However, at higher filtration rising velocity and lower chemical dose value, the turbidity removal declines. This may be due to the effect of faster filtration velocity forces particles to penetrate into the filter bed as described earlier in this chapter.

The analysis using full factorial design conducted on the other two types of medium (i and iii) proved that the media depth had the most significant effect at the 0.05 level. Therefore to improve process performance, it is obvious that we should begin by adjusting the factor, which had the biggest effect.

6.9.3 Discussion of the 2⁴ factorial design results

2⁴ factorial design was done in order to investigate the effect of the medium shape (factor D) on the removal of turbidity. The first attempt was to investigate the effect of the medium type by comparing medium (i) and medium (ii) and the second attempt was to compare the best performing medium in the first attempt and medium (iii). Figures 6.22 and 6.23 show the effect of medium size in which medium i ($d_{50} = 3.03$ mm) was compared to medium ii ($d_{50} = 3.30$ mm).

mm). Medium (i) was indicated by the low level (1) of factor D and medium (ii) was indicated by the high level (2).

As can be seen from the Figures medium (ii) performed better than medium (i) since using medium (ii) leads to more particles (turbidity) are to be removed. And that could be referred to the fact that medium (ii) is a sharp-edged cubic that could lead to a more compacted media within the filter bed and could also be due to the surface properties between these two media.

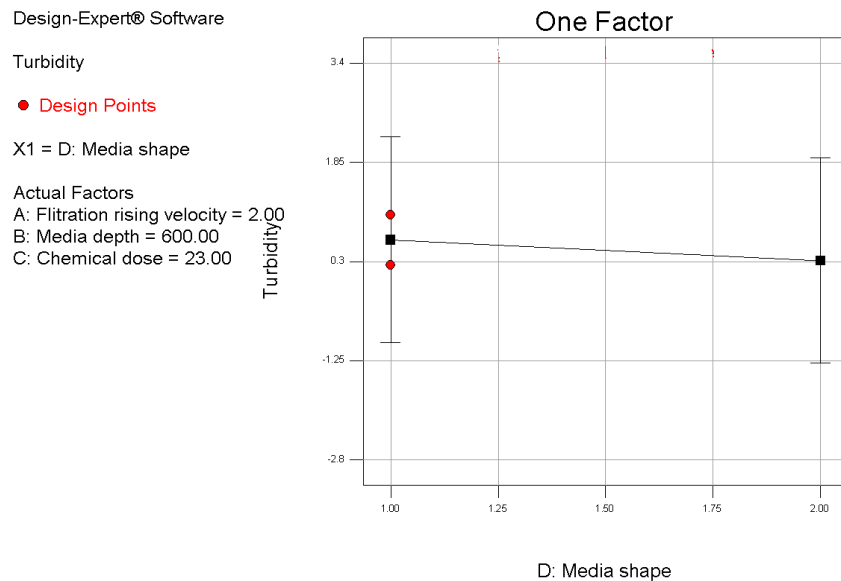


Figure 6.20: Effect of medium shape on Turbidity (a).

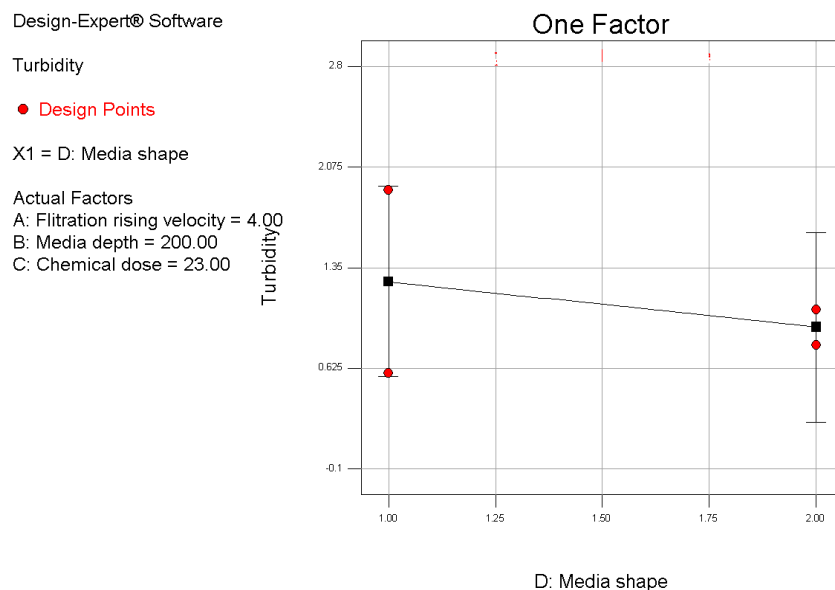


Figure 6.21: Effect of the medium shape on Turbidity (b).

It must be noted that the medium type is involved in an interaction. Therefore it can not be interpreted that factor D (medium shape) by itself affect the response (Turbidity). Figure 6.24 shows the relationship between the medium shape-chemical dose interaction and turbidity removal. Figure 6.24 indicates that the maximum turbidity removal was achieved with medium (ii) when the chemical dose was at high level. On the other hand there was no significant difference between the performances of both media at the low level of chemical dose (factor C). That proves the point that medium shape does not affect the response by itself, its importance appears to have a significant effect when it is combined with the effect of chemical dose

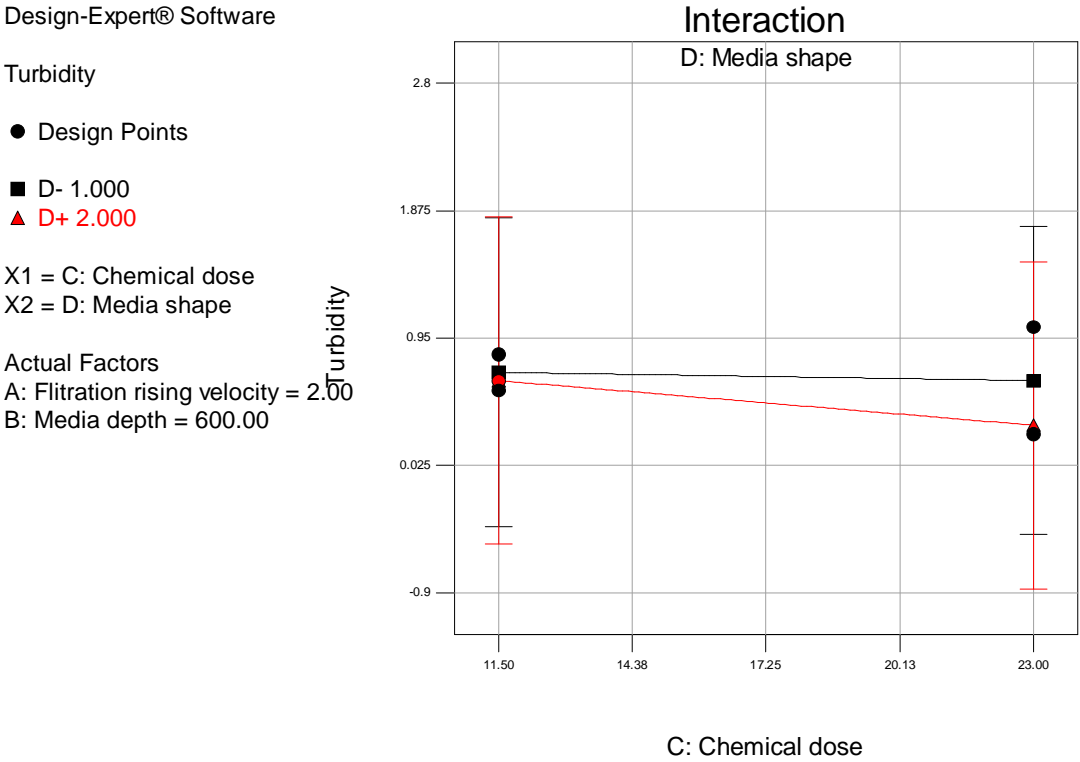


Figure 6.22: Effect of interaction CD.

Based on the previous 2^4 statistical results which showed that medium (ii) outperforms medium (i) in terms of turbidity removal at certain condition of chemical dose. Thus, in the next section medium (ii) is considered for comparison with medium (iii), which has a different shape (disc-shaped). Medium (ii) this time is indicated by the low level (1) of factor D and medium (iii) is indicated by the high level (2). Based on ANOVA and Pareto chart (Figure 6.25) the media

depth (factor B) is by far the most important factor affecting the turbidity removal. No other factors or interactions appear to be significant. The chemical dose-media shape interaction and the effect of the medium shape also appear to have an influential effect on the process.

Design-Expert® Software
Turbidity

- A: Filtration rising velocity
- B: Media depth
- C: Chemical dose
- D: Media shape
- Positive Effects
- Negative Effects

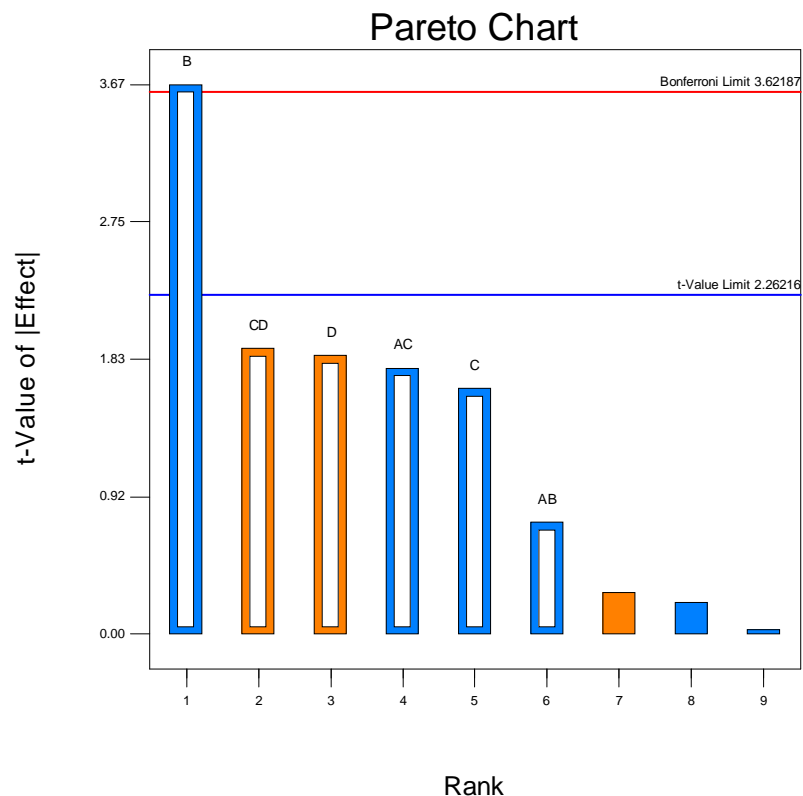


Figure 6.23: Pareto chart of main effects in the factorial 2^4 design.

The effect of medium shape (factor D) can be further interpreted in Figures 6.26 and 6.27. Figure 6.26 indicates that when the chemical dose was at high level there was a significantly large difference between the performance of medium ii (indicated by 1) and medium iii (indicated by 2). Medium ii appears to perform better than medium iii in terms of turbidity removal. However, when the chemical dose decreases to a low level there was no significant difference between the performances of both media (Figure 6.27).

Design-Expert® Software

Turbidity

X1 = D: Media shape

Actual Factors

A: Filtration rising velocity = 2.00

B: Media depth = 200.00

C: Chemical dose = 23.00

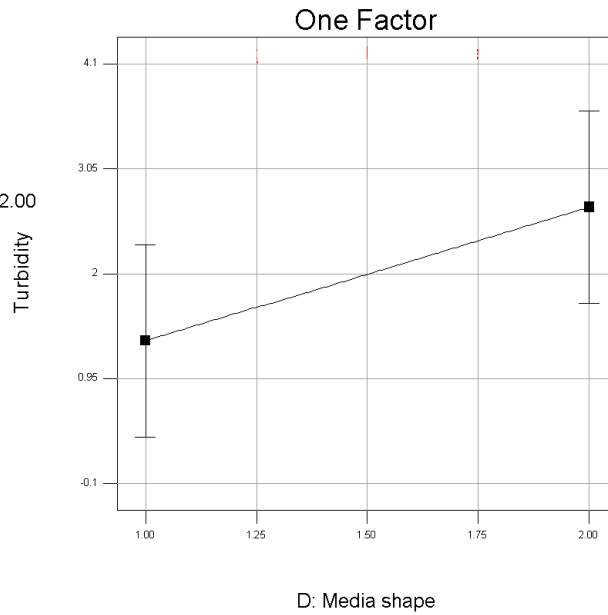


Figure 6.24: Effect of the medium shape on Turbidity at optimal chemical dose.

Design-Expert® Software

Turbidity

● Design Points

X1 = D: Media shape

Actual Factors

A: Filtration rising velocity = 2.00

B: Media depth = 600.00

C: Chemical dose = 11.50

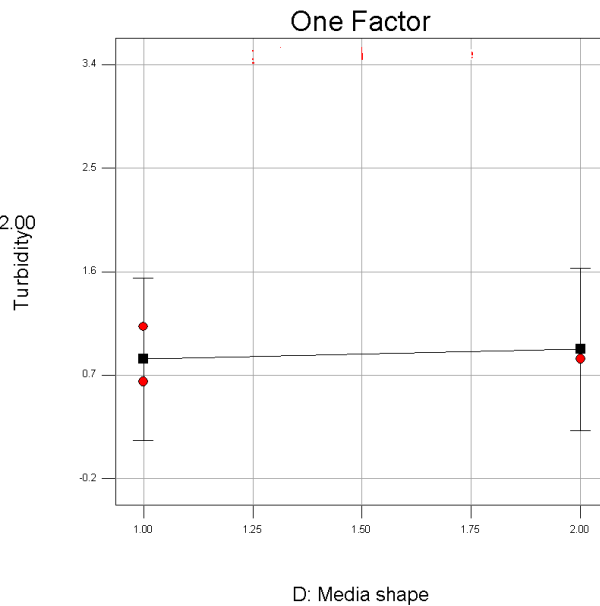


Figure 6.25: Effect of the medium shape on Turbidity at low level of chemical dose.

Figure 6.28 shows the effect of chemical dose-medium shape interaction. As seen in Figure 6.28 medium (ii) outperforms medium (iii). The best turbidity removal was achieved with medium (ii) and optimal (high level) chemical dose. A reasonable explanation is given in sections 6.6.3. and 6.6.5

Turbidity

● Design Points

■ D- 1.000

▲ D+ 2.000

X1 = C: Chemical dose

X2 = D: Media shape

Actual Factors

A: Filtration rising velocity = 2.00

B: Media depth = 200.00

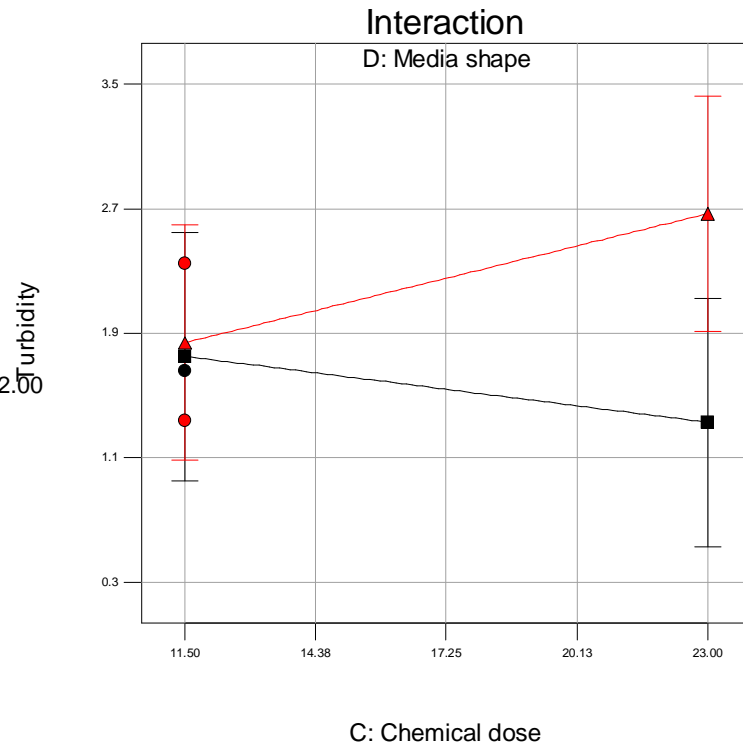


Figure 6.26: Effect of interaction CD.

It can be concluded that the analysis using 2^4 factorial design reveals that medium size and surface roughness play a role in enhancing turbidity removal. It can also be concluded that medium ii (sharp-edged cubic) outperforms medium iii (disc-shaped). Despite the fact that medium (ii) has a smaller size than that of medium (iii), the better performance could also be attributed to the medium shape and surface properties. Medium ii ($d_{50} = 3.30$ mm) has a cubic shape with sharp sides and a rough surface, while medium iii ($d_{50} = 4.07$ mm) has a disc shape with a smooth surface. Detailed interpretation of the effect of medium size and medium shape can be found in the previous sections of this chapter.

7 Conclusions

A study on a pilot plant (diameter of 0.3 m and height of 2.8 m) was conducted to observe a contact flocculation filtration process using floating medium. The aim of the floating medium filter pilot plant was to provide results that would allow investigation into the effects of the physical properties (size and shape) of the media on the performance of a floating medium filter.

The pilot plant was fed with an artificial water solution (250 mg/L bentonite). Visual observation of flocculation and solids removal in the column was possible. Filtrate turbidity was measured and filtration tests were continued until the turbidity rose significantly, at which point breakthrough was assumed to have been reached. Breakthrough times ranged between 2 and 7 hours, which is considered short and was due to the high solids loading of the feed solution. Pressure tappings allowed headloss to be monitored during experiments.

In this study, three factors that could possibly affect the filtration process were investigated. These included the filtration rate, the filter bed depth and the chemical coagulant dosage. The best conditions to remove particles (turbidity) were found to be: (i) filtration rate at $36.8 \text{ L/m}^2 \cdot \text{min}$, allowing slower clogging interstitial spaces within the medium grains and hence longer filter run time, (ii) filter bed depth of 600 mm, allowing particles to have the opportunity to potentially interact with more medium grains, and hence the chance for particle attachment to and within media grains, and (iii) chemical coagulant dosage of 23 mg/L, allowing a greater number and bigger size of flocs to be formed.

Decreasing the medium size increases the surface area and tortuosity of the filter bed, while decreasing the interstitial spaces within the medium grains. All these factors led to increase the turbidity removal as it was observed with the smaller medium (2.28 mm). Filtrate quality with 0.4 NTU was achieved by using medium size of 2.28 mm and voidage of 0.31. However, the increase in removal efficiency is counterbalanced by an increase in the headloss development. Headloss development experienced by the smaller medium was higher (109 mm of H_2O) than

that experienced by the three other media (42 mm of H₂O). Both headloss readings were at breakthrough time.

Results and experimental observations of headloss development along the filter bed showed that the effective bed depth (the minimum depth that produces the best water quality of filtrate) reduces with reduction in effective medium size. The effective bed depth for the smaller medium (2.28 mm) was \approx 0.2 to 0.3 m of 0.6 m depth, while the effective bed depth for the three other media (3.03, 3.30 and 4.07 mm) was greater than 0.3 m. These findings suggest that larger-size medium and greater depths might be a more optimal filter design from the standpoint of turbidity removal and headloss development.

Shape of medium grains leads to various grains packing, which changes the liquid flow through the filter bed. The more compact the filter bed the less the voidage, the better the particle removal. Although the size of media experimented in this study was inconsistent, the shape of some media such as medium ii (angular medium) led to better performance compared to medium iii (smooth disc-shaped medium). Angular granular medium grains result in low filter bed voidage (0.36) as they can readily interlock. However, these findings should be further investigated with consistent medium size in order to confirm the aforementioned conclusion.

In a FMF, when linear low density polyethylene (LLDPE) powder ($d_{50} = 600 \mu\text{m}$) was used as the filter medium, the filtration process (particle removal) occurred in the first few centimeters of the filter bed. This indicates that the FMF acts as a surface filter when LLDPE powder is used on its own. This surface filtration led to an excellent filtrate quality (0.14 NTU). Although the performance of the filter was excellent, loss of filter media during backwash was unavoidable.

The experimental results reported in this study showed that the chemical coagulant dosage and flocculation time are important factors affecting floc size. Larger-size flocs were formed with higher coagulant dosage (23 mg/L) and long flocculation time (≥ 20 minutes).

The statistical analysis indicated that media depth has the most significant effect on turbidity removal. The statistical analysis also indicated that medium size play a role on the turbidity removal.

For high turbid feed water (as it was in this study), the filter run time is very short and it lies between 2 and 7 hours because the greatest portion of suspended solids is retained within the filter bed itself. Consequently, every 2 to 7 hours interval, the FMF is to be backwashed. Therefore, it can be said that the FMF can not be used as a complete treatment process for high turbid water. However, it could be used as a pre-filter, prior to low-pressure membrane drinking water filtration technology.

Although optimization of backwashing conditions was not targeted in this study, the optimization of the hydraulic backwash load is very important in making the process economically competitive. An effective backwash strategy in terms of the hydraulic load of backwashing water as well as backwashing volume should be incorporated into the operation procedure of upflow floating media filter.

Recommendations

Based on the findings of this study, the following recommendations for further studies are made.

- Medium shape should be further investigated with consistent medium size.
- Pilot scale experiments should be conducted to study the effect of various feed water turbidities.
- Experiments should be carried out to investigate the effect of using different coagulants such as alum.
- FMF should be tested for treating surface water which contains natural organic matter (NOM) in order to investigate its performance in removing NOM.

References

- Adin, A., Baumann, E.R. and Cleasby, A.L., 1979. The application of filtration theory to pilot plant design. *Journal of the American Water Works Association*, **71**(1), 17-27.
- Adin, A. and Rebhun, M., 1974. High rate contact flocculation filtration with cationic polyelectrolytes, *Journal of the American Water Works Association*, **66**(2), 109-117.
- Ahmed, H., 1996. The effects of flux rate and solids accumulation on small size particle accumulation in expandable granular bead filters. Masters thesis, Louisiana State University, USA.
- Amirtharajah, A., 1988. Some theoretical and conceptual views of filtration. *Journal of the American Water Works Association*, **80**(12), 36-46.
- Arndt, R.E. and Wagner, E.J., 2003. Filtering myxobolus cerebralis triactinomyxons from contaminated water using rapid sand filtration. *Aquacultural Engineering*, **29**, 77-91.
- An-shu, L., 1982. Technical comparison of direct filtration and contact-flocculation filtration processes. Masters thesis No. 84-18, Asian Institution of Technology, Bangkok.
- Bache, D.H. and Rassol, E.R., 2001. Characteristics of alumino-humic flocs in relation to DAF performance, *Water Science. Technol.* **43** (8), 203–208.
- Baker, M.N., 1981. The quest for pure water. Second edition. Vol. 1. Denver, CO: American Water Works Association\
- Bellelo, S. M., 2006. Evaluation of media influence and practical applications for the use of static low density media filters in domestic wastewater treatment. Masters thesis, Louisiana State University and Agricultural and Mechanical College, USA.
- Ben Aim, R., Shanoun A., Visvanathan, C. and Vigneswaran, S., 1993. New filtration media and their use in water treatment. *Proceedings of the World Filtration Congress*, Nagoya, Japan, pp. 273-276.

- Benedek, A. and Bancsi, J.J., 1977. Comparative evaluation of commercial polyelectrolytes for flocculating alum precipitated domestic wastewater. *Progress in Water Technology*, **9**, 33-42.
- Boller, M., 1993. Filter mechanisms in roughing filters. *Journal of Water Supply Research. Technol. Aqua*. **42**(3): 174-85
- Camp, T.R., 1964. Theory of water filtration. *Journal of the Sanitary Engineering Division, ASCE*, **90**(SA4), 1-30.
- Carmen, P.C., 1937. Fluid flow through granular bed. *Transactions Institution Chemical Engineers*, **15**, 150-166.
- Chiemchaisri, C., Panchawaranon, C., Rutchatanunti, S., Kludpiban, A., Ngo, H.H. and Vigneswaran, S., 2003. Development of floating plastic media filtration system for water treatment and wastewater reuse. *Environmental Science and Health*, **38**(10), 2359-2368.
- Collins, M.R., Eighmy, T.T. and Malley, J.P.(Jr.), 1991. Evaluating modifications to slow sand filters. *Journal of the American Water Works Association*, **83**(9), 62–70.
- Collins, MR., Westersmund, CM., Cole, JO., Roccaro, JV., 1994. Evaluation of roughing filtration design variables. *American Water Works Association Research Foundation and American Water Works Association*
- Culp, G.L and Culp, R.L., 1974. *New Concepts in Water Purification*, New York: van Nostrand Reinhold. pp. 51-108.
- Delphos, P. J. and Wesner, G. M., 2005. *Mixing, Coagulation, and Flocculation*. In: Barath, E.E. *Water Treatment Plant Design*. 4th edition. New York: McGraw-Hill Professional.
- El Etriby, H.K. and Menlibai, M., 1997. Sewage tertiary treatment using floating media filters. Second International water technology conference, Alexandria, Egypt,
- Ergun, S., 1952. Fluid flow through packed columns. *Chemical Engineering Progress*, **48**(2), 89-94.
- Fernlund, J.M., 1998. The effect of particle form on sieve analysis: a test by image analysis. *Engineering Geology*, **50**(1-2), 111-124.

- Fitzpatrick, C.S.B., 1998. Media properties and their effect on filter performance and backwashing. *Water Science and Technology*, **38**(6), 105-111.
- Fogel, D. Isaac-renton, J., Guasparini, R., Moorehead, W. and Onger, J., 1993. Removing giardia and cryptosporidium by slow sand filtration. *Journal of the American Water Works Association*, **85**(11), 77-84.
- Galvis, G., 1999. Development and evaluation of multistage filtration plants. PhD thesis, University of Surry, United Kingdom.
- Hamann, C.L. and McKinney, R.E., 1968. Upflow filtration process. *Journal of the American Water Works Association*, **60**(9), 1023-1039.
- Higgins, T.E., 1981. Treatment of Plating Waste Waters by Ferrous Reduction, Sulfide Precipitation, Coagulation and Upflow Filtration; NTIS Report EPG-R-8104: Washington, DC, 1981. pp. 1-187.
- Hultman, B., Jonsson, K. and Plaza, E., 1994. Combined nitrogen and phosphorous removal in a full-scale continuous up-flow sand filter. *Water Science and Technology*, **29**(10-11), 127-134.
- Hutchion, W. and Foley, D.P., 1974. Operational and experimental results of direct filtration. *Journal of the American Water Works Association*, **66**(2), 79-87.
- Ives, K.J., 1961. Filtration using radioactive algae. *Journal of the Sanitary Engineering Division, ASCE*, **87**(SA3), 23-37.
- Ives, K.J., 1970. Rapid filtration. *Water Research* 4:201-223.
- Iwai, S. and Kitao, T., 1994. Wastewater treatment with microbial films. Lancaster, EUA: Technomic Publishing. p. 178-184.
- Iwatani, Akitoshi and Muragame, JP., 1980. Filter apparatus using floating filter medium. United States Patent 4198301.
- Jaccarino, R. Filter Treatment Using Upflow Filtration. *Water Engineering Management*, 1991, June, 22

- Jegatheesan, V., and Vigneswaran, S. (2005) *Deep bed filtration: Mathematical models and observations*. Critical Reviews in Environmental Science and Technology, 35 . pp. 515-569.
- Jellison, K., Dick, R. and Weber-Shirk, M., 2000. Enhanced ripening of slow sand filters. *Journal of Environmental Engineering*, **126**(12), 1153-1157.
- Logsdon, G. S., Neden, D.G., Ferguson, A.M.D. and LaBonde, S. D., 1993. Testing of direct filtration for treatment of high turbidity water. *Journal of the American Water Works Association*, **85**(12), 39-46
- Metcalf and Eddy Inc., 1991. *Wastewater Engineering Treatment, Disposal, and Reuse*. 3rd edition. Boston: McGraw-Hill.
- Monk, R.D.G. and Gagnon, A.P., 1985. A new method of filter monitoring. *Public Works*, **116**(10), 68
- Montgomery, D.C., 1997 *Design and Analysis of Experiments*. 4th edition. New York, NY: Wiley & Sons.
- Montgomery, D.C. and Runger, G.C., 2003. *Applied Statistics and Probability for Engineers*. 3rd edition. New York, NY: Wiley & Sons.
- Narin, M., 1994. Pilot scale flocculation filter study for surface water filtration. Masters thesis EV-94-17, Asian Institute of Technology, Bangkok.
- Ngo, H.H. and Vigneswaran, S., 1995. Application of floating media filters in water and wastewater treatment with contact-flocculation filtration arrangement. *Water Research*, **29**(9), 2211-2213.
- Odira, P.M.M.A., 1985. Upflow filter in Flocculation and direct filtration of water of high turbidity. Publication No. 37, Tampere University of Technology, Tampere, Finland.
- Ødegaard, H. and Helness, H., 1999. Floating filters for particle removal in sewage treatment. *Journal of the Chartered Institution of Water and Environmental Management*, **13**(5), 338-342.
- O' Melia, C.R. and Stumm, W., 1967. Theory of water filtration. *Journal of the American Water Works Association*, AWWA, **59**(11), 1393.

- Peladan, J.G., Lemmel, H. and Pujol, R., 1996. High nitrification rate with upflow biofiltration. *Water Science and Technology*, **34**(1-2), 347-353.
- Ranjit, K.R., 2001. Design of experiments using the TAGUCHI approach. New York, NY: Wiley & Sons.
- Reynolds, T.D. and Richards, P., 1982. Unit Operations and Processes in Environmental Engineering. 2nd edition. Boston: PWS Publishing Company. pp. 131-169.
- Ripperger, S., 1989. Microfiltration. In: Vigneswaran, S. and Ben Aim, R. (eds). Water, Wastewater and Sludge Filtration. CRC Press: Florida.
- Rhodes, M., 2008. Introduction to Particle Technology. 2nd edition. Chichester: Wiley & Sons. pp.153-156.
- Schwarzkopf, S.H., 2006. Liquid filtration apparatus and method embodying super-buoyant filtration particles. European Patent EP1680362.
- Shea, T.G., Gates, W.E. and Argaman, Y.A., 1971. Experimental evaluation of operating variables in contact flocculation. *Journal of the American Water Works Association*, **63**(1), 41-48.
- Stanley, D.R., 1955. Sand filtration studies with radio-tracers. *Journal of American Society of Civil Engineers*, **81**, 592
- Stuckenberg, J.R. and Hesby, J.C., 1991. Pilot testing the Haberer process in the United States. *Journal of the American Water Works Association*, **83**(9), 90-96.
- Sundarakumar, R., 1996. Pilot scale study on floating media filtration for surface water treatment. Masters thesis EV-96-31, Asian Institute of Technology, Bangkok.
- Tchobanoglous, G. and Burton, F.L., 1991. Wastewater Engineering Treatment, Disposal, and Reuse. 3rd Ed., McGraw-Hill, New York.
- Tobiason, JE. And Vigneswaran, S., 1994. Evaluation of a modified model for deep bed filtration. *Journal of Water Research*. 28:335-342

Trochim, W.M.K., 2006. Research Methods Knowledge Base, "Factorial Designs". <<http://www.socialresearchmethods.net/kb/expfact.htm>> (Accessed: 10/05/2009.)

Trussell, R.Rhodes., Trussell, Albert.R., Lang, John.S., and Tate, Carol.H., 1980. Recent developments in filtration system design. *Journal of the American Water Works Association*, **72**(12), 705-710.

Wagener, C.A., 2003. Evaluation of static low density media filters for use in domestic wastewater treatment. Masters thesis, Louisiana State University, USA.

Weber, W.J., 1972. Physicochemical Process for Water Quality Control. New York: Wiley-Interscience.

Wegelin, M., 1986. Horizontal flow roughing filtration, a design construction and operation manual. IRCWD Report No 06/86, Switzerland.

Werellagama, D.R. and Induka, B., 1993. Application of the floto filter unit for contact flocculation filtration of surface waters. Masters thesis EV-93-26, Asian Institute of Technology, Bangkok.

Tchobanoglous, G. and Schroeder, E.D., 1985. Water Quality Characteristics, Modeling, Modification. Reading, MA Addison-Wesley Publishing.

Uthus, L., Hoff, I. and Horvli, I., 2005. Evaluation of grain shape characterization methods for unbound aggregates. In: Proceedings of the 7th International Conference on the Bearing Capacity of Roads, Railways and Airfields, Trondheim, Norway.

La Leva di Archimede, Water: The importance of water. Available: <http://www.laleva.cc/environment/water.html> (Accessed: 15/03/2009)

Wang, S., Terdkiatburana, T. and Tade, M.O., 2008. Single and co-adsorption of heavy metals and humic acid on fly ash. *Journal of Separation and Purification Technology*, **58**, 353-358.

Yan, W.L. and Bai, Renbi., 2005. Adsorption of lead and humic acid on chitosan hydrogel beads. *Journal of Water Research*. **39**(4), 688-698.

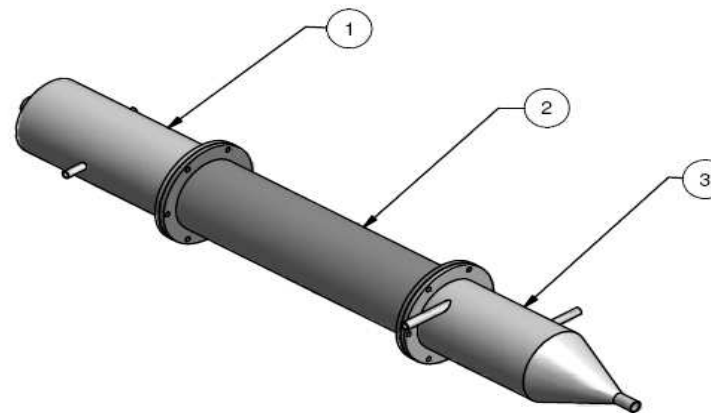
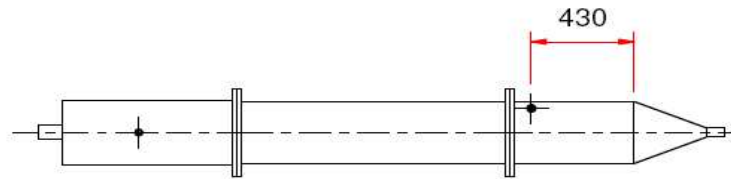
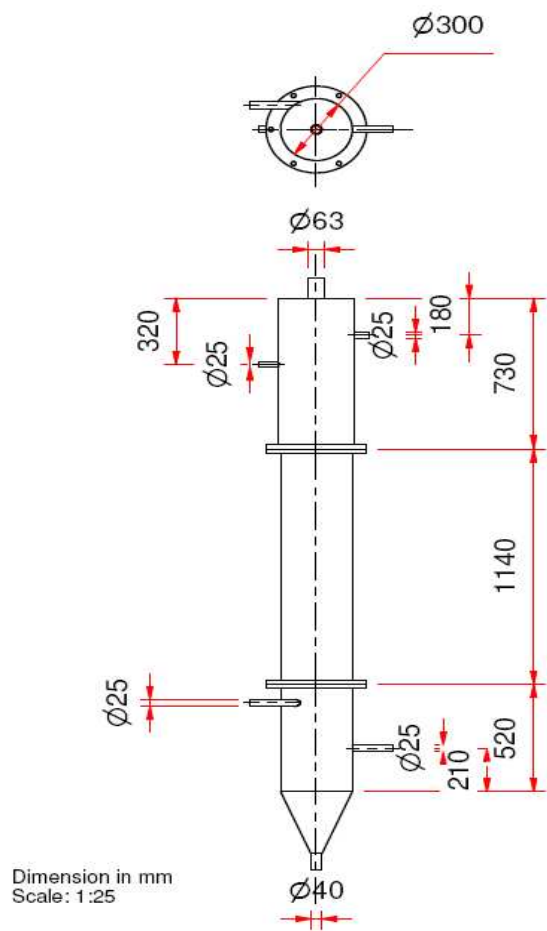
Yao, K.M., Habibian, M.T. and O'Melia, C.R., 1971. Water and wastewater filtration: concepts and applications. *Environmental Science and Technology*, **5**(11), 1105-1112

Zamani, A. and Maini, B., 2009. Flow of dispersed particles through porous media - Deep bed filtration. *Journal of Petroleum Science and Engineering*, **69**, 71-88.

Zouboulis, A., Lazaridis, N. and Grohmann, A., 2002. Toxic metals removal from waste waters by upflow filtration with floating filter medium. I. The case of zinc. *Separation Science and Technology*, **37**(2), 403-416

Appendix A

Pilot plant design drawings



1	TOP SECTION	1	PVC
2	MIDDLE SECTION	1	PVC
3	BOTTOM SECTION	1	PVC

Figure A.1: Filter column.

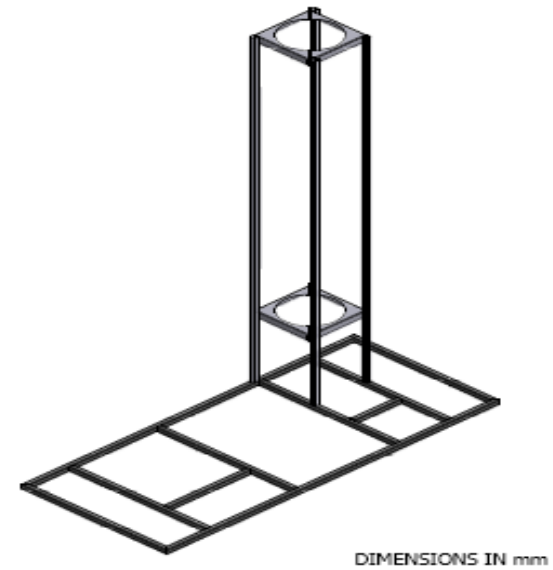
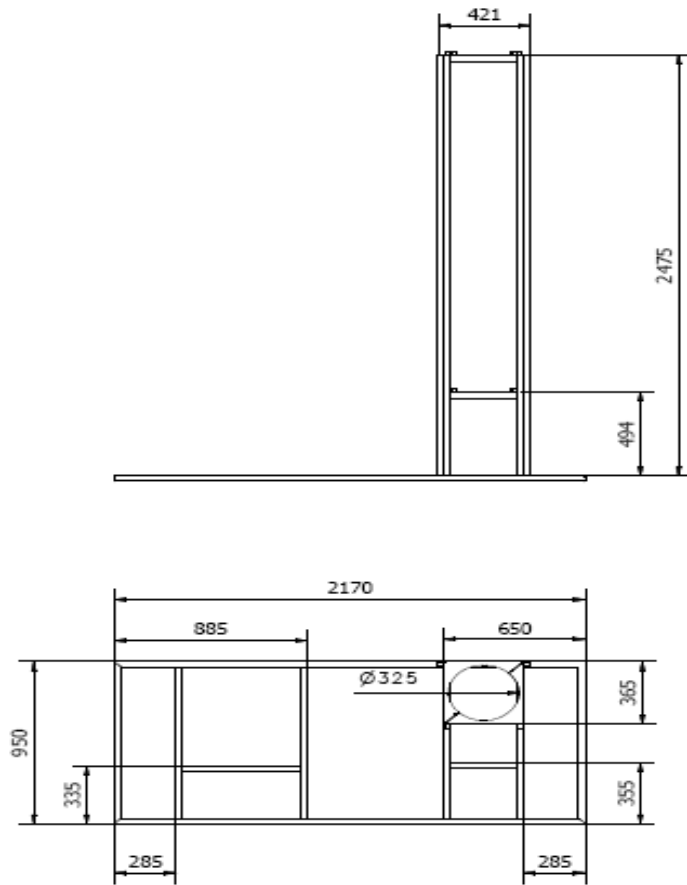


Figure A.2: Frame.

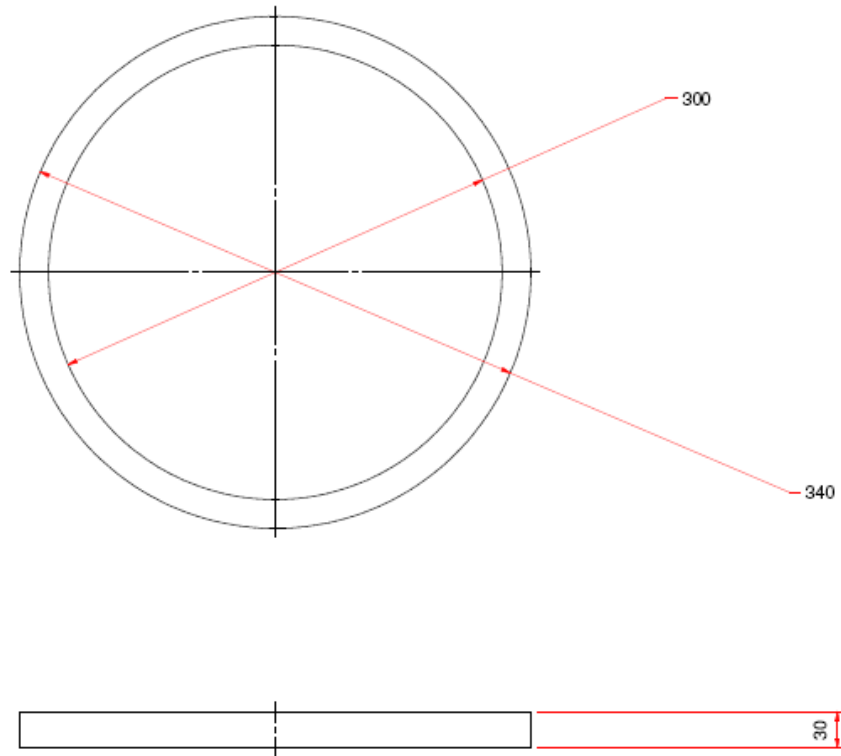
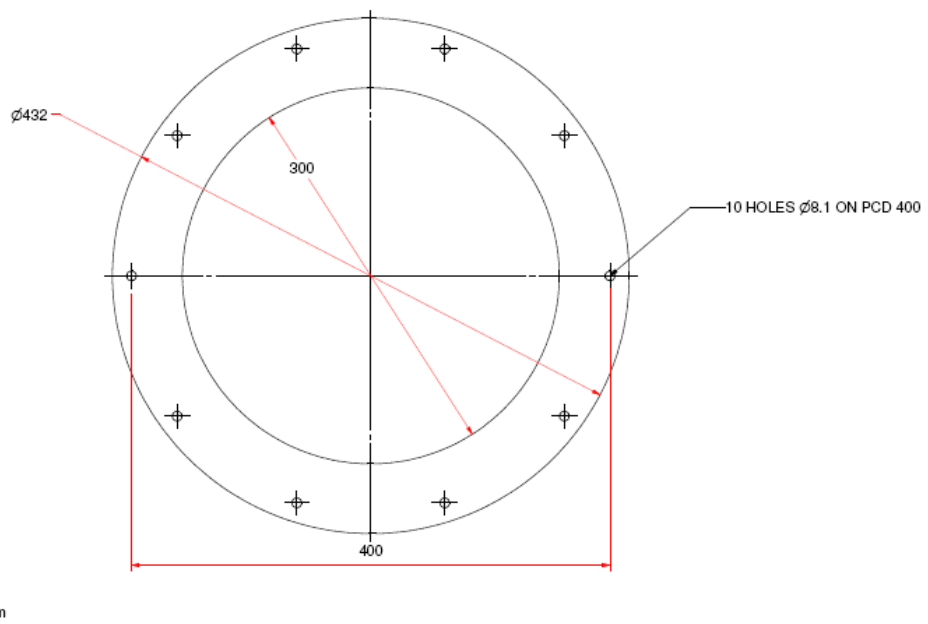
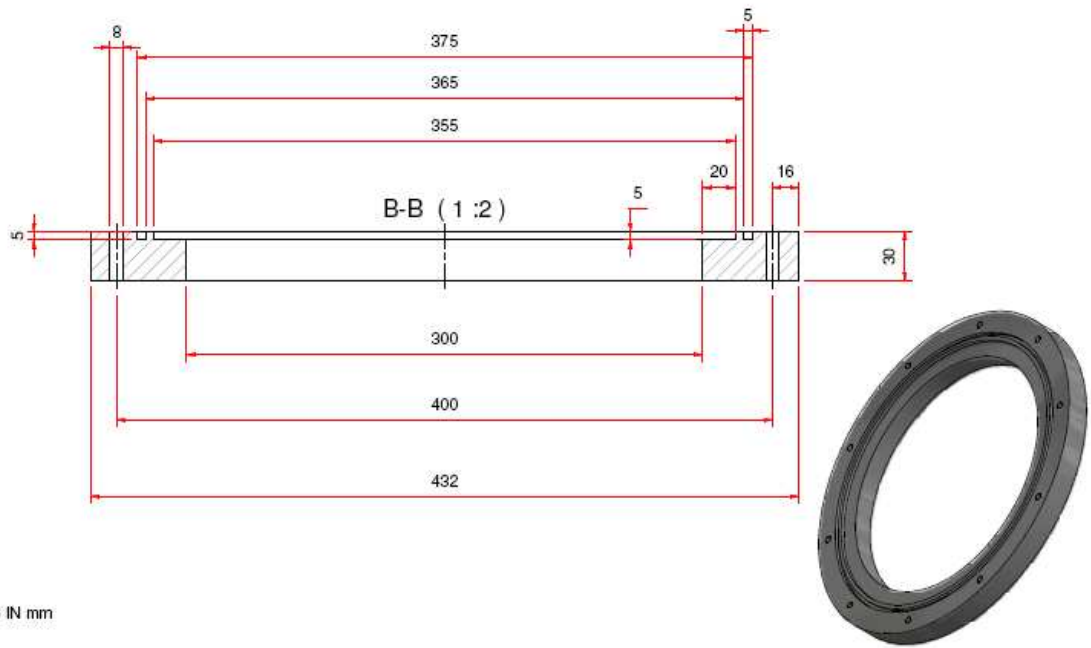


Figure A.3: Blank (support) flange.



DIMENSIONS IN mm

Figure A.4: Top flange.



DIMENSIONS IN mm

Figure A.5: Bottom flange.

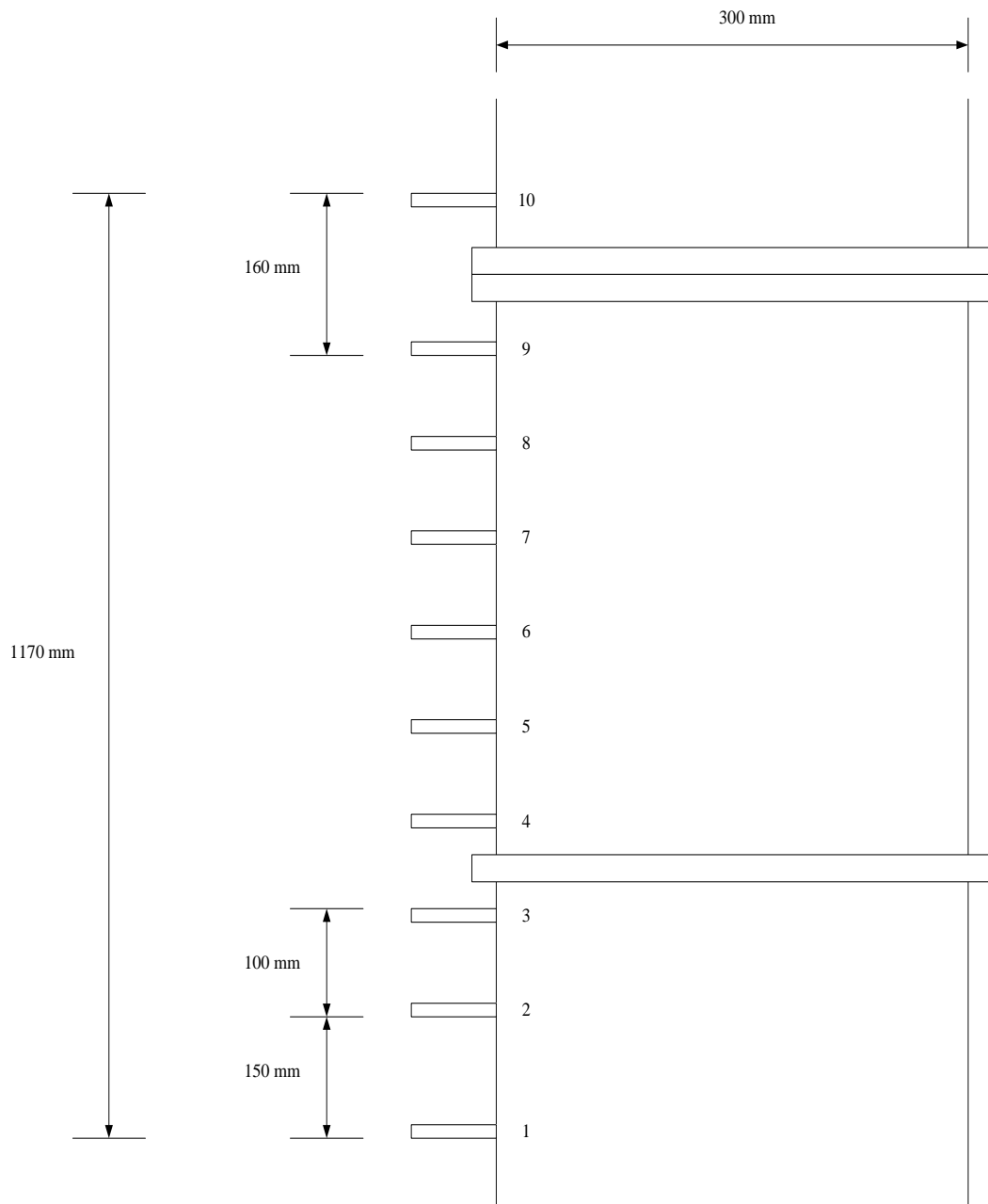


Figure A.6: Piezometer points.

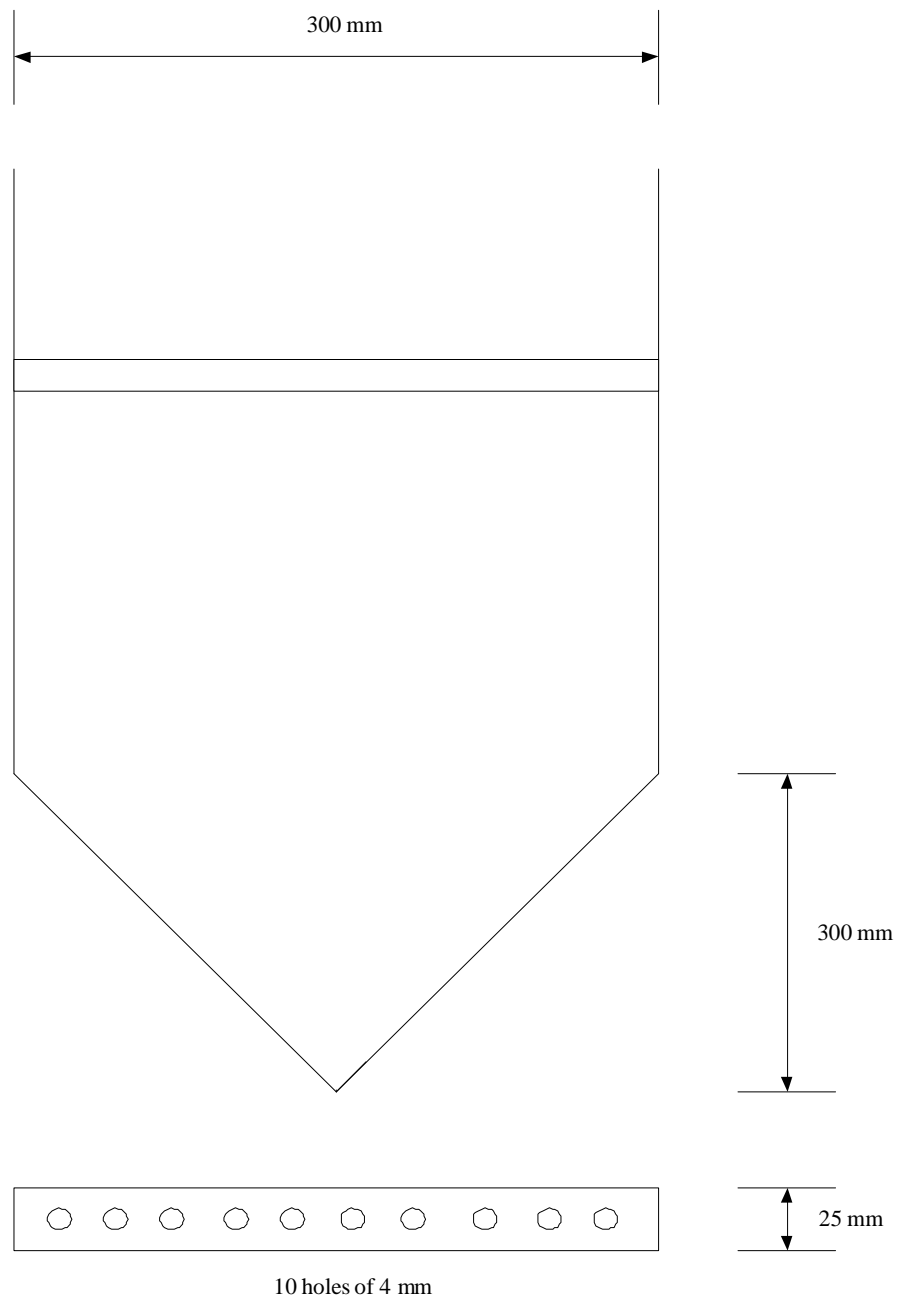


Figure A.7: Air inlet system.

Appendix B

Calculations

Table B.1: Calculated media properties of medium i

Exp.Run	Filtration velocity (m/h)	Interstitial velocity (m/h)	Reynolds number in filter bed (-)	Reynolds number in pipe (-)	Dean number (-)	Modified Dean number (-)	Headloss across filter bed (cm)	Velocity gradient in filter bed (s^{-1})
1	2	9.03	2.97	13.86	4.65	4.646	1.02	63.17
2	4	18.07	5.93	27.72	9.30	9.29	1.58	111.19
3	2	9.03	2.97	13.86	4.65	4.646	2.3	54.77
4	4	18.07	5.93	27.72	9.30	9.29	4.15	104.04
5	2	9.03	2.97	13.86	4.65	4.646	1.25	69.93
6	4	18.07	5.93	27.72	9.30	9.29	3.04	154.22
7	2	9.03	2.97	13.86	4.65	4.646	4.2	74.01
8	4	18.07	5.93	27.72	9.30	9.29	3.45	94.86
9	3	13.55	4.45	20.79	6.98	6.97	3.15	96.14
10	3	13.55	4.45	20.79	6.98	6.97	2.10	78.50
11	3	13.55	4.45	20.79	6.98	6.97	2.05	77.56

Table B.2: Calculated media properties of medium ii

Exp.Run	Filtration velocity (m/h)	Interstitial velocity (m/h)	Reynolds number in filter bed (-)	Reynolds number in pipe (-)	Dean number (-)	Modified Dean number (-)	Headloss across filter bed (cm)	Velocity gradient in filter bed (s ⁻¹)
1	2	5.09	3.37	13.86	4.65	4.646	2.25	74.04
2	4	10.18	6.75	27.72	9.30	9.29	1.5	85.50
3	2	5.09	3.37	13.86	4.65	4.646	3.13	50.42
4	4	10.18	6.75	27.72	9.30	9.29	4.25	83.10
5	2	5.09	3.37	13.86	4.65	4.646	1.1	51.77
6	4	10.18	6.75	27.72	9.30	9.29	1.75	92.35
7	2	5.09	3.37	13.86	4.65	4.646	4.02	57.14
8	4	10.18	6.75	27.72	9.30	9.29	5.7	96.23
9	3	7.63	5.06	20.79	6.98	6.97	3.15	75.88
10	3	7.63	5.06	20.79	6.98	6.97	3.00	74.05
11	3	7.63	5.06	20.79	6.98	6.97	2.05	61.22

Table B.3: Calculated media properties of medium iii

Exp.Run	Filtration velocity (m/h)	Interstitial velocity (m/h)	Reynolds number in filter bed (-)	Reynolds number in pipe (-)	Dean number (-)	Modified Dean number (-)	Headloss across filter bed (cm)	Velocity gradient in filter bed (s ⁻¹)
1	2	7.82	3.47	13.86	4.65	4.646	1.55	67.75
2	4	15.64	6.95	27.72	9.30	9.29	3.07	134.84
3	2	7.82	3.47	13.86	4.65	4.646	3.53	59.03
4	4	15.64	6.95	27.72	9.30	9.29	5.75	106.54
5	2	7.82	3.47	13.86	4.65	4.646	1.58	68.40
6	4	15.64	6.95	27.72	9.30	9.29	2.16	113.10
7	2	7.82	3.47	13.86	4.65	4.646	3.62	59.77
8	4	15.64	6.95	27.72	9.30	9.29	5.67	105.80
9	3	11.73	5.21	20.79	6.98	6.97	3.10	82.97
10	3	11.73	5.21	20.79	6.98	6.97	3.02	81.90
11	3	11.73	5.21	20.79	6.98	6.97	2.62	76.28

Table B.4: Calculated media properties of medium iv

Exp.Run	Filtration velocity (m/h)	Interstitial velocity (m/h)	Reynolds number in filter bed (-)	Reynolds number in pipe (-)	Dean number (-)	Modified Dean number (-)	Headloss across filter bed (cm)	Velocity gradient in filter bed (s ⁻¹)
2	4	15.73	4.60	27.72	4.65	4.646	6.52	197.63
4	4	15.73	4.60	27.72	9.30	9.29	10.9	147.54
5	2	7.87	2.30	13.86	4.65	4.646	4.8	119.91
7	2	7.87	2.30	13.86	9.30	9.29	8.52	92.23

Sieving analysis

The sieving analysis was done in order to determine the d_{50} diameter. The cumulative percentage values for the four different media and LLDPE powder are shown in the following tables.

Table B.5: Sieving analysis of medium i

Sieve size (μm)	Geometric mean (μm)	Mass (g)	Cumulative mass undersize (g)	Cumulative % undersize
+4750	4750	0.6	500	100
+4000-4750	4358.9	17.4	499.4	99.88
+3350-4000	3660.6	468.5	482	96.4
+2800-3350	3062.7	13.5	13.5	2.7
+2360-2800	2570.6	0		
+2000-2360	2172.56	0		
+1700-2000	1843.91	0		
-1700	1700	0		
Total		500		

Table B.6: Sieving analysis of medium ii

Sieve size (μm)	Geometric mean (μm)	Mass (g)	Cumulative mass undersize (g)	Cumulative % undersize
+4750	4750	3.1	499.4	100
+4000-4750	4358.9	21.6	496.3	99.38
+3350-4000	3660.6	383.6	474.7	95.05
+2800-3350	3062.7	76.0	91.1	18.24
+2360-2800	2570.6	10.3	15.1	3.02
+2000-2360	2172.56	2.0	4.8	0.96
+1700-2000	1843.91	2.5	2.8	0.56
-1700	1700	0.3	0.3	0.06
Total		499.4		

Table B.7: Sieving analysis of medium iii

Sieve size (μm)	Geometric mean (μm)	Mass (g)	Cumulative mass undersize (g)	Cumulative % undersize
+4750	4750	89.8	499.7	100
+4000-4750	4358.9	371.2	409.9	82.03
+3350-4000	3660.6	36.5	38.7	7.74
+2800-3350	3062.7	1.8	2.2	0.44
+2360-2800	2570.6	0.1	0.4	0.08
+2000-2360	2172.56	0.1	0.3	0.06
+1700-2000	1843.91	0.2	0.2	0.04
-1700	1700	0		
Total				

Table B.8: Sieving analysis of medium iv

Sieve size (μm)	Geometric mean (μm)	Mass (g)	Cumulative mass undersize (g)	Cumulative % undersize
+4750	4750	0	499.4	100
+4000-4750	4358.9	0	499.4	100
+3350-4000	3660.6	0	499.4	100
+2800-3350	3062.7	11.3	499.4	100
+2360-2800	2570.6	334.2	488.1	97.74
+2000-2360	2172.56	116.3	153.9	30.82
+1700-2000	1843.91	37.2	37.6	7.53
-1700	1700	0.4	0.4	0.08
Total		499.4		

Table B.9: Sieving analysis of LLDPE powder

Sieve size (μm)	Geometric mean (μm)	Mass (g)	Cumulative mass undersize (g)	Cumulative % undersize
+1000	1000	75.2	477.7	100
+850-1000	921.95	58.5	372.5	83.20
+710-850	776.85	45.4	314.0	70.13
+600-710	652.69	72.4	268.6	60.00
+500-600	547.72	46.7	196.2	43.81
+425-500	460.98	44.0	149.5	33.40
+300-425	357.1	59.8	105.5	23.56
+250-300	273.86	29.1	45.7	10.21
-250	250	16.6	16.6	3.70
Total		447.7		

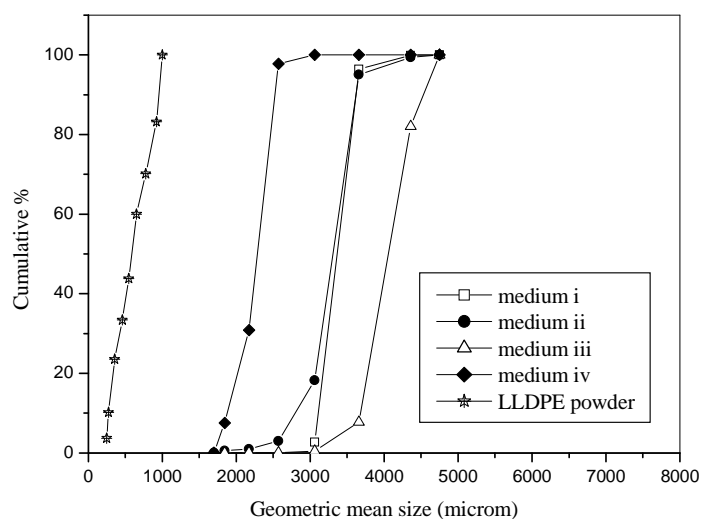


Figure B.1: Cumulative % curves for the floating medium particles.

The d_{50} diameters of the four media were read from Figure B.1 as follows:

Medium i $d_{50} = 3.03$ mm

Medium ii $d_{50} = 3.30$ mm

Medium iii $d_{50} = 4.07$ mm

Medium iv $d_{50} = 2.28$ mm

LLDPE powder $d_{50} = 0.60$ mm

Appendix C

Dosing pump and Jar test

Dosing pump calibration using water:

Table C.1: Dosing pump calibration (replicate 1)

Speed percentage (%)	Volume (ml)	Time (sec)	Flow rate (ml/min)
10	9	46.5	11.61
30	20	30.7	39.10
50	34	31.3	65.18
60	56	37.6	89.36
70	36.5	21.1	103.79
90	37	16.2	137.04
100	29	11	158.18

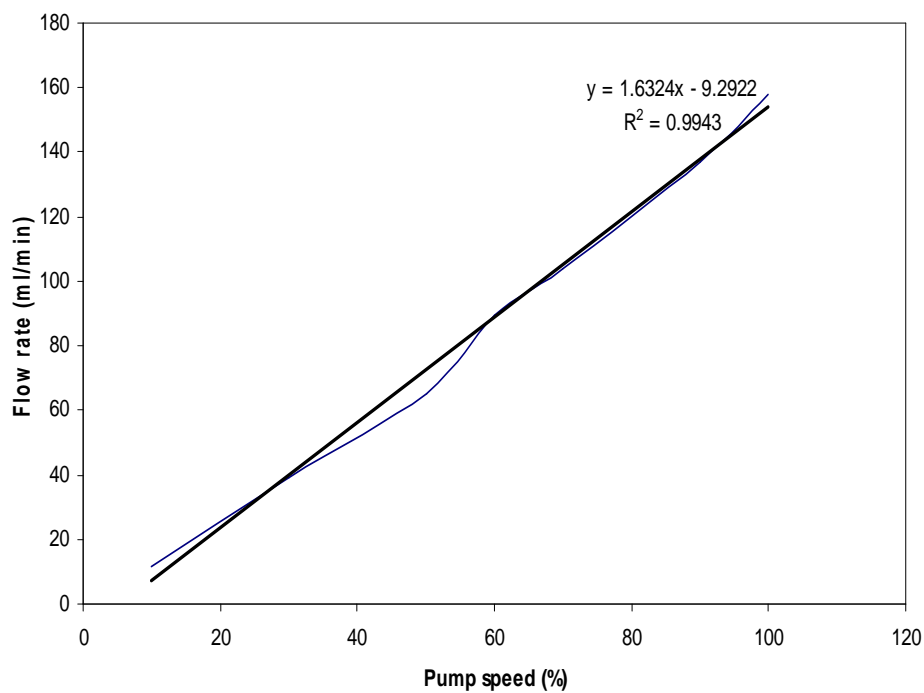


Figure C.1: Dosing pump calibration curve (speed percentage vs. flow rate) using water.

Table C.2: Dosing pump calibration (replicate 2)

Speed percentage (%)	Volume (ml)	Time (sec)	Flow rate (ml/min)
10	10	40.1	14.96
20	18.5	44.8	24.78
30	28.5	36.9	46.34
40	30	29.1	61.86
50	28.5	22.9	74.67
60	23	15.5	89.03
70	37	20.5	108.29
80	32	15.5	123.87
90	45	20.5	131.71
100	64	27	142.22

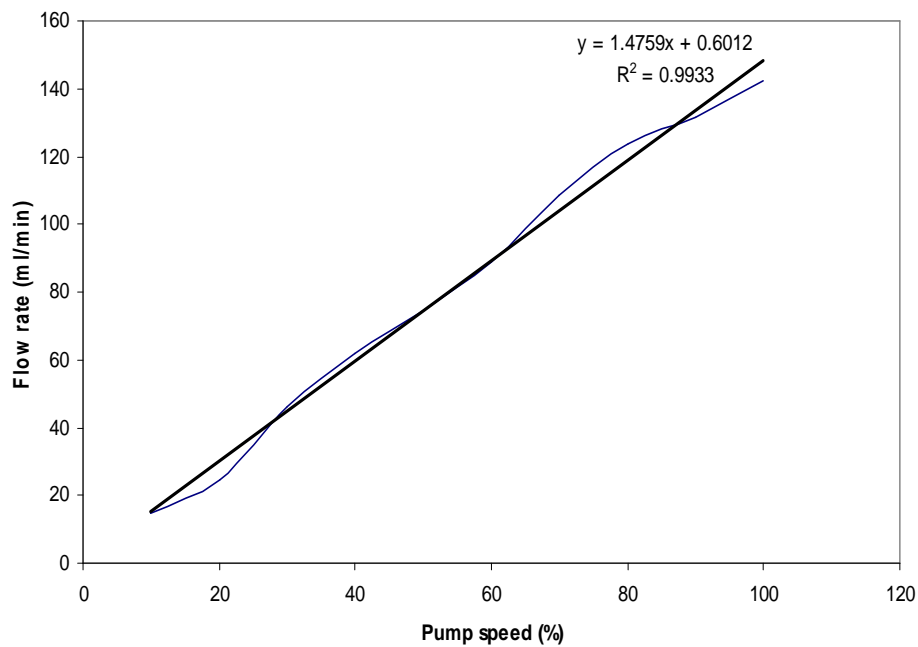


Figure C.2: Dosing pump calibration curve (speed percentage vs. flow rate) using water.

Table C.3: Dosing pump calibration (replicate 3)

Speed percentage (%)	Volume (ml)	Time (min)	Flow rate (ml/min)
10	67	4	16.75
30	148	3	49.33
50	240	3	80
70	170	1.5	113.33
90	213	1.5	142

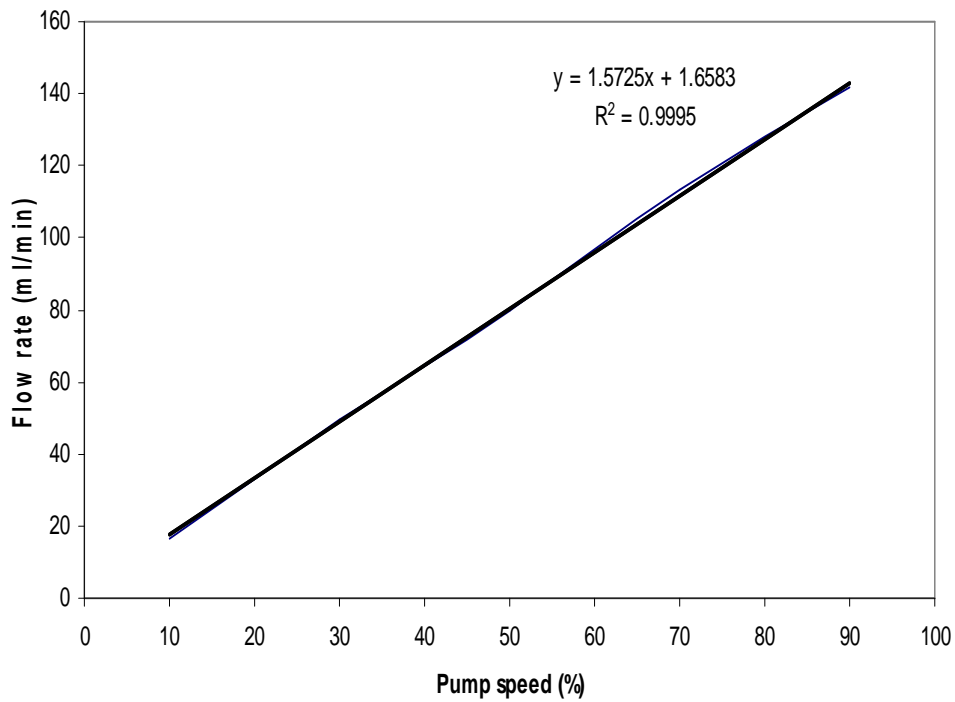


Figure C.3: Dosing pump calibration curve (speed percentage vs. flow rate) using water.

Table C.4: Dosing pump calibration (replicate 4)

Speed percentage (%)	Volume (ml)	Time (min)	Flow rate (ml/min)
20	40	3	13.33
40	100	1.5	66.67
50	152	2	76
60	186	2	93
70	220	2	110
80	196	1.5	130.67
100	207	1.33	155.64

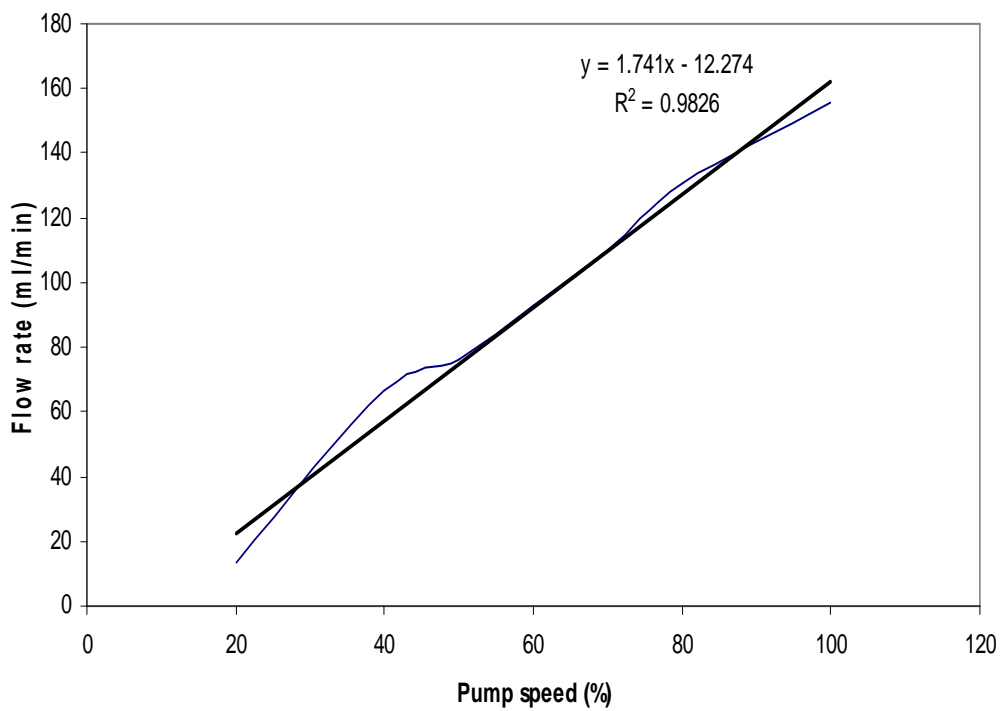


Figure C.4: Dosing pump calibration curve (speed percentage vs. flow rate) using water.

Jar tests

The purpose of jar tests was to establish the correct dose of coagulant to use. The optimum dose depends upon the raw water to be treated. The jar tests were carried out with synthetic raw water. The conditions of the synthetic raw water used in this study were as follows:

Feed water: concentration = 250 mg/L bentonite, Turbidity = 68.24 NTU

Coagulant: ferric sulphate.

Tables C.5 and C.6 summarise the laboratory jar testing results on synthetic raw water. Figures C.5 and C.6 show the filtrate turbidity profiles for various ferric sulphate doses.

Table C.5: Jar tests results (experiment 1)

Coagulant dosage (mg/L)	pH	Turbidity (NTU)
8	5.03	0.84
12.5	5.00	0.50
17	5.00	0.60
21	4.98	0.60
25	5.00	0.32
29	5.05	0.32

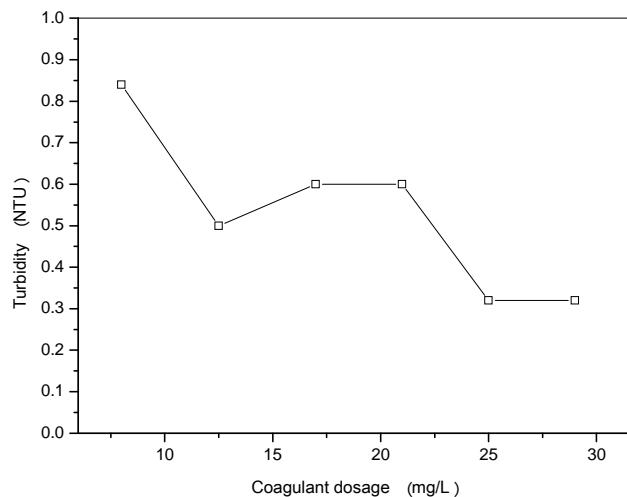


Figure C.5: Coagulant dosage vs. turbidity

Table C.6: Jar tests results (experiment 2)

Coagulant dosage (mg/L)	pH	Turbidity (NTU)
17	5.00	0.80
21	5.98	0.77
23	4.97	0.39
25	4.98	0.33
27	4.98	0.34
29	4.99	0.34

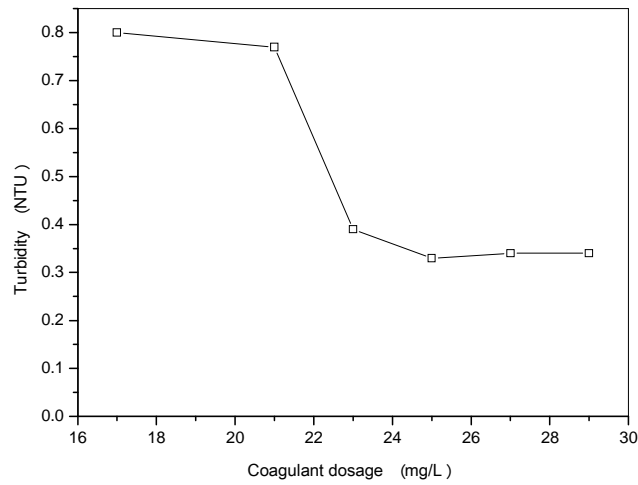


Figure C.6: Coagulant dosage vs. turbidity

Appendix D

Turbidity and headloss profiles

Appendix 1: Summary of results

The turbidity and headloss profiles for experimental runs # 1 to # 42 are given in the following pages. This summary gives the operational conditions.

Table D.1: Summary of pilot plant experimental runs # 1 to # 42

Experimental run	Medium	Filtration rising velocity (m/h)	Medium depth (mm)	Chemical dose (mg/l)	Backwash method
1	medium i	2	200	11.5	Air + water
2	medium i	4	200	11.5	Air + water
3	medium i	2	600	11.5	Air + water
4	medium i	4	600	11.5	Air + water
5	medium i	2	200	23	Air + water
6	medium i	4	200	23	Air + water
7	medium i	2	600	23	Air + water
8	medium i	4	600	23	Air + water
9	medium i	3	400	17.25	Air + water
10	medium i	3	400	17.25	Air + water
11	medium i	3	400	17.25	Air + water
12	medium i	2	200	11.5	Air + water
13	medium i	4	200	11.5	Air + water
14	medium i	2	600	11.5	Air + water
15	medium i	4	600	11.5	Air + water
16	medium ii	2	200	23	Air + water
17	medium ii	4	200	23	Air + water
18	medium ii	2	600	23	Air + water
19	medium ii	4	600	23	Air + water
20	medium ii	3	400	17.25	Air + water
21	medium ii	3	400	17.25	Air + water
22	medium ii	3	400	17.25	Air + water
23	medium iii	2	200	11.5	Water only

24	medium iii	4	200	11.5	Air + water
25	medium iii	2	600	11.5	Air + water
26	medium iii	4	600	11.5	Air + water
27	medium iii	2	200	23	Air + water
28	medium iii	4	200	23	Air + water
29	medium iii	2	600	23	Air + water
30	medium iii	4	600	23	Water only
31	medium iii	3	400	17.25	Water only
32	medium iii	3	400	17.25	Air + water
33	medium iii	3	400	17.25	Air + water
34	medium iv	2	200	23	Air + water
35	medium iv	4	200	11.5	Air + water
36	medium iv	2	600	23	Air + water
37	medium iv	4	600	11.5	Air + water
38	LLDPE powder	4	200	23	Air + water
39	LLDPE powder	2	600	23	Air + water
40	Combined media	2	600	23	Air + water
41	Combined media	4	600	11.5	Air + water
42	Combined media	4	600	23	Air + water

denotes an experimental run

Appendix 2 Turbidity and headloss

Factorial design experimental runs

Medium = medium i; filtration velocity = 2 m/h; medium depth = 200 mm and chemical dose = 11.5 mg/L.

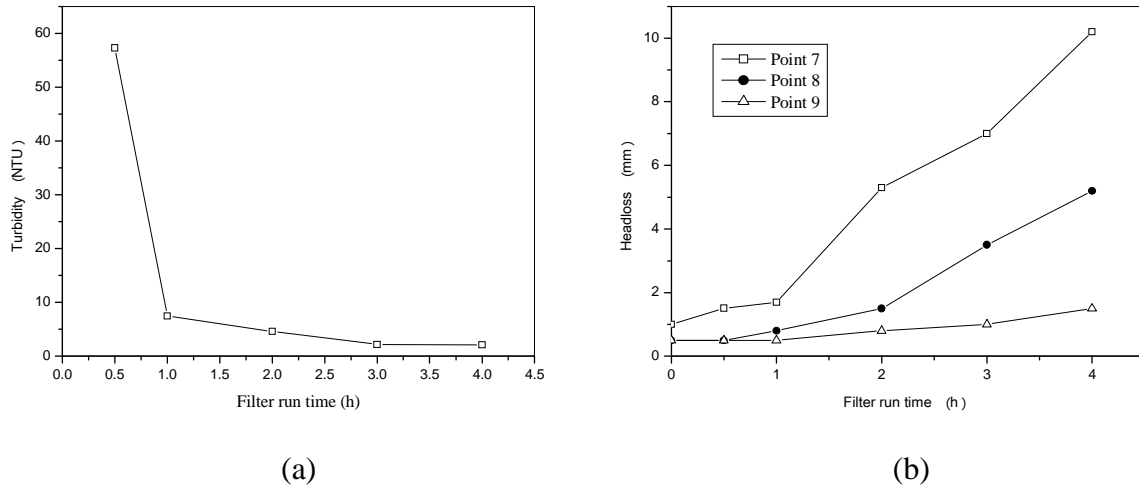


Figure D.1.a: Filtrate turbidity vs. filter run time, b: Headloss profile vs. time (run 1, medium i).

Medium = medium i; filtration velocity = 4 m/h; medium depth = 200 mm and chemical dose = 11.5 mg/L.

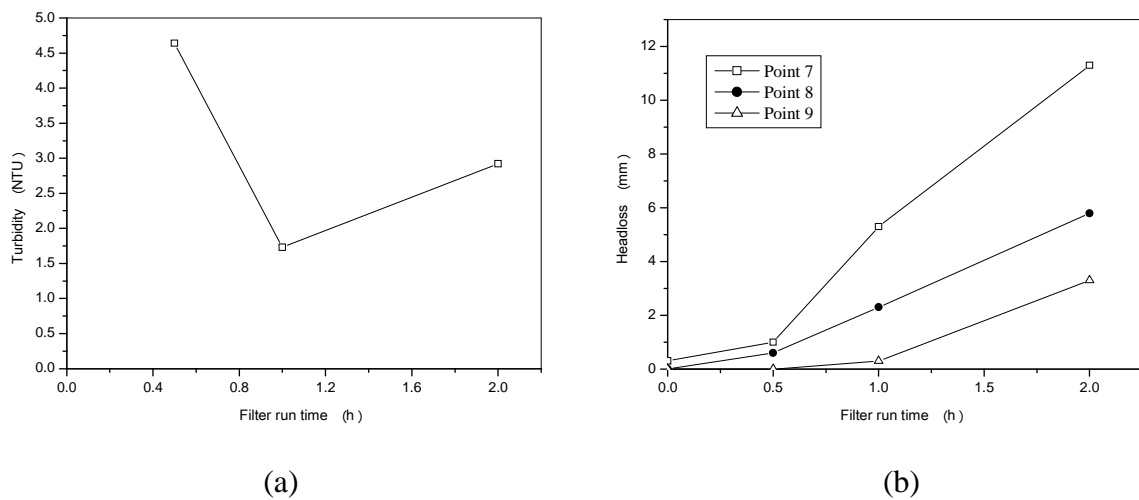


Figure D.2.a: Filtrate turbidity vs. filter run time, b: Headloss profile vs. time (run 2, medium i).

Medium = medium i; filtration velocity = 2 m/h; medium depth = 600 mm and chemical dose = 11.5 mg/L.

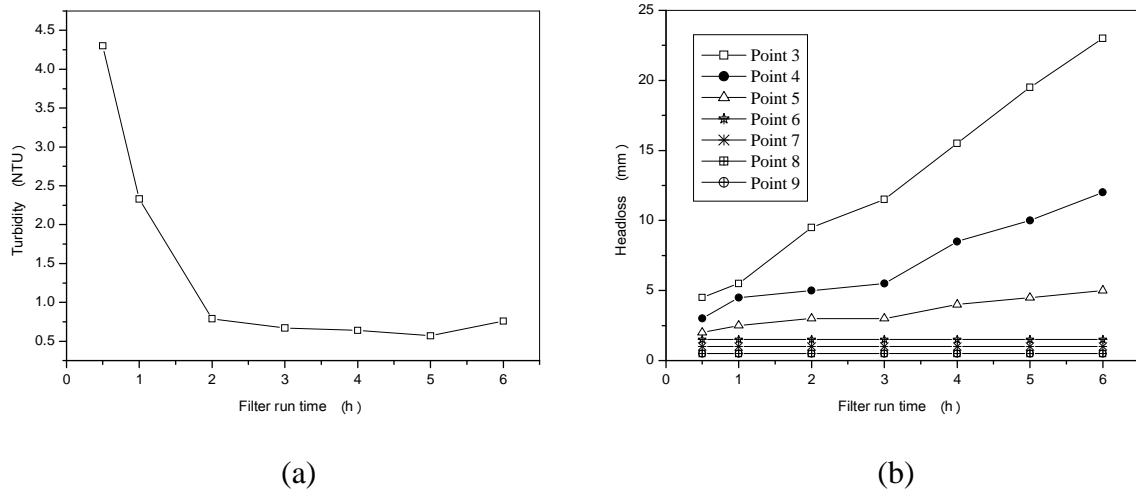


Figure D.3.a: Filtrate turbidity vs. filter run time, b: Headloss profiles vs. time (run 3, medium i).

Medium = medium i; filtration velocity = 4 m/h; medium depth = 600 mm and chemical dose = 11.5 mg/L.

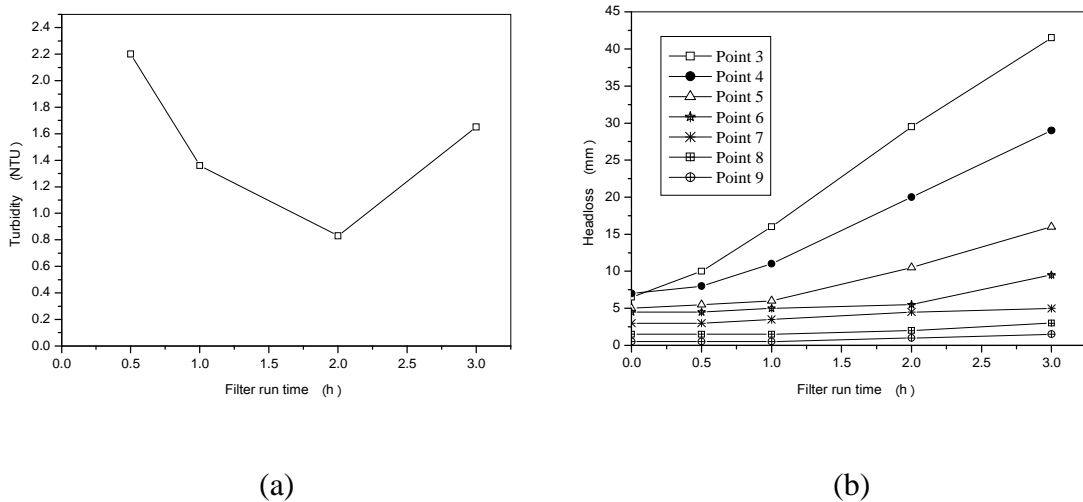


Figure D.4.a: Filtrate turbidity vs. filter run time, b: Headloss profiles vs. time (run 4, medium i).

Medium = medium i; filtration velocity = 2 m/h; medium depth = 200 mm and chemical dose = 23 mg/L.

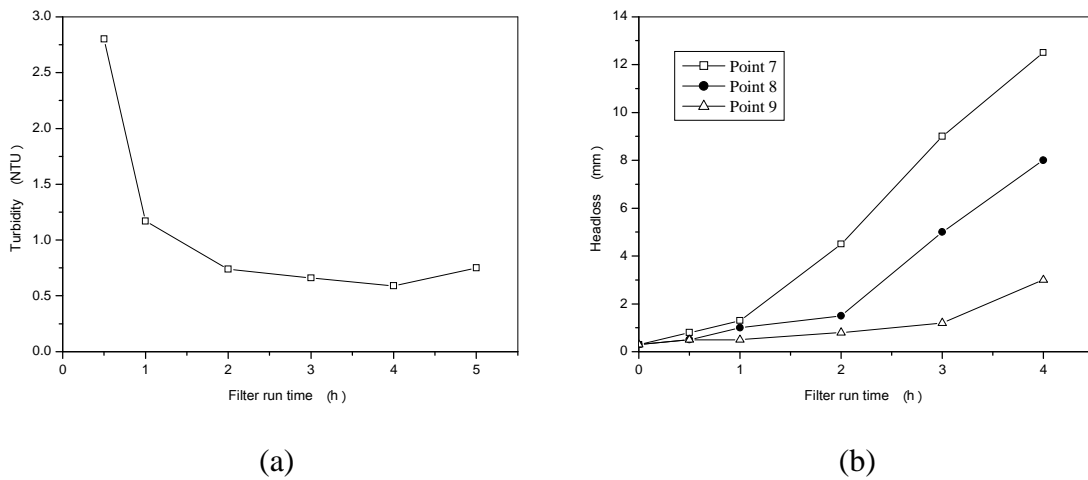


Figure D.5.a: Filtrate turbidity vs. filter run time, b: Headloss profiles vs. time (run 5, medium i).

Medium = medium i; filtration velocity = 4 m/h; medium depth = 200 mm and chemical dose = 23 mg/L.

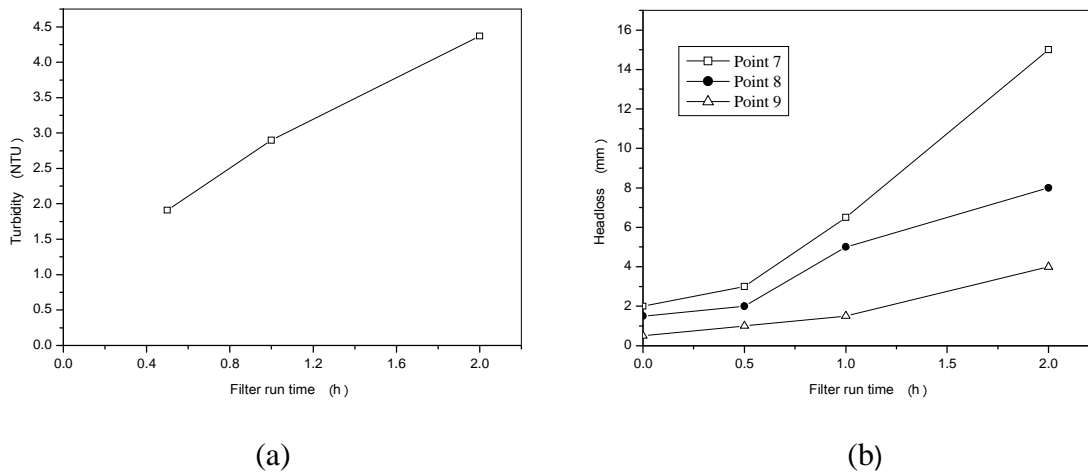


Figure D.6.a: Filtrate turbidity vs. filter run time, b: Headloss profiles vs. time (run 6, medium i).

Medium = medium i; filtration velocity = 2 m/h; medium depth = 600 mm and chemical dose = 23 mg/L.

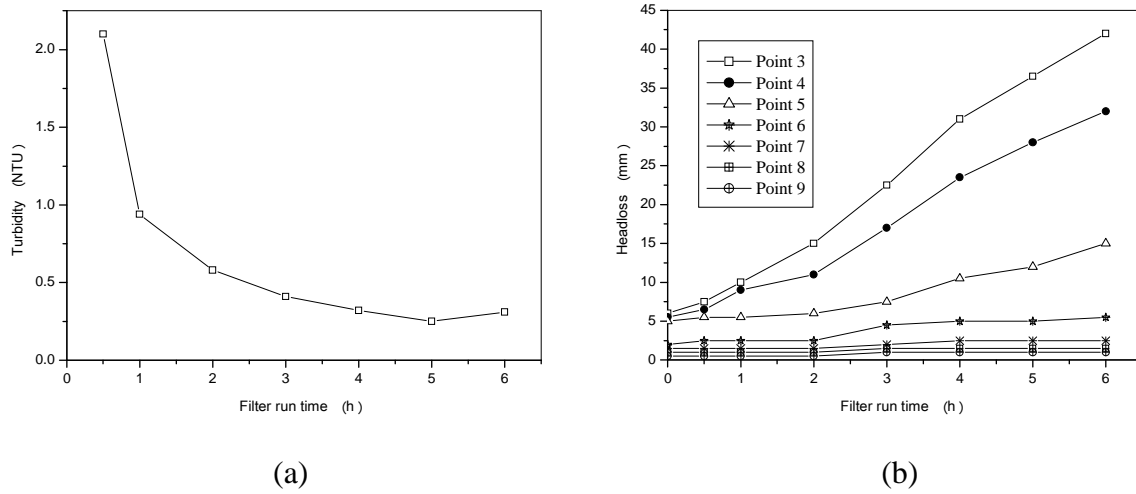


Figure D.7.a: Filtrate turbidity vs. filter run time, b: Headloss profiles vs. time (run 7, medium i).

Medium = medium i; filtration velocity = 4 m/h; medium depth = 600 mm and chemical dose = 23 mg/L.

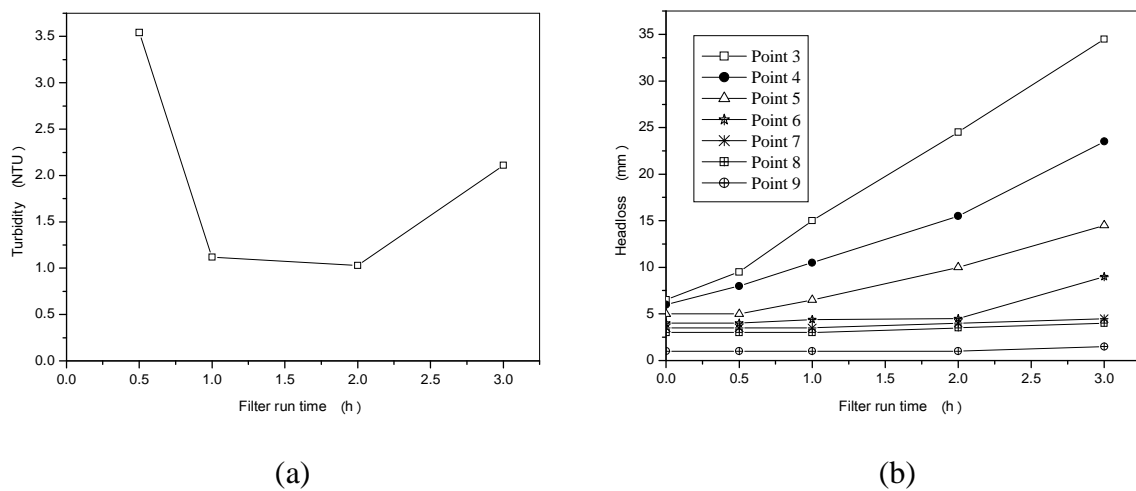


Figure D.8.a: Filtrate turbidity vs. filter run time, b: Headloss profiles vs. time (run 8, medium i).

Medium = medium i; filtration velocity = 3 m/h; medium depth = 400 mm and chemical dose = 17.25 mg/L.

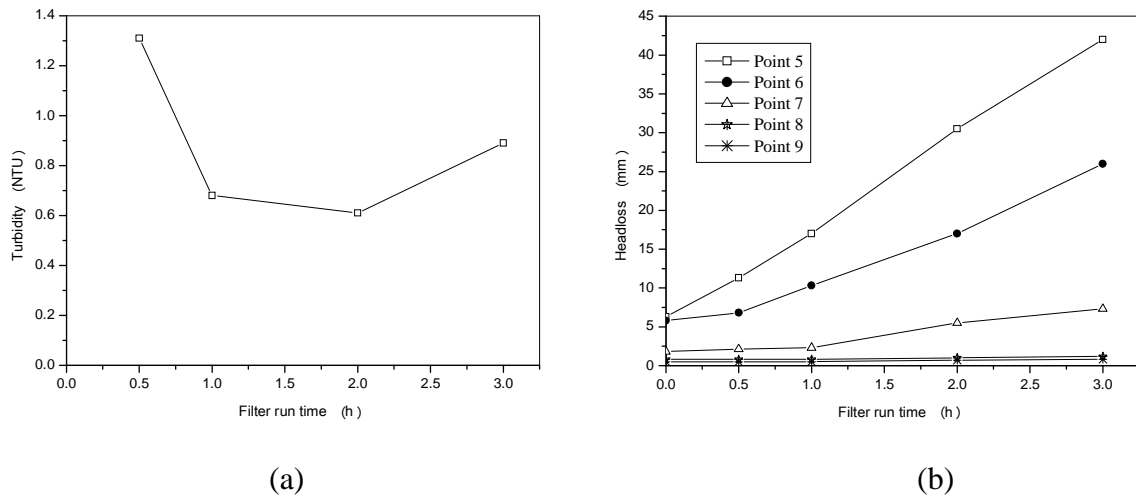


Figure D.9.a: Filtrate turbidity vs. filter run time, b: Headloss profiles vs. time (run 9, medium i).

Medium = medium i; filtration velocity = 3 m/h; medium depth = 400 mm and chemical dose = 17.25 mg/L.

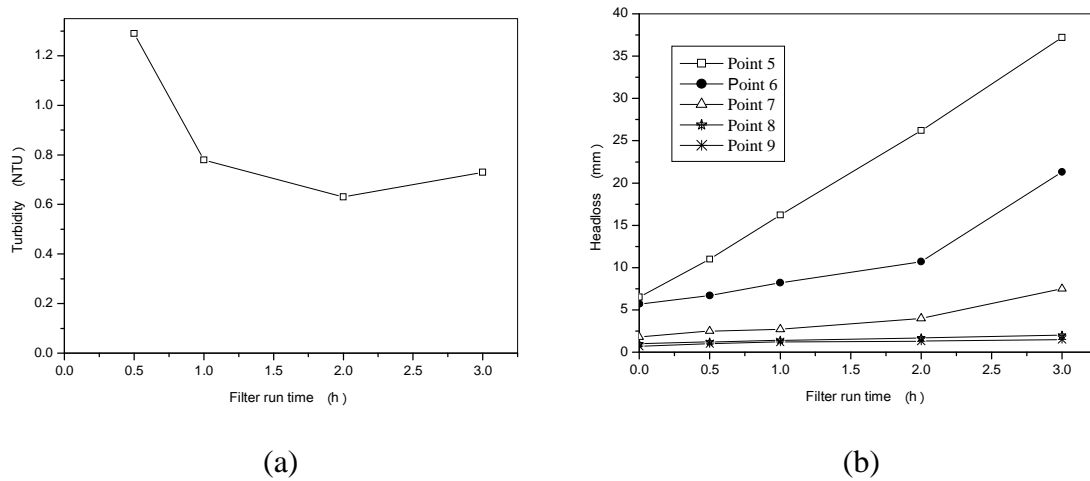


Figure D.10.a: Filtrate turbidity vs. filter run time, b: Headloss profiles vs. time (run 10, medium i).

Medium = medium i; filtration velocity = 3 m/h; medium depth = 400 mm and chemical dose = 17.25 mg/L.

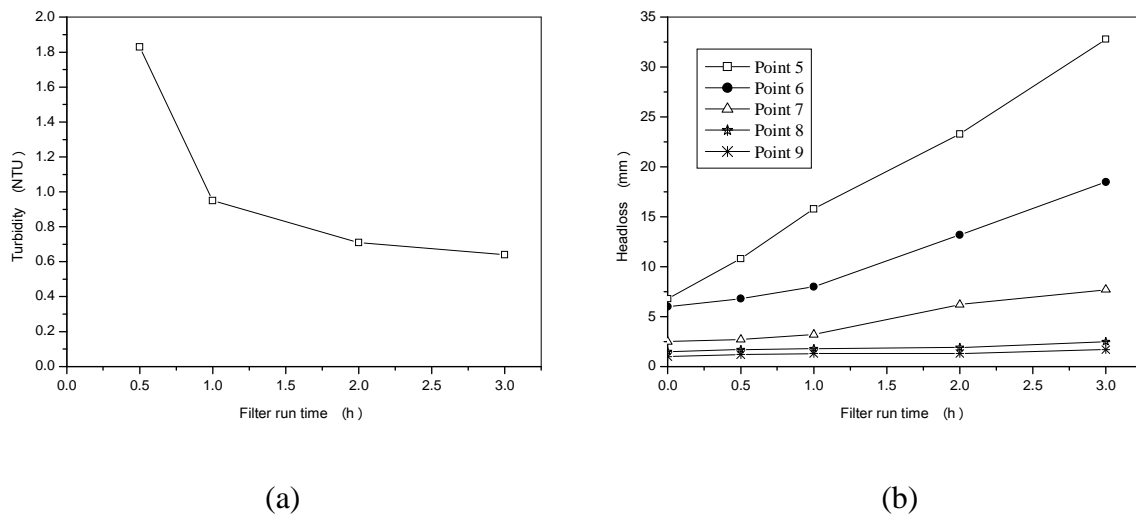


Figure D.11.a: Filtrate turbidity vs. filter run time, b: Headloss profiles vs. time (run 11, medium i).

Medium = medium ii; filtration velocity = 2 m/h; medium depth = 200 mm and chemical dose = 11.5 mg/L.

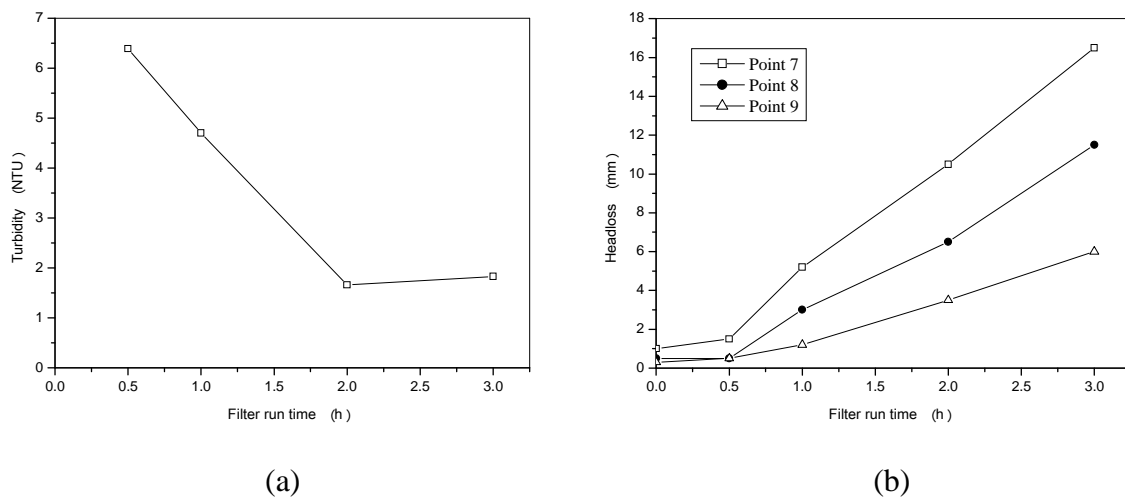


Figure D.1.a: Filtrate turbidity vs. filter run time, b: Headloss profiles vs. time (run 1, medium ii).

Medium = medium ii; filtration velocity = 4 m/h; medium depth = 200 mm and chemical dose = 11.5 mg/L.

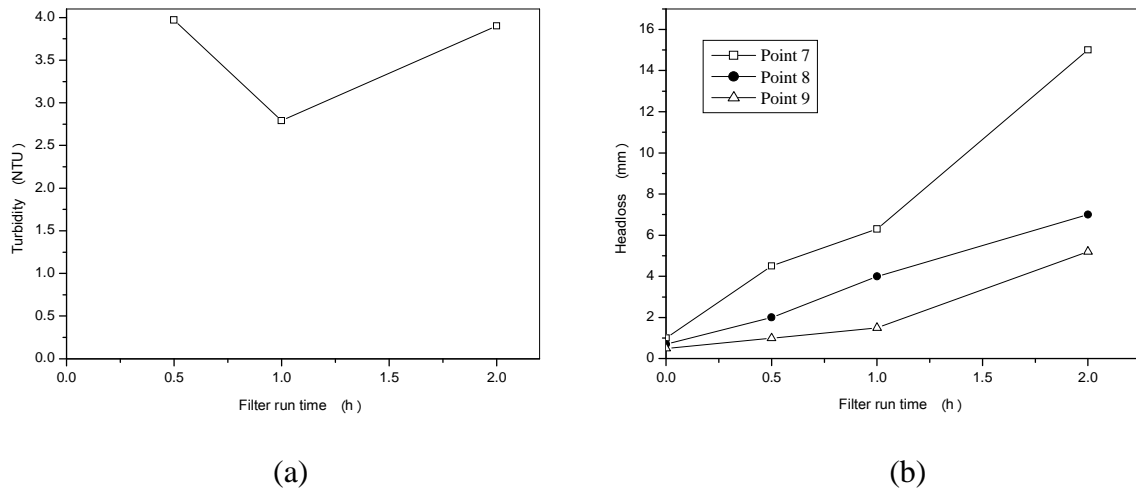


Figure D.2.a: Filtrate turbidity vs. filter run time, b: Headloss profiles vs. time (run 2, medium ii).

Medium = medium ii; filtration velocity = 2 m/h; medium depth = 600 mm and chemical dose = 11.5 mg/L.

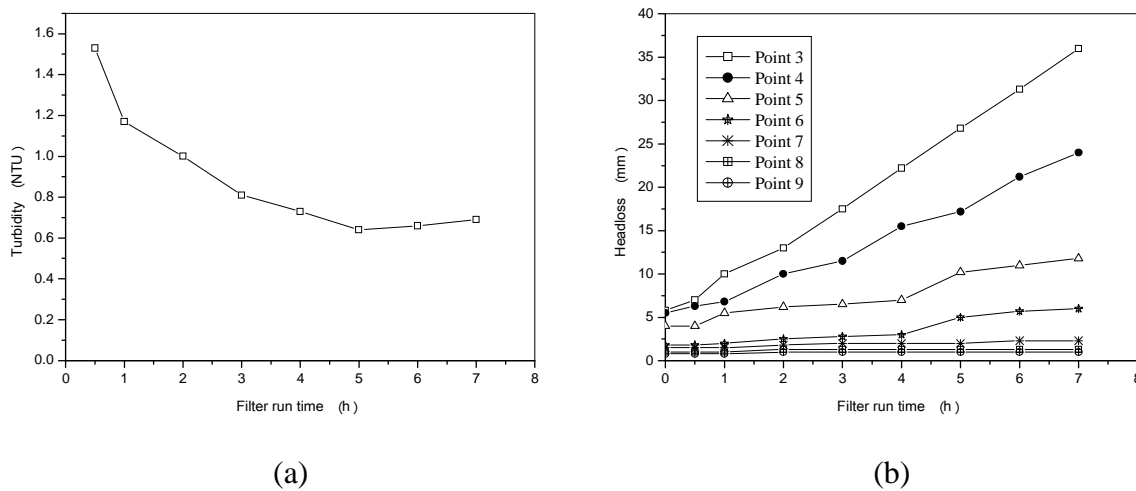


Figure D.3.a: Filtrate turbidity vs. filter run time, b: Headloss profiles vs. time (run 3, medium ii).

Medium = medium ii; filtration velocity = 4 m/h; medium depth = 600 mm and chemical dose = 11.5 mg/L.

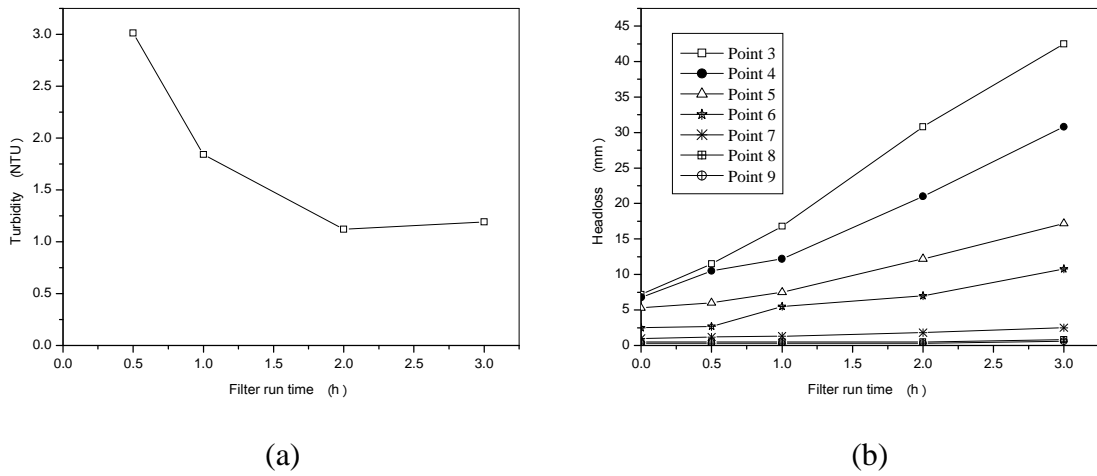


Figure D.4.a: Filtrate turbidity vs. filter run time, b: Headloss profiles vs. time (run 4, medium ii).

Medium = medium ii; filtration velocity = 2 m/h; medium depth = 200 mm and chemical dose = 23 mg/L.

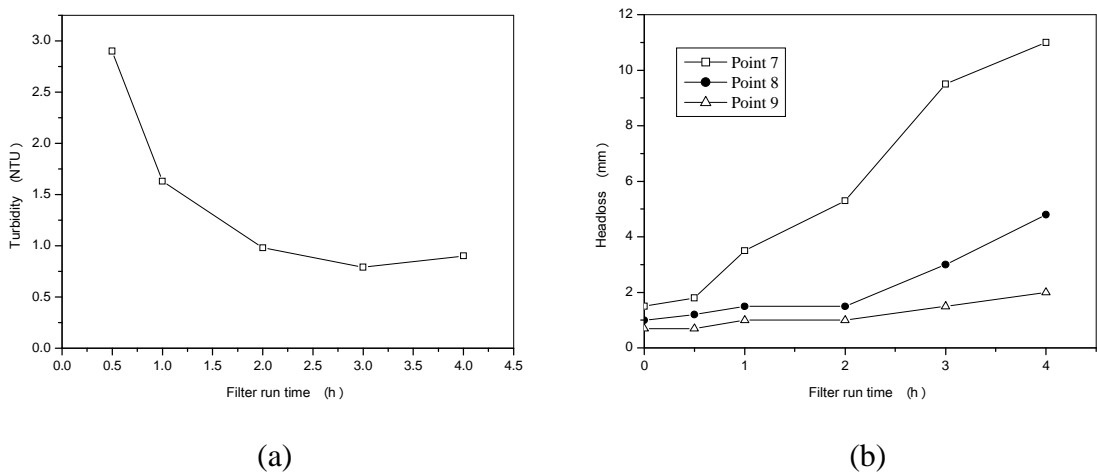


Figure D.5.a: Filtrate turbidity vs. filter run time, b: Headloss profiles vs. time (run 5, medium ii).

Medium = medium ii; filtration velocity = 4 m/h; medium depth = 200 mm and chemical dose = 23 mg/L.

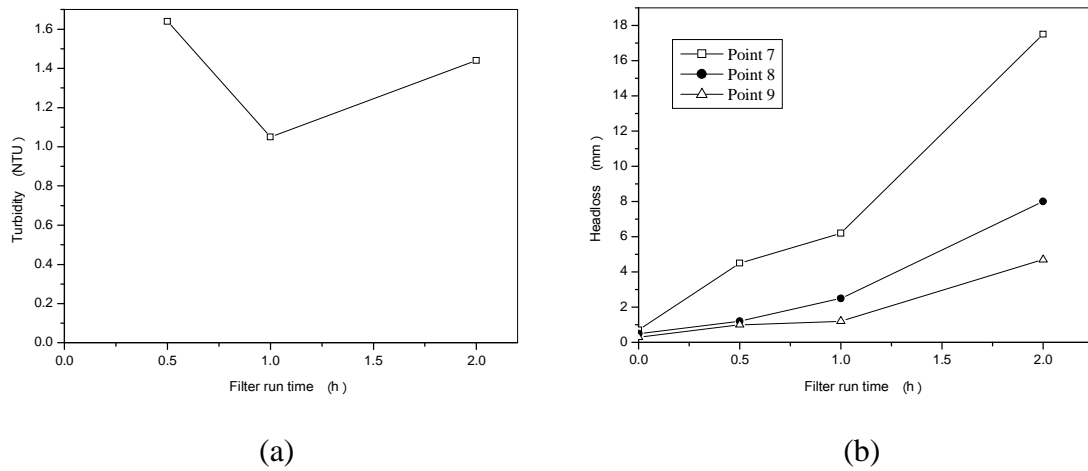


Figure D.6.a: Filtrate turbidity vs. filter run time, b: Headloss profiles vs. time (run 6, medium ii).

Medium = medium ii; filtration velocity = 2 m/h; medium depth = 600 mm and chemical dose = 23 mg/L.

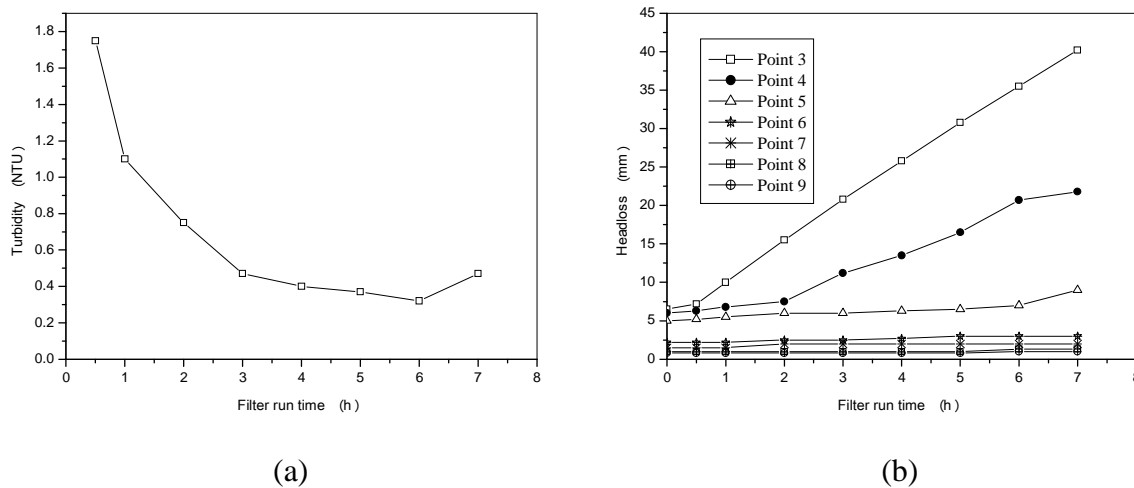


Figure D.7.a: Filtrate turbidity vs. filter run time, b: Headloss profiles vs. time (run 7, medium ii).

Medium = medium ii; filtration velocity = 4 m/h; medium depth = 600 mm and chemical dose = 23 mg/L.

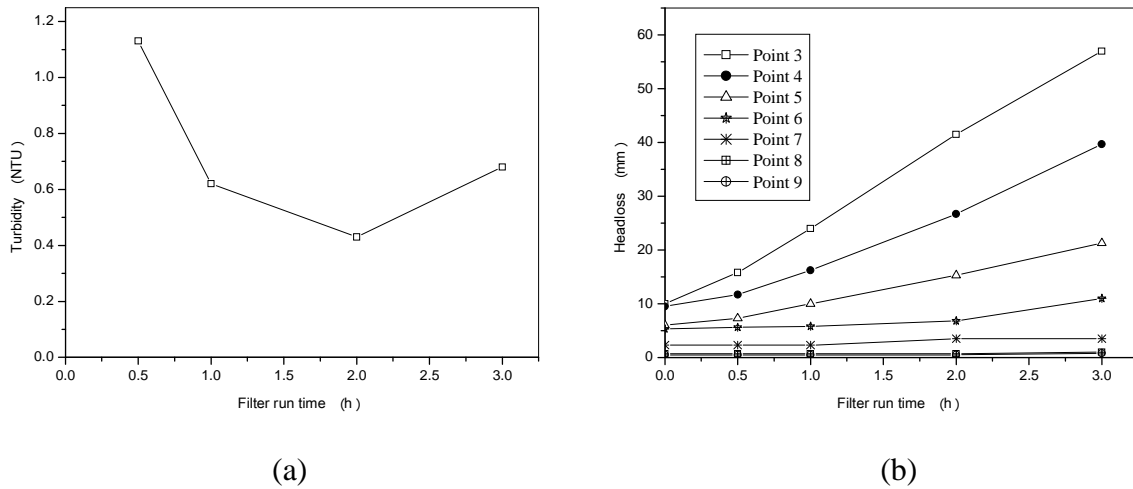


Figure D.8.a: Filtrate turbidity vs. filter run time, b: Headloss profiles vs. time (run 8, medium ii).

Medium = medium ii; filtration velocity = 3 m/h; medium depth = 400 mm and chemical dose = 17.25 mg/L.

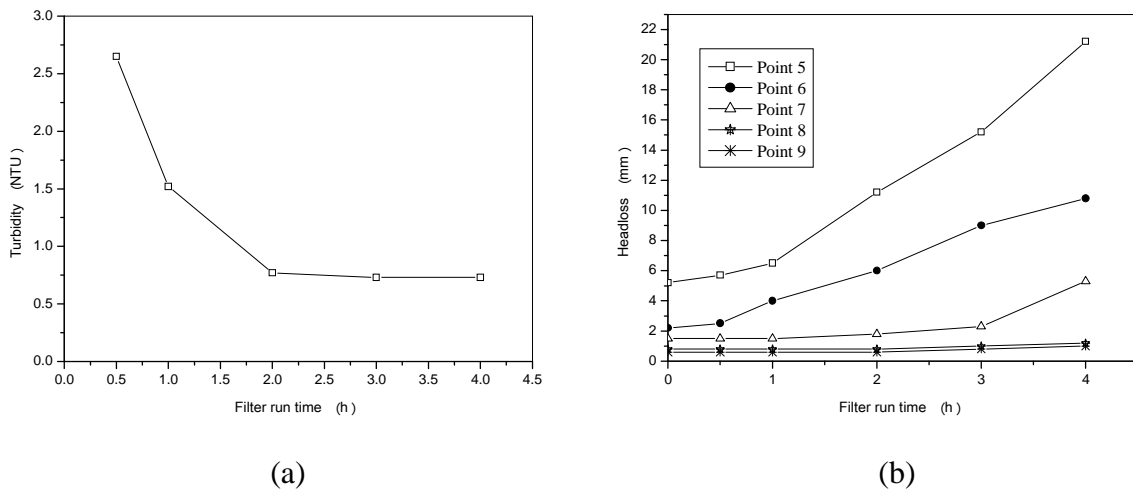


Figure D.9.a: Filtrate turbidity vs. filter run time, b: Headloss profiles vs. time (run 9, medium ii).

Medium = medium ii; filtration velocity = 3 m/h; medium depth = 400 mm and chemical dose = 17.25 mg/L.

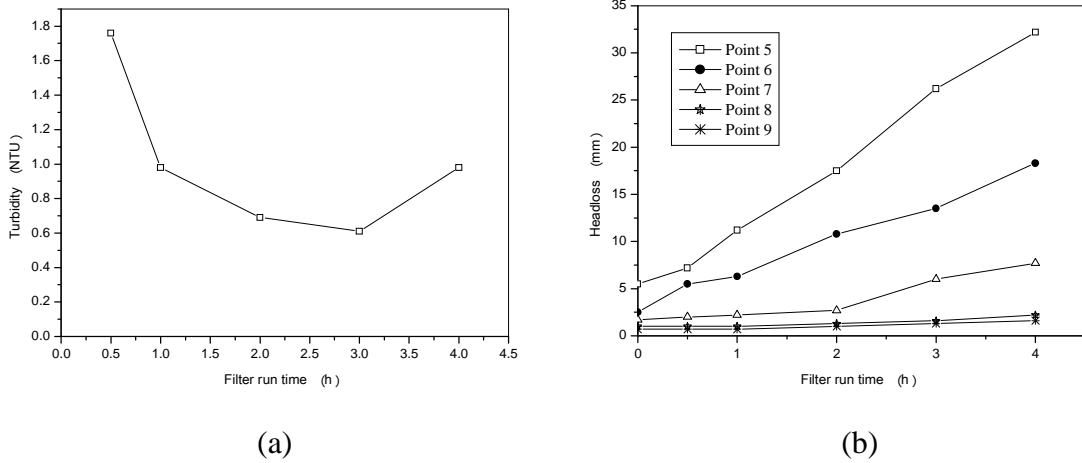


Figure D.10.a: Filtrate turbidity vs. filter run time, b: Headloss profiles vs. time (run 10, medium ii).

Medium = medium ii; filtration velocity = 3 m/h; medium depth = 400 mm and chemical dose = 17.25 mg/L.

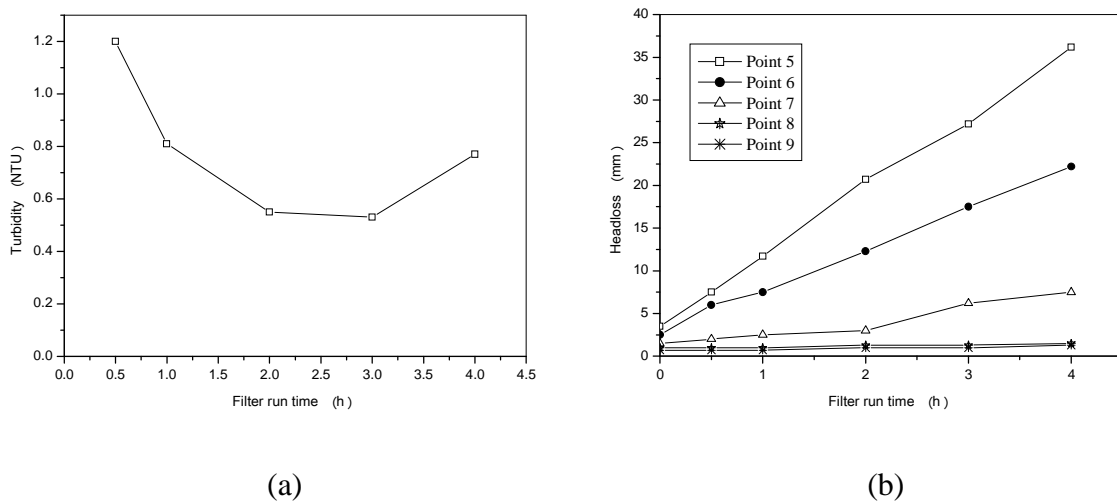


Figure D.11.a: Filtrate turbidity vs. filter run time, b: Headloss profiles vs. time (run 11, medium ii).

Medium = medium iii; filtration velocity = 2 m/h; medium depth = 200 mm and chemical dose = 11.5 mg/L.

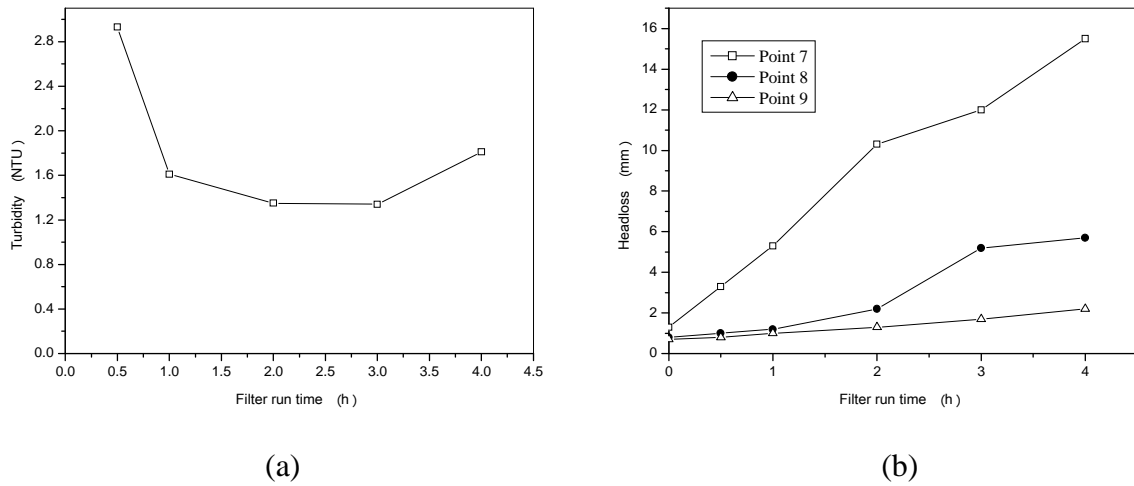


Figure D.1.a: Filtrate turbidity vs. filter run time, b: Headloss profiles vs. time (run 1, medium iii).

Medium = medium iii, filtration velocity = 4 m/h; medium depth = 200 mm and chemical dose = 11.5 mg/L.

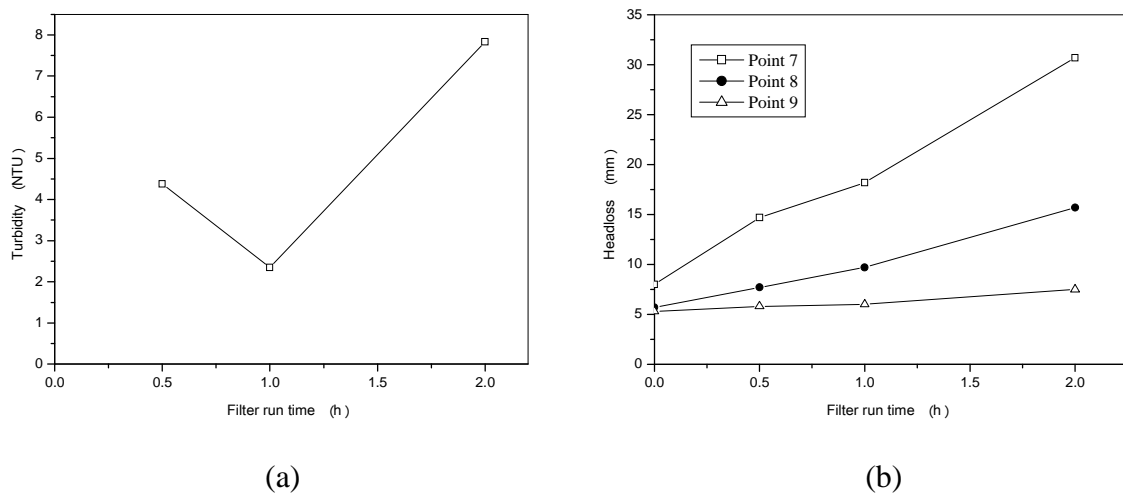


Figure D.2.a: Filtrate turbidity vs. filter run time, b: Headloss profiles vs. time (run 2, medium iii).

Medium = medium iii; filtration velocity = 2 m/h; medium depth = 600 mm and chemical dose = 11.5 mg/L.

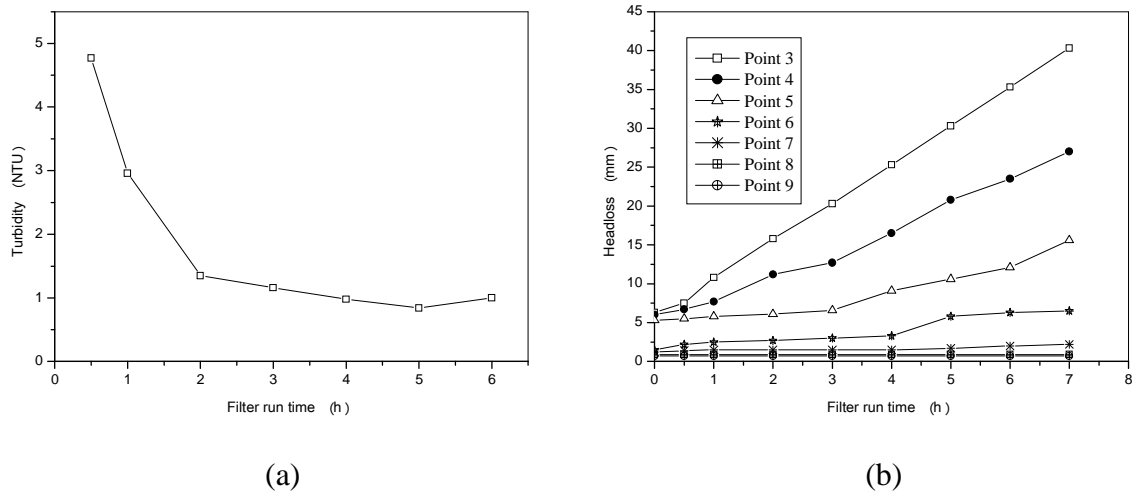


Figure D.3.a: Filtrate turbidity vs. filter run time, b: Headloss profiles vs. time (run 3, medium iii).

Medium = medium iii; filtration velocity = 4 m/h; medium depth = 600 mm and chemical dose = 11.5 mg/L.

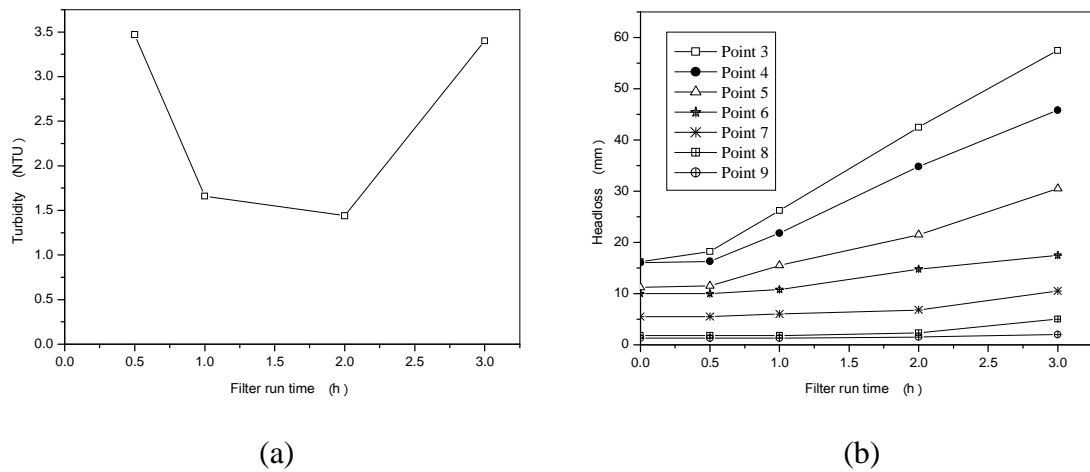


Figure D.4.a: Filtrate turbidity vs. filter run time, b: Headloss profiles vs. time (run 4, medium iii).

Medium = medium iii; filtration velocity = 2 m/h; medium depth = 200 mm and chemical dose = 23 mg/L.

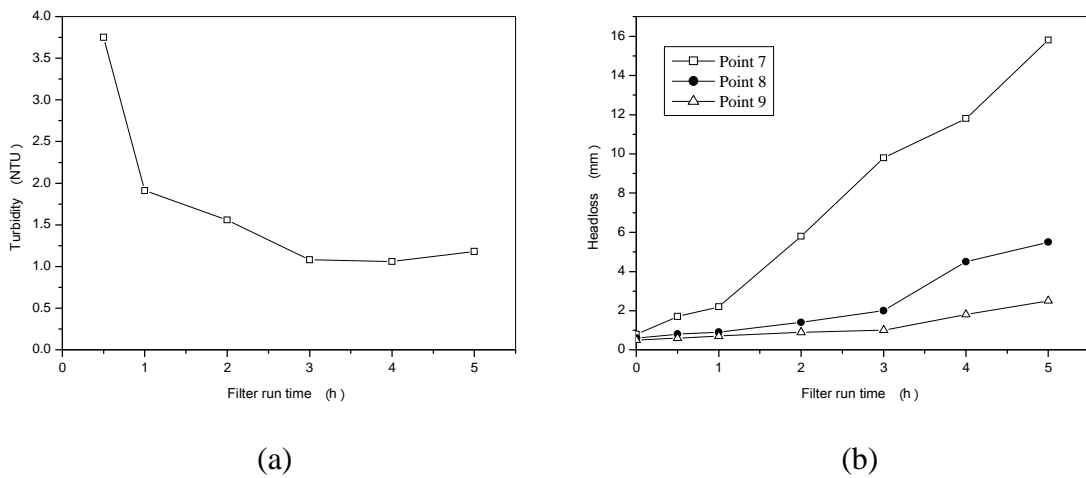


Figure D.5.a: Filtrate turbidity vs. filter run time, b: Headloss profiles vs. time (run 5, medium iii).

Medium = medium iii; filtration velocity = 4 m/h; medium depth = 200 mm and chemical dose = 23 mg/L.

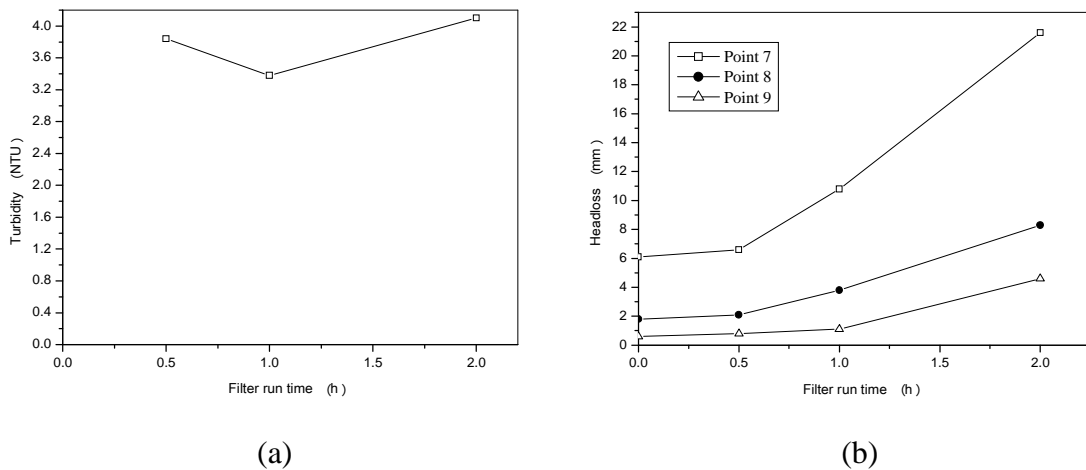


Figure D.6.a: Filtrate turbidity vs. filter run time, b: Headloss profiles vs. time (run 6, medium iii).

Medium = medium iii; filtration velocity = 2 m/h; medium depth = 600 mm and chemical dose = 23 mg/L.

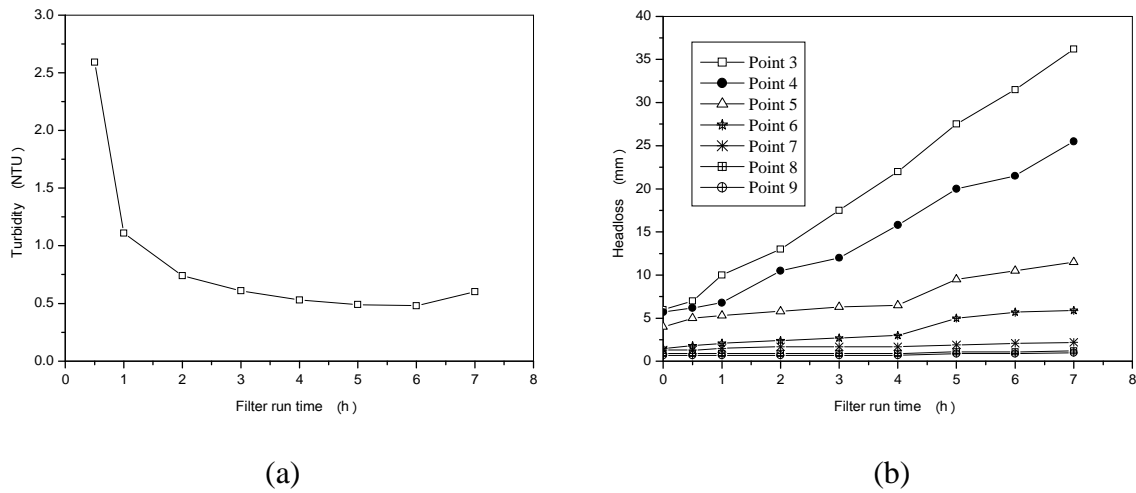


Figure D.7.a: Filtrate turbidity vs. filter run time, b: Headloss profiles vs. time (run 7, medium iii).

Medium = medium iii; filtration velocity = 4 m/h; medium depth = 600 mm and chemical dose = 23 mg/L.

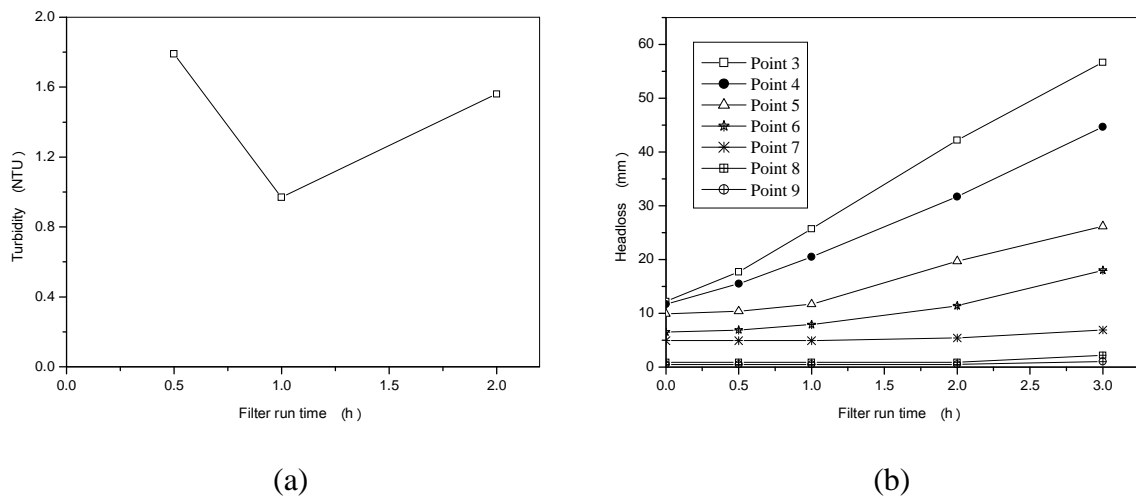


Figure D.8.a: Filtrate turbidity vs. filter run time, b: Headloss profiles vs. time (run 8, medium iii).

Medium = medium iii; filtration velocity = 3 m/h; medium depth = 400 mm and chemical dose = 17.25 mg/L.

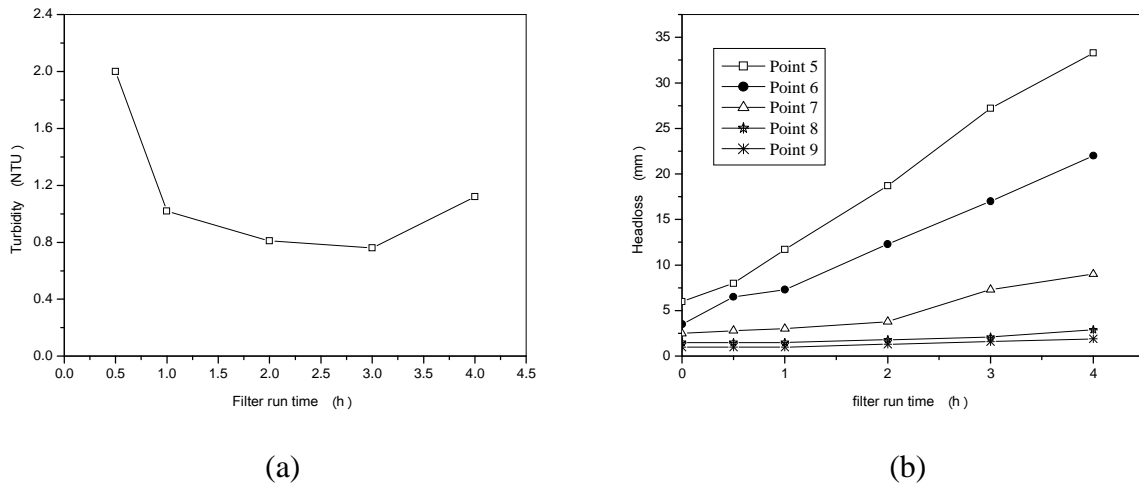


Figure D.9.a: Filtrate turbidity vs. filter run time, b: Headloss profiles vs. time (run 9, medium iii).

Medium = medium iii; filtration velocity = 3 m/h; medium depth = 400 mm and chemical dose = 17.25 mg/L.

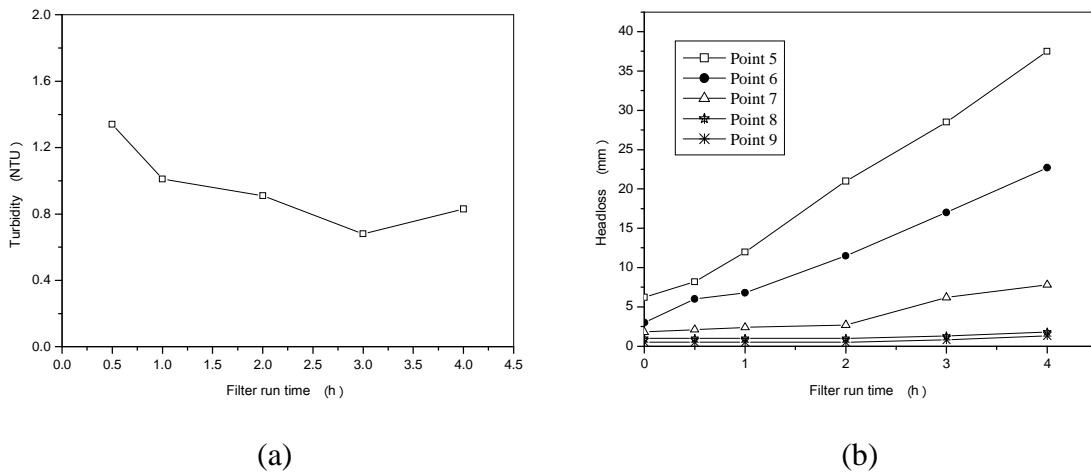
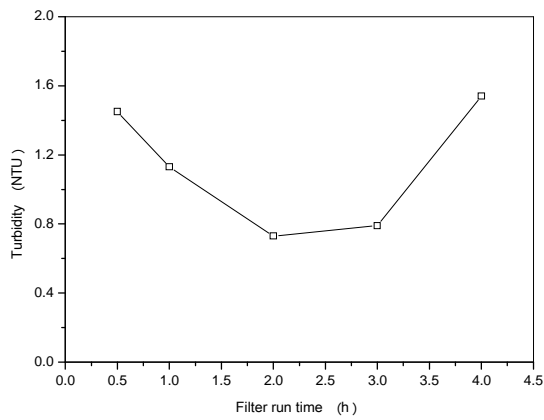
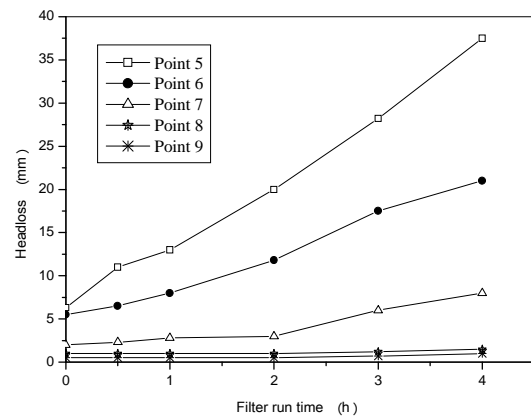


Figure D.10.a: Filtrate turbidity vs. filter run time, b: Headloss profiles vs. time (run 10, medium iii).

Medium = medium iii; filtration velocity = 3 m/h; medium depth = 400 mm and chemical dose = 17.25 mg/L.



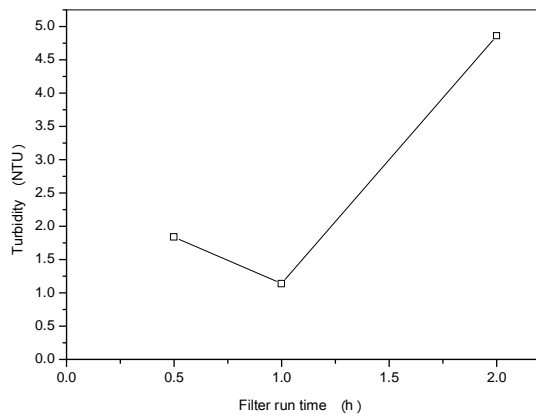
(a)



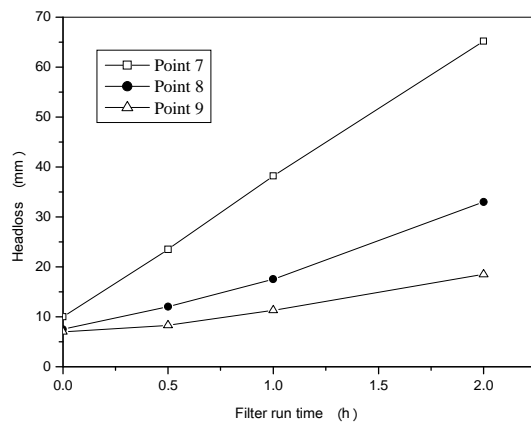
(b)

Figure D.11.a: Filtrate turbidity vs. filter run time, b: Headloss profiles vs. time (run 11, medium iii).

Medium = medium iv; filtration velocity = 4 m/h; medium depth = 200 mm and chemical dose = 11.5 mg/L.



(a)



(b)

Figure D.2.a: Filtrate turbidity vs. filter run time, b: Headloss profiles vs. time (run 2, medium iv).

Medium = medium iv; filtration velocity = 4 m/h; medium depth = 600 mm and chemical dose = 11.5 mg/L.

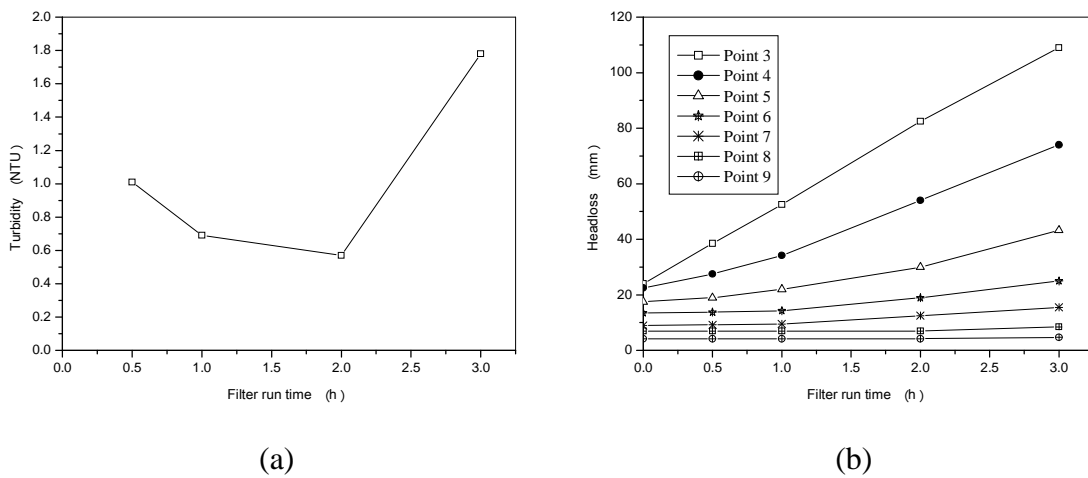


Figure D.4.a: Filtrate turbidity vs. filter run time, b: Headloss profiles vs. time (run 4, medium iv).

Medium = medium iv; filtration velocity = 2 m/h; medium depth = 200 mm and chemical dose = 23 mg/L.

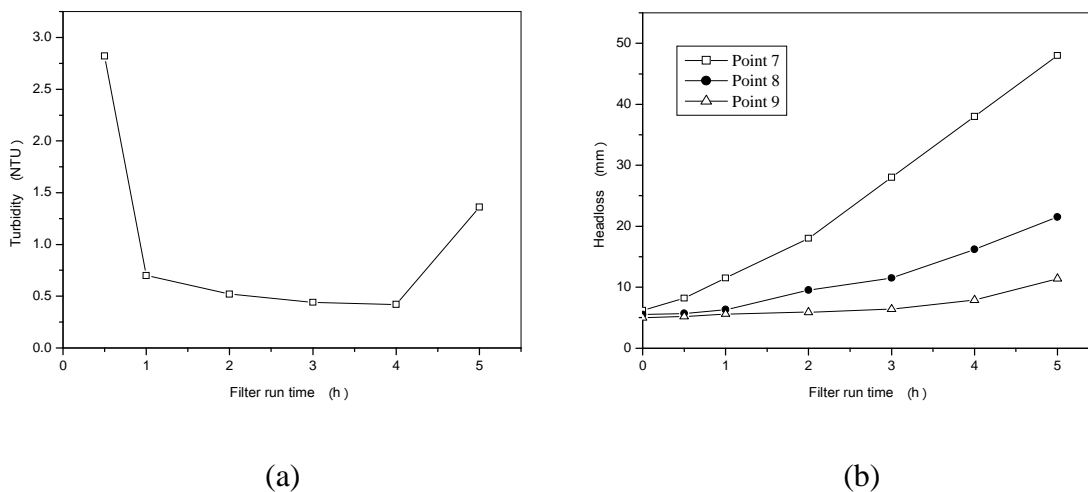


Figure D.5.a: Filtrate turbidity vs. filter run time, b: Headloss profiles vs. time (run 5, medium iv).

Medium = medium iv; filtration velocity = 2 m/h; medium depth = 600 mm and chemical dose = 23 mg/L.

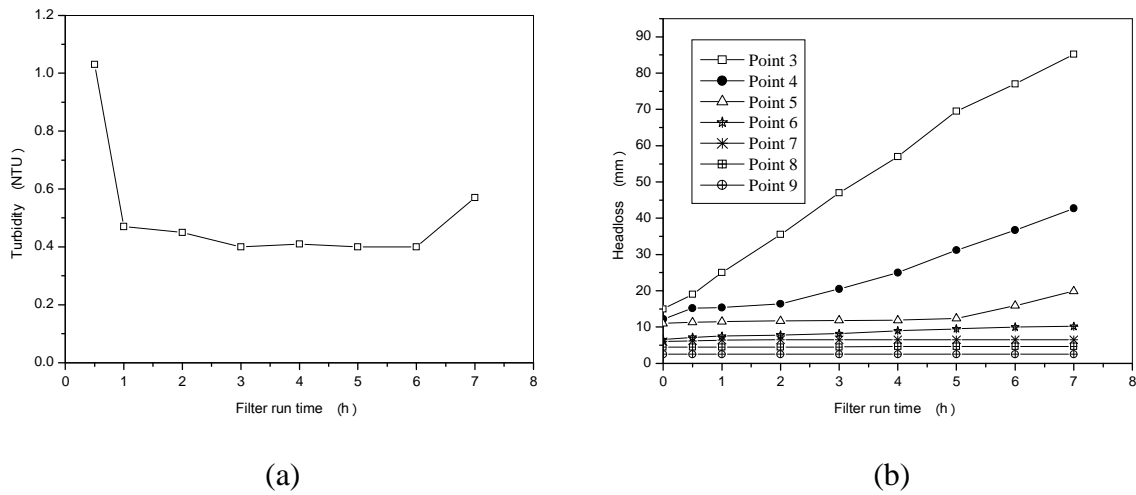


Figure D.7.a: Filtrate turbidity vs. filter run time, b: Headloss profiles vs. time (run 7, medium iv).

Medium = LLDPE powder; filtration velocity = 4 m/h; medium depth = 200 mm and chemical dose = 23 mg/L.

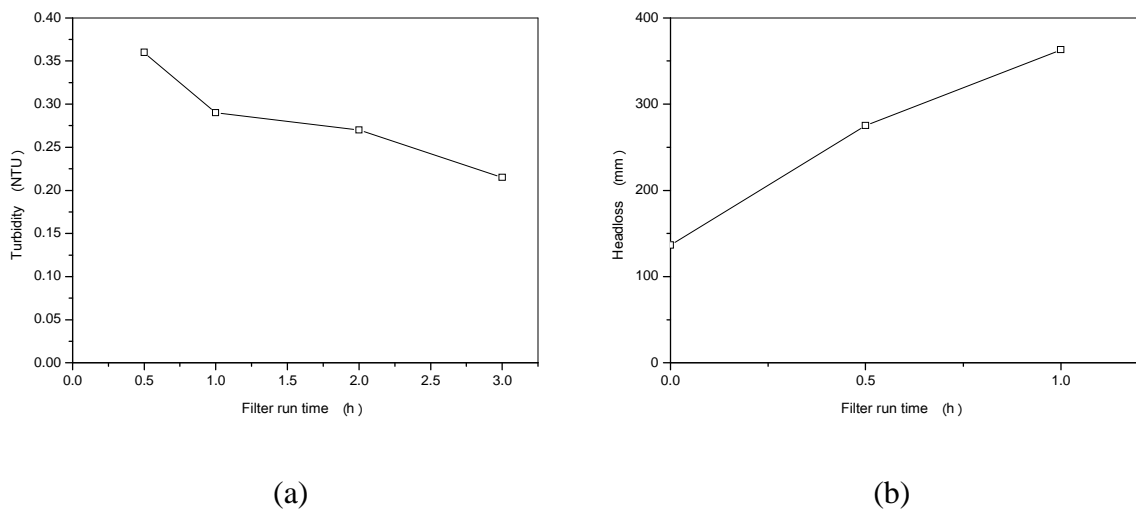
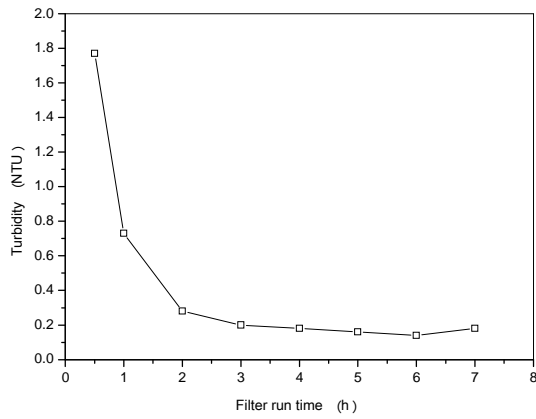
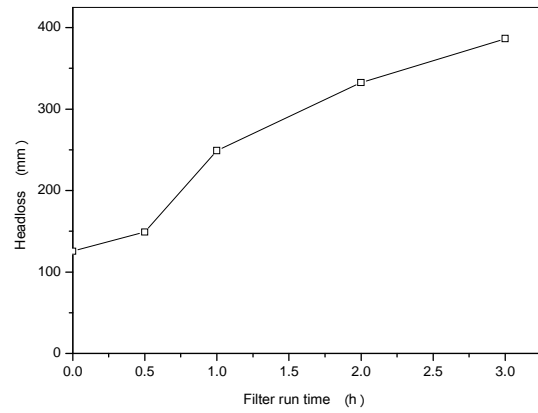


Figure D.6.a: Filtrate turbidity vs. filter run time, b: Headloss profiles vs. time (run 6, LLDPE powder).

Medium = LLDPE powder; filtration velocity = 2 m/h; medium depth = 600 mm and chemical dose = 23 mg/L.



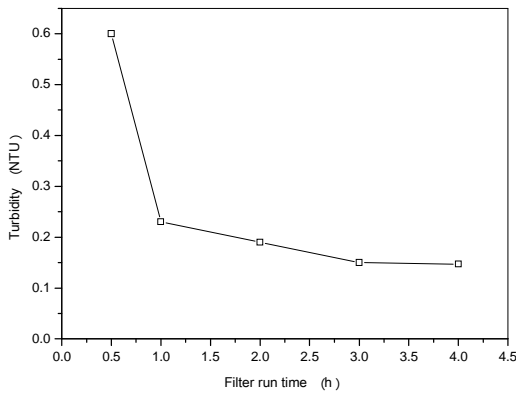
(a)



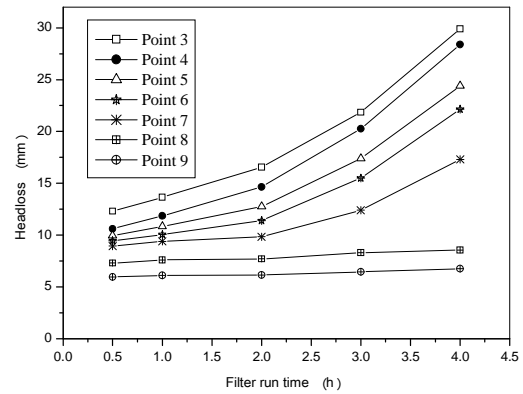
(b)

Figure D.7.a: Filtrate turbidity vs. filter run time, b: Headloss profiles vs. time (run 7, LLDPE powder).

Medium = combined (75% medium ii and 25% LLDPE powder); filtration velocity = 4 m/h; medium depth = 600 mm and chemical dose = 11.5 mg/L.



(a)



(b)

Figure D.4.a: Filtrate turbidity vs. filter run time, b: Headloss profiles vs. time (run 4, combined media).

Medium = combined (75% medium ii and 25% LLDPE powder); filtration velocity = 2 m/h; medium depth = 600 mm and chemical dose = 23 mg/L.

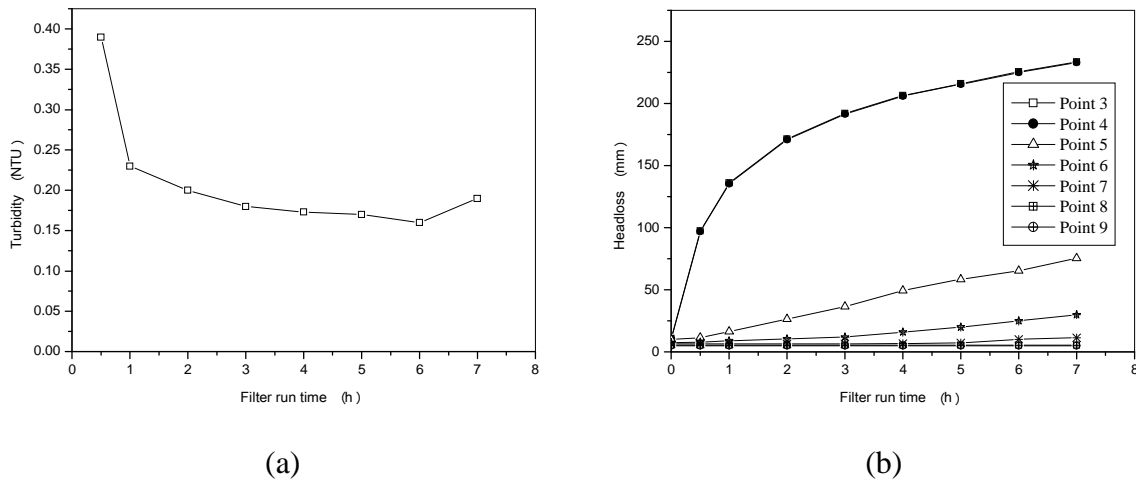


Figure D.7.a: Filtrate turbidity vs. filter run time, b: Headloss profiles vs. time (run 7, combined media).

Medium = combined (75% medium ii and 25% LLDPE powder); filtration velocity = 4 m/h; medium depth = 600 mm and chemical dose = 23 mg/L.

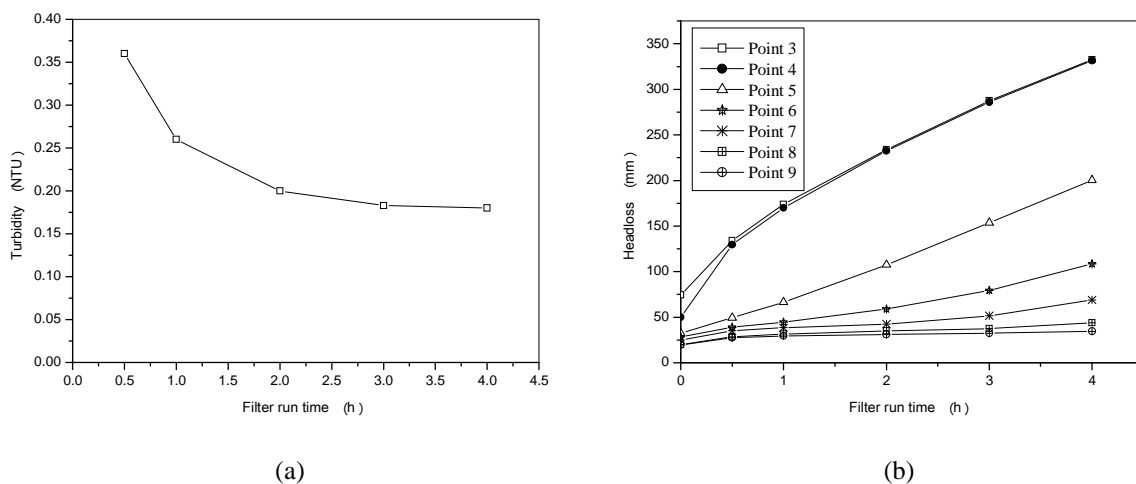


Figure D.8.a: Filtrate turbidity vs. filter run time, b: Headloss profiles vs. time (run 8, combined media).

Appendix E

Factorial design results

Discussion of the 2³ factorial design results of medium i

- **Factor significance using t-test**

The importance of each factor is shown in the Pareto Chart (Figure E.1), which graphically displays the magnitudes of the effects from the results obtained. The effects are sorted from largest to smallest.

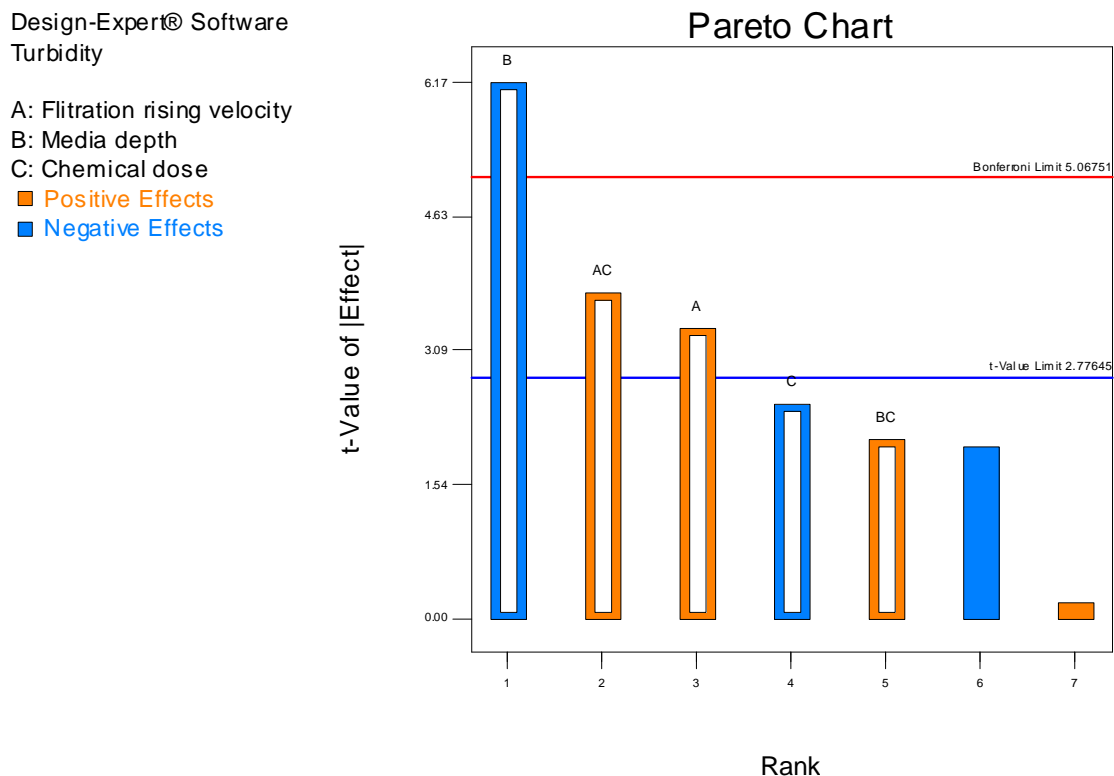


Figure E.1: Pareto chart.

The Pareto chart clearly shows that media depth (factor B) is the most important factor affecting the removal of turbidity followed by the filtration rising velocity-chemical dose interaction (AC), and filtration rising velocity (factor A) when a t-value limit of 2.77645 adjustment is done. The conclusion from this Figure is also supported by the ANOVA in the next section.

- **Analysis of variance**

According to the ANOVA (Table E.1), the *F* values to be 14.72, which implies that the terms in the model have a significant effect of the response.

Table E.1: Reproduced summary of ANOVA

Source	Sum of squares	df	Mean square	F value	p-value (Prob > F)
Model	3.23	5	0.65	14.72	0.011
A-Filtration rising velocity	0.49	1	0.49	11.15	0.0288
B-Media depth	1.67	1	1.67	38.11	0.0035
C-Chemical dose	0.27	1	0.27	6.06	0.0695
AC	0.62	1	0.62	14.02	0.02
BC	0.19	1	0.19	4.23	0.1087
Curvature	0.55	1	0.55	12.45	0.0243
Residual	0.18	4	0.044		
Lack of Fit	0.18	2	0.088	375.64	0.0027
Pure Error	4.67E-04	2	2.33E-04		
Cor Total	3.96	10			

Based on the ANOVA results, the final mathematical equation (regression model) in terms of coded factors (confidence level above 95%) as determined by Design-expert software for media (i) is given below:

$$\text{Turbidity} = 1.13 + 0.25A - 0.46B - 0.18C + 0.28AC + 0.15BC$$

Figure E.2 show response surface plots for the relationship between filtration rising velocity, and chemical dose on the removal of turbidity. As can be seen in Figure E.2 at lower filtration rising velocity of 2 m/h, the chemical dose value needed for maximum turbidity removal was at 23 mg/l (high level). However, at higher filtration rising velocity and lower chemical dose value, the turbidity removal declines.

Design-Expert® Software

Turbidity

○ Design points below predicted value



X1 = A: Filtration rising velocity
X2 = C: Chemical dose

Actual Factor
B: Media depth = 400.00

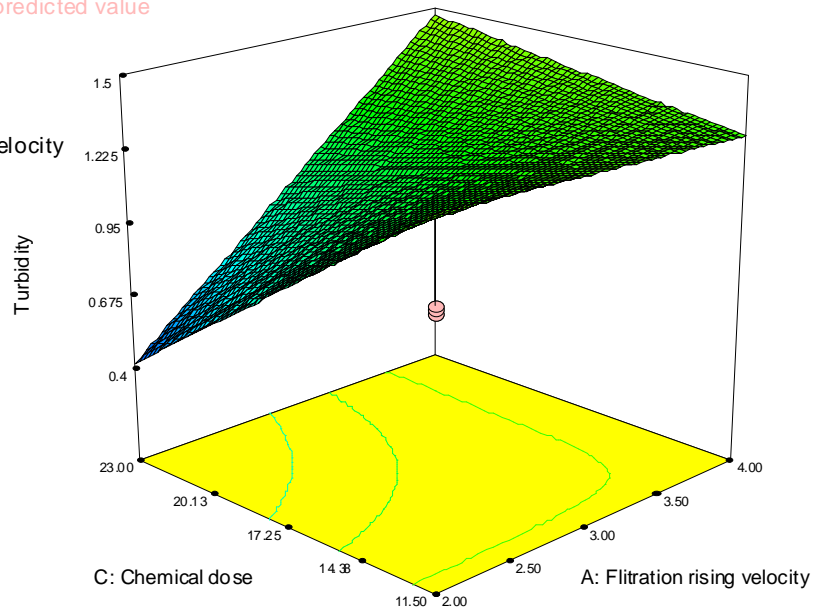


Figure E.2: 3D response surface graph for turbidity removal vs. filtration rising velocity and chemical dose.

Discussion of the 2^3 factorial design results of medium iii

- **Factor significance using t-test**

The importance of each factor is shown in the Pareto Chart (Figure E.3), which graphically displays the magnitudes of the effects from the results obtained. The effects are sorted from largest to smallest.

In the case of media iii, the Pareto shows that filtration rising velocity (factor A) is the most important factor affecting the removal of turbidity followed by the media depth (factor B). It is also shown that filtration rising velocity-media depth interaction (AB), has a significant effect on the response when a t-value limit of 2.77645 adjustment is done. The conclusion from this Figure is also supported by the ANOVA in the next section.

A: Filtration rising velocity
B: Media depth
C: Chemical dose
■ Positive Effects
■ Negative Effects

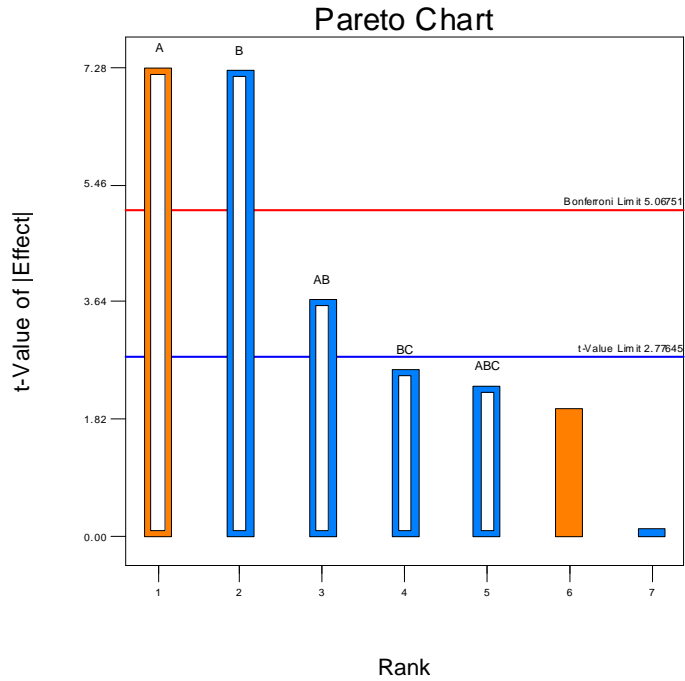


Figure E.3: Pareto chart.

- **Analysis of variance**

According to the ANOVA (Table E.2), the model F-value of 26.31 implies the model is significant. There is only a 0.37% chance that a “model F-value” this large could occur due to noise. Values of “Prob > F” less than 0.05 indicate model terms are significant. In this case A, B, AB are significant model terms.

Table E.2: Reproduced summary of ANOVA

Source	Sum of squares	df	Mean square	F value	p-value (Prob > F)
Model	6.05	5	1.21	26.31	0.0037
A-Filtration rising velocity	2.44	1	2.44	53.07	0.0019
B-Media depth	2.42	1	2.42	52.59	0.0019
AB	0.63	1	0.63	13.63	0.021
BC	0.31	1	0.31	6.78	0.0598
ABC	0.25	1	0.25	5.48	0.0793
Curvature	1.26	1	1.26	27.33	0.0064
Residual	0.18	4	0.046		
Lack of Fit	0.18	2	0.09	55.35	0.0177
Pure Error	3.27E-03	2	1.63E-03		
Cor Total	7.49	10			

Based on the ANOVA results, the final mathematical equation (regression model) in terms of coded factors (confidence level above 95%) as determined by Design-expert software for media (iii) is given below:

$$\text{Turbidity} = 1.48 + 0.55A - 0.55B - 0.28AB - 0.20BC - 0.18ABC$$

Figures E.4 and E.5 show the relationship between filtration rising velocity, and media depth since their interaction has a significant effect. It can be concluded that the best turbidity removal was achieved when the filtration rising velocity was at the lower level, media depth at the higher level, and chemical dose at the higher level. On the other hand the least turbidity removal was achieved when the filtration rising velocity was the higher level, media depth at the lower level and chemical dose at the higher level. This conclusion can also be drawn from by the response surface plots shown in Figure E.6

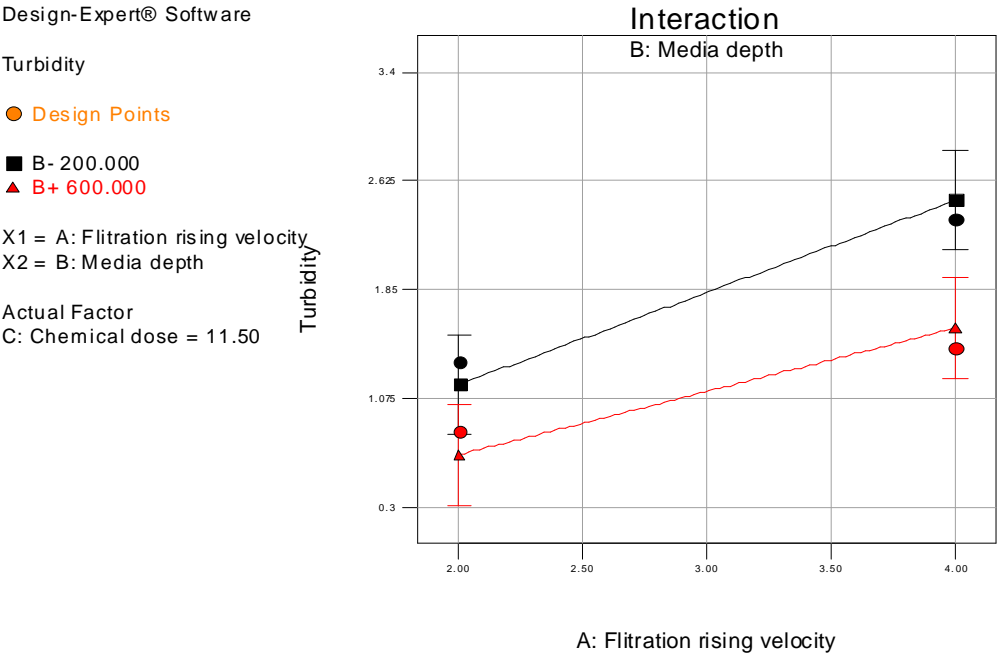


Figure E.4: Effect of interaction AB at low level of chemical dose.

Design-Expert® Software

Turbidity

● Design Points

■ B- 200.000

▲ B+ 600.000

X1 = A: Filtration rising velocity

X2 = B: Media depth

Actual Factor

C: Chemical dose = 23.00

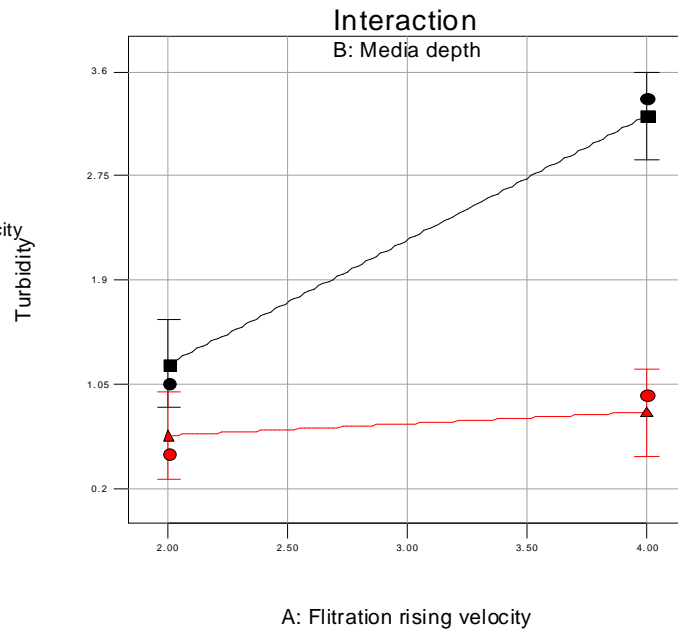


Figure E.5: Effect of interaction AB at high level of chemical dose.

Design-Expert® Software

Turbidity

● Design points above predicted value

○ Design points below predicted value

3.38

0.48

X1 = A: Filtration rising velocity

X2 = B: Media depth

Actual Factor

C: Chemical dose = 23.00

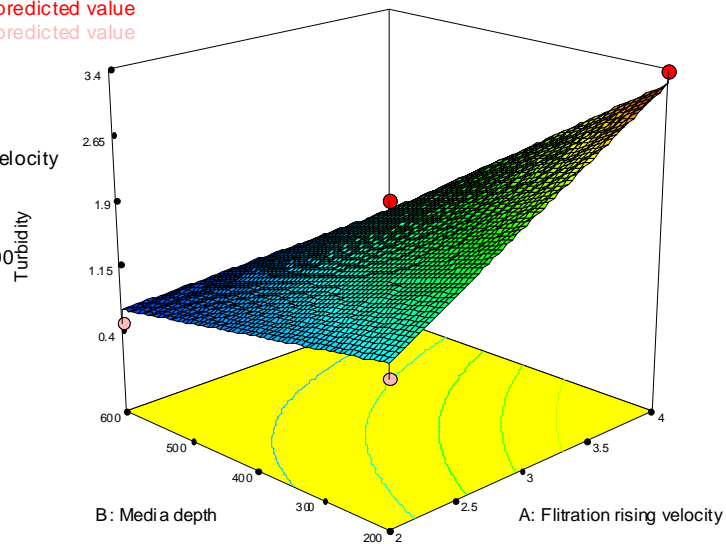


Figure E.6: 3D response surface graph for turbidity removal vs. filtration rising velocity and media depth.

Appendix F

Materials and equipment data sheet

Food Grade
 Bentonite

Revised 08/13/01

VOLCLAY® KWK FOOD GRADE

General Description	Fine granular sodium bentonite with an average particle size between 20 and 70 mesh.																		
Functional Use	Used in the "fining" step of processing wine, juice, cider, and vinegar for the removal of suspended solids. Particularly useful in preventing cloudiness and removing heat-sensitive proteins.																		
Purity	Hydrous aluminum silicate comprised principally of the clay mineral montmorillonite. Volclay KWK Food Grade meets all requirements of the Food Chemical Codex.																		
Chemical Formula	Diocahedral smectite, an expanding layer silicate: $(Na,Ca)_{0.33}(Al_{1.67}Mg_{0.33})Si_4O_{10}(OH)_2 \cdot nH_2O$																		
Elemental Composition	Typical analysis – moisture free. <table border="0"> <tr><td>SiO₂</td><td>83.02 %</td></tr> <tr><td>Al₂O₃</td><td>21.08 %</td></tr> <tr><td>Fe₂O₃</td><td>3.25 %</td></tr> <tr><td>FeO</td><td>0.35 %</td></tr> <tr><td>MgO</td><td>2.87 %</td></tr> <tr><td>Na₂O</td><td>2.57 %</td></tr> <tr><td>CaO</td><td>0.65 %</td></tr> <tr><td>Trace</td><td>0.72 %</td></tr> <tr><td>LOI</td><td>5.64 %</td></tr> </table>	SiO ₂	83.02 %	Al ₂ O ₃	21.08 %	Fe ₂ O ₃	3.25 %	FeO	0.35 %	MgO	2.87 %	Na ₂ O	2.57 %	CaO	0.65 %	Trace	0.72 %	LOI	5.64 %
SiO ₂	83.02 %																		
Al ₂ O ₃	21.08 %																		
Fe ₂ O ₃	3.25 %																		
FeO	0.35 %																		
MgO	2.87 %																		
Na ₂ O	2.57 %																		
CaO	0.65 %																		
Trace	0.72 %																		
LOI	5.64 %																		
Moisture	Maximum 12% as shipped.																		
Dry Particle Size	Maximum 1.0% retained on 16 mesh. Maximum 35.0% retained on 20 mesh. Maximum 3.5% passing 70 mesh.																		
Wet Particle Size	Minimum 94% finer than 200 mesh (74 microns). Minimum 92% finer than 325 mesh (44 microns).																		
pH	8.0 - 10.5 @ 5% solids.																		
Free Swell	Minimum 20 mls per 2 grams clay.																		
Packaging	50 or 100 pound multi-wall paper bags, or bulk.																		



A wholly-owned subsidiary of AMCOL International Corporation



THE INFORMATION AND DATA CONTAINED HEREIN ARE BELIEVED TO BE ACCURATE AND RELIABLE. AMERICAN COLLOID COMPANY MAKES NO WARRANTY OF ANY KIND AND ACCEPTS NO RESPONSIBILITY FOR THE RESULTS OBTAINED THROUGH APPLICATION OF THIS INFORMATION.

LLDPE - Product Data Sheet

LP 3040/10 LLDPE

Date of Issue: February 2002

Print Date: July 2002

Information

Polymer technology centre
P O Box 72
Modderfontein 1645
South Africa

Tel: +27 (0) 11 458 0700
Fax: +27 (0) 11 458 0734

Polyethylene sales

Sasol Polymers
Johannesburg
Tel: +27 (0) 11 790 1250
Cape Town
Tel: +27 (0) 21 686 7740
Durban
Tel: +27 (0) 31 267 0777

www.sasol.com/polymers



Sasol Polymers Polythene Business

Masterbatch

Melt index: 20 Density: 0.924

Features

Excellent melt flow
Colourable
Excellent colour retention
Powder
Butene copolymer

Additives

Antioxidant

Applications

Base polymer for masterbatch

Performance properties - LP 3040/10

Test	Value	Unit	Test method
MFI (190°C/2.16kg)	20	g/10min	ASTM D1238
Nominal density	0.924	g/cm ³	ASTM D1505
Bulk density	350	kg/m ³	ASTM D1895
Particle size	90% < 1000	µm	ASTM D1921
Tensile strength at yield	13	MPa	ASTM D638 ¹⁾
Impact energy at -40°C	15	J/mm	ASTM D3029
ESCR F ₅₀	0.5	hr	ASTM D1693 ²⁾

¹⁾ Crosshead speed 500mm/min

²⁾ 100% Igepal C0630

Processing

LP 3040/10 processes over a wide range of temperatures. A typical melt temperature would be 180°C to 250°C. LP 3040/10 can be used for various pigment concentrations, due to its high flow properties.

Presentation

Supplied in powder form packed in 25kg bags.

Food Packaging

This material complies with F&DA regulation 177.1520 when used unmodified and according to good manufacturing practices for food contact applications. Accordingly, this material may be used in all food contact applications (except holding food during cooking).

Explosion Hazard

While care is taken to keep the amount of sub 150µm particles to a minimum, some fines will always be present in the powder. These fines can, under certain conditions, pose an explosion hazard. We recommend that the processing equipment has adequate grounding at all times and good housekeeping be practised throughout the facility.

Storage

As ultraviolet light may cause a change in the material, all resins should be protected from direct sunlight during storage.


Handling

Workers should be protected from the possibility of skin or eye contact with molten polymer. Safety glasses are suggested as a minimal precaution to prevent possible mechanical or thermal injury to the eyes. Fabrication areas should be ventilated to carry away fumes or vapours.

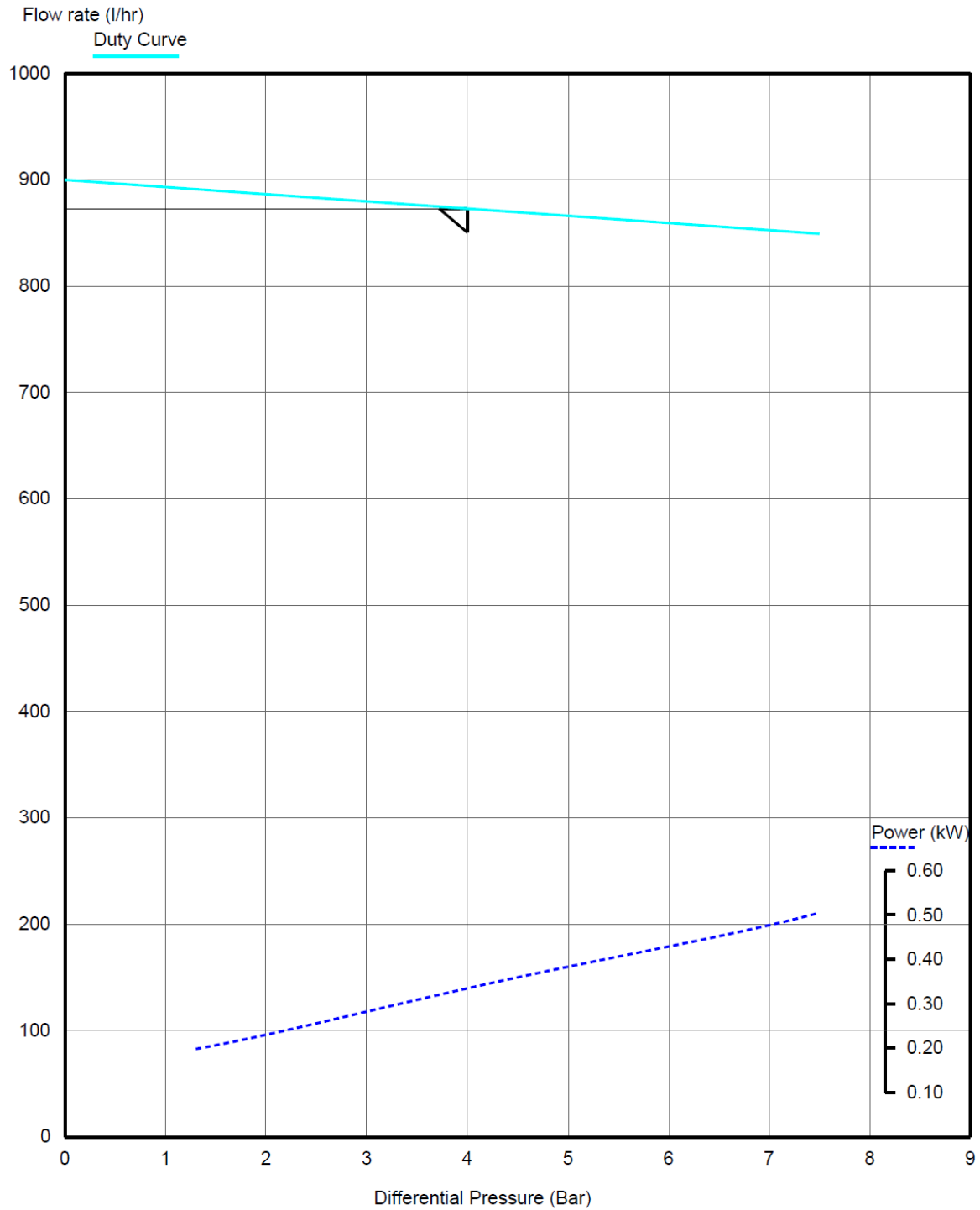
Combustibility

Polyethylene resins will burn when supplied with adequate heat and oxygen. They should be handled and stored away from contact with direct flames and/or other ignition sources. In burning, polyethylene resins contribute high heat and may generate a dense black smoke. Fires can be extinguished by conventional means, with water and water mist preferred. In enclosed areas, fire fighters should be provided with self-contained breathing apparatus.

This information is based on our current knowledge and experience. In view of many factors that may affect processing and application, this data does not relieve processors from the responsibility of carrying out their own tests and experiments, neither does it imply any legally binding assurance of certain properties or of suitability for a specific purpose. It is the responsibility of those to whom we supply our products to ensure that any proprietary rights and existing laws and legislation are observed.

 DENORCO Ref DEFAULT	MONO		2/1
	DUTY POINT Head 4 Bar Flow 872.8 l/hr SG 1 Viscosity cSt	Power Abs 0.335 kW Motor Size 0.75 kW Pump Speed 920 RPM	Abrasion NONE NPSHr Inlet/Outlet 25 mm Minimum starting Torque 5 Nm

Ver 5.91



SSCX

CLOSE-COUPLED, SINGLE-IMPELLER CENTRIFUGAL PUMP FEATURING AXIAL SUCTION AND RADIAL DISCHARGE

Single impeller centrifugal pumps manufactured from stainless steel AISI 304 with 2 poles enclosed self-ventilated internally cooled asynchronous motor. Recommended for pumping clear water and liquids that are chemically non aggressive in domestic, agricultural and industrial sector.

- **IMPELLER AND DIFFUSER IN AISI 304 STAINLESS STEEL**
- **HIGH RELIABILITY**
- **HIGH HYDRAULIC EFFICIENCY**



Applications

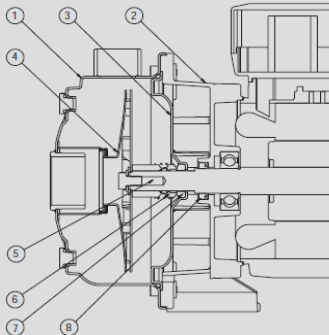
- Booster sets
- Irrigation
- Handling of non aggressive water and liquids
- Gardening

Usage limitations

- Type of liquid: chemically non aggressive clean water and liquids with no suspended solids
- Max liquid temperature: 90°C
- Max. operating pressure: 8 bar (PN8)

Motor

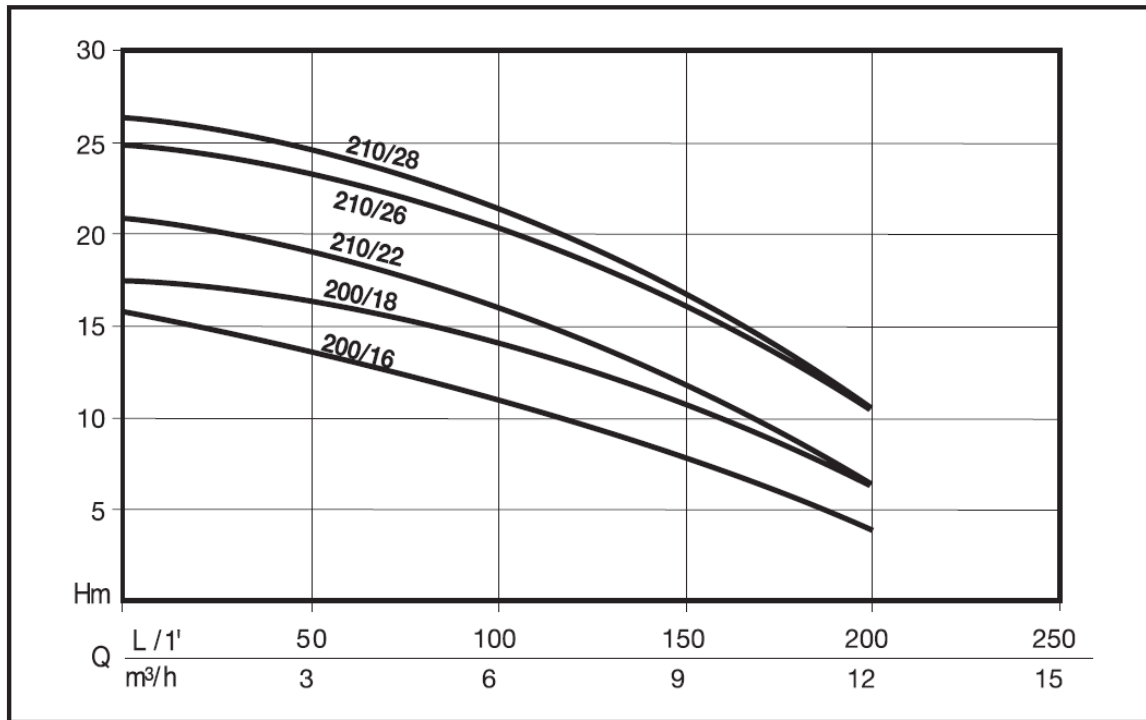
- Enclosed, externally ventilated
- IP55 protection level
- Class F insulation
- Single phase power supply with capacitor permanently activated and thermal protection built into the motor winding
- Three phase power supply with external protection provided by the user
- Rotation speed 2850rpm
- Suitable for continuous use



DESIGN FEATURES

Component	Material
1 Pump body	Stainless steel X5 CrNi 18-10 EN1.4301 (AISI 304)
2 Motor bracket	Aluminum AISI 12 UNI 5076
3 Seal housing	Stainless steel X5 CrNi 18-10 EN1.4301 (AISI 304)
4 Impeller	Stainless steel X5 CrNi 18-10 EN1.4301 (AISI 304)
5 Motor shaft (hydraulic end)	Stainless steel X5 CrNi 18-10 EN1.4301 (AISI 304)
6 Rotating assembly mechanical seal	Graphite
7 Fixed assembly mechanical seal	Ceramic
8 O-rings	NBR 70Shore

TABLE OF HYDRAULIC PERFORMANCE



PUMP PERFORMANCE

CODE	MODEL	Nominal Power		Absorbed Power		VOLTAGE	Amp.	μF.	Q	Discharge head in meters							
		HP	kW	HP	kW					0	20	40	80	120	160	200	
										L/1'	0	20	40	80	120	160	200
										m³/h	0	1,2	2,4	4,8	7,2	9,6	12
N4600010	SSCX 200/16M	0,75	0,55	1	0,75	1 ~ 230 V	3,5	12,5	Discharge head in meters	16	14,5	14	12,5	9,5	6,5	4	
N4600020	SSCX 200/16T					3 ~ 230 ÷ 400 V	3,1-1,8										
N4600030	SSCX 200/18M	1	0,75	1,2	0,9	1 ~ 230 V	4	16		18	17	16	15	13	10,5	6	
N4600040	SSCX 200/18T					3 ~ 230 ÷ 400 V	3,1-1,8										
N4600050	SSCX 210/22M	1,15	0,85	1,5	1,1	1 ~ 230 V	4,9	25		21,5	20	19	17	15	11	6	
N4600060	SSCX 210/22T					3 ~ 230 ÷ 400 V	3,8-2,2										
N4600070	SSCX 210/26M	1,35	1	1,9	1,4	1 ~ 230 V	6,7	25		25,5	24	23	21,5	19	15,5	10	
N4600080	SSCX 210/26T					3 ~ 230 ÷ 400 V	5-2,9										
N4600090	SSCX 210/28M	1,5	1,1	2,1	1,55	1 ~ 230 V	7,3	25		27	25,5	24,5	23	19,5	16	10	
N4600100	SSCX 210/28T					3 ~ 230 ÷ 400 V	5,6-3,2										

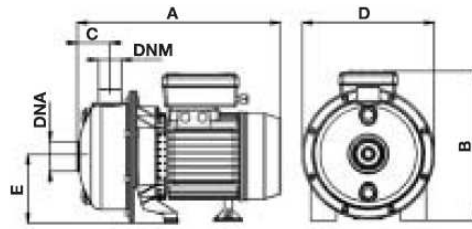


TABLE OF SIZES AND WEIGHTS

Model	Dimensions mm.							Weight
	A	B	C	D	E	DNA	DNM	kg
SSCX 200/16	320	240	50,5	210	105	1" 1/4	1"	8,7
SSCX 200/18	320	240	50,5	210	105	1" 1/4	1"	9,5
SSCX 210/22	350	250	50,5	210	105	1" 1/4	1"	12,1
SSCX 210/26	350	250	50,5	210	105	1" 1/4	1"	13,6
SSCX 210/28	350	250	50,5	210	105	1" 1/4	1"	13,8

GB - 1" ED. 092006 - COD. NV260P890